

Instituto de Neurociencias
Universidad Miguel Hernández-CSIC

**Thalamic control of cortical plasticity following
input deprivation**

Memoria de Tesis Doctoral

Verónica Moreno Juan

Directora de Tesis:

Guillermina López-Bendito, PhD

San Juan de Alicante, 2018

Programa de Doctorado en Neurociencias



San Juan de Alicante, 11th of December 2017

DOCTORAL THESIS BY COMPENDIUM OF PUBLICATIONS

To whom it may concern:

The doctoral thesis developed by me, Verónica Moreno Juan, with title: “***Thalamic control of cortical plasticity following input deprivation***”, is a compendium of publications and includes the following publication in which I am the first author:

Prenatal thalamic waves regulate cortical area size prior to sensory processing

Verónica Moreno-Juan, Anton Filipchuk, Noelia Antón-Bolaños, Cecilia Mezzera, Henrik Gezelius, Belen Andrés, Luis Rodriguez-Malmierca, Rafael Susín, Olivier Schaad, Michael Rutlin, Sacha Nelson, Sebastien Ducret, Miguel Valdeolmillos, Filippo M. Rijli and Guillermina López-Bendito

Nature Communications 2017 Feb 3;8:14172. Doi: 10.1038/ncomms14172

I declare that this publication will not be used in any other thesis.

Yours sincerely,

Verónica Moreno Juan

San Juan de Alicante, 11th of December 2017

DOCTORAL THESIS BY COMPENDIUM OF PUBLICATIONS

To whom it may concern:

The doctoral thesis developed by Verónica Moreno Juan, with title: “***Thalamic control of cortical plasticity following input deprivation***”, includes a publication in *Nature Communications* (doi: 10.1038/ncomms14172), corresponding to the main topic of the dissertation.

As the director of this PhD. Thesis and the corresponding author of the article, I declare that Ms. Verónica Moreno Juan is a first author of the article and is a major contributor of the work presented in this publication. I declare that this publication will not be used in any other thesis.

This article was published in a journal that belongs to the first quartile (Q1) for the corresponding discipline according to the last Journal Citation Reports (JCR).

Nature Communications: Impact factor 12.124 (2016 Q1 Multidisciplinary Sciences)

Yours sincerely,

Guillermina López-Bendito



INFORME DE LA COMISION ACADEMICA DEL PROGRAMA DE DOCTORADO EN NEUROCIENCIAS

Por la presente, la Comisión Académica del Programa de Doctorado en Neurociencias:

Informa FAVORABLEMENTE el depósito de la Tesis presentada por Dña. Verónica Moreno Juan

Realizada bajo la dirección de la Dra. Gullermina López-Bendito,

Titulada: ***Thalamic control of cortical plasticity following input deprivation.***

Presentada por compendio de publicaciones.

San Juan de Alicante 7 Diciembre 2017

Dr. Miguel Valdeolillos

Coordinador del programa de Doctorado en Neurociencias

Cada vez más cerca del final de esta etapa y ahora por fin ha llegado la hora de escribir uno de los capítulos más importantes de este libro.

No puedo empezar sino por agradecerle a mi directora de tesis, mi jefa, Guille. Gracias por haberme dado la oportunidad de elegir este camino, que ha sido más duro de lo que pensaba, pero sin dudarlo volvería a escogerlo mil veces más. Has sido mi mentora, mi profesora, mi jefa y mucho más que eso. Me llevo muchísimos buenos recuerdos de todas las discusiones científicas que hemos tenido, conversaciones intensas en el despacho, incluso los días de limpieza pasándolos con miedo a que me tirases algo de la nevera, gracias por todos los buenos ratos. Durante estos años hemos vivido muchos momentos, he madurado mucho a tu lado y he aprendido más que nunca a ser yo. Quiero agradecerte de corazón que me hayas dado la oportunidad de conocer mundo y poder compartir mis ideas sin fronteras, sin duda es una de las partes más bonitas de este trabajo, y sin ti nunca hubiera sido posible. Y por supuesto, quiero darte las gracias por la confianza que has depositado en mí durante todos estos años, porque me has hecho sentir muy privilegiada. Gracias por todo esto y mucho más Guille.

Quiero empezar por agradecer a Luis y Belén, sois mis motores de cada día, no puedo imaginarme el laboratorio sin vosotros. Ya lo sabéis, pero para que quede constancia sois parte de mi familia y ojalá os pudiera llevar en mi mochilita allá donde vaya en el futuro, pero como sé que es prácticamente imposible, y no lo digo por el tamaño de la mochila, me conformaré con teneros cerca de espíritu y veros las caras todas las veces que podamos. Os quiero muchísimo y gracias y más gracias por todo lo que habéis hecho por mi.

Leti, Ana, Mar e Irene... mis chicas, los días a vuestro lado son mucho mejores. A las peques, os aconsejo paciencia, todo llega al final, a Ana quiero darle las gracias por acogernos en su familia y por ser una más de nosotros con tanta facilidad. A mi Letiti, tras alguna que otra exaltación de la amistad, me toca dejarla por escrito, eres una persona increíble y una trabajadora excepcional, y como amiga de las pocas que existen. Ojalá tengas todo lo que te mereces en esta vida, te deseo toda la felicidad del mundo.

A Rafa, gracias por tu paciencia, por tu tiempo y tus risas, gracias por haber estado conmigo todos estos años, eres una parte fundamental de este libro y de mi vida, gracias!

Aleja, tu llegada ha sido de lo mejor que ha pasado este año en el labo. Antes de compis ya éramos amigos, y ahora es genial contar con un amigo más en el laboratorio. Gracias por todos los momentos que me has dado estos años y por ser como eres. No lo diré muchas más veces por si nos toca otro, pero el mundo necesita más gente como tú!

A Teresa, la última en llegar, todo lo que te espera! Quiero darte la bienvenida a nuestra casa y espero que sigas integrándote como hasta ahora, que nosotros somos mucho más majos que los yanquis!

Agradecimientos

A Noe, hemos pasado por muchísimo las dos, ojalá hubiera sido todo diferente. Ya te queda menos para acabar esta etapa, mucho ánimo para el último empujón.

A Helena, llevamos muchos años juntas pasando buenos y malos momentos y quiero aprovechar para darte las gracias por todas las veces que me has ayudado. Te deseo muchísima felicidad para ti y para tus peques.

A Fran y Miguel, gracias por estar siempre disponibles cuando os he necesitado y por toda vuestra ayuda y consejos.

Ceci, no puedo enumerar todas las cosas que he aprendido de ti, han sido muchísimas. Gracias por estar conmigo desde el principio y por los buenos y malos momentos que hemos pasado juntas, aunque estés lejos desde hace tiempo, no me olvido de ti, gracias Cecuci.

No me olvido de Anton, Edu, Henrik y Mar, que ya no están en el labo, pero que también han sido parte fundamental de esta historia. Antón, tu ausencia se nota todos los días, ya no es lo mismo entrar al labo sin tus piropos... quiero darte las gracias por todos los buenos momentos que hemos pasado, y por haber compartido conmigo el núcleo de esta tesis. Te echo de menos! Edu, te echamos de menos, tu capa de ranciedad nos la vamos sorteando por días, pero ninguno la lleva con tanta elegancia como tú! Ojalá nos visitaras más a menudo!! Henrik, gracias por todos estos años, has sido una de las mejores personas que me he cruzado en este camino. Gracias por tu ayuda y por compartir todo lo que sabes con nosotros. Te echo muchísimo de menos, y he de reconocerlo... ahora hasta me gusta escuchar a ABBA porque me recuerda a ti! Mar, la mami, echo mucho de menos tus consejos y quiero agradecerte la ayuda y la confianza que siempre me has brindado, esto también va por ti.

Mi Abraham... A ti va dedicada esta tesis, por ser un indispensable en mi vida, por estar siempre cuando te necesito y cuando no! Por aguantar mis manías y hacer que me sienta una princesa siempre que estamos juntos. Por nuestros viajes, nuestras nocheviejas, nuestros cánticos perjudicados y todos nuestros momentos. Ojalá podamos celebrar esto juntos aquí y en París. Eres un ejemplo a seguir en todos los ámbitos de tu vida. Te quiero y te deseo todo lo bueno de este mundo, porque poca gente como tú se lo merece tanto.

Vir, vidrierita mía, este trocito es para ti, ojalá pudiera explayarme más pero ya se está haciendo pesado, imagínate si pusiera aquí todo lo que mereces que te diga públicamente! Eres alguien fundamental en mi vida, desde la carrera hasta ahora, y lo que queda! Hemos vivido muchísimo juntas, más cosas buenas que malas, pero incluso en las malas siempre nos hemos apoyado la una en la otra. Empezamos nueva etapa, y te me vas lejos, pero algo me dice que como siempre, acabaremos muy cerca! Te quiero muchísimo y te deseo muchísima suerte en todo lo que te está por llegar.

Marilyn, mi marilyna, ya estás casi! Y no digo con la tesis... vas a ser mamá! (por si no te habías enterado)!! Ha sido la mejor noticia en mucho tiempo! Quiero darte las

gracias por todo el apoyo que me has dado durante este tiempo y por tu amistad, soy muy afortunada de poder contar contigo.

Cris, eres un pilar de esta historia. Gracias por todos los momentos que has compartido conmigo, por nuestras risas y nuestros llantos. Y sobre todo, por tu brownie, esta tesis hubiera sido mucho menos dulce sin él. Te deseo lo mejor y te voy a dar todo el ánimo que pueda para esta última carrera!

Giovanni, mi compi, mi amigo y confidente. Gracias por haber estado a mi lado durante todos estos años, por nuestras rutas, nuestras charlas y por haberme acogido. En fin, por ser tan especial. Te echo muchísimo de menos.

A Pili, llevamos juntas desde hace mucho tiempo y estaremos juntas durante muchísimo más. Gracias por estar siempre a mi lado y por regalarme tus sonrisas.

Gente del INA, gracias por vuestro ánimo, vuestras sonrisas y saludos en los pasillos, también por vuestro apoyo y ayuda. En especial gracias a mis chicas del animalario, a Mari, Vero, Fany y Lorena. También quería agradecer a Virtu, Maite, Ruth y a Giovanna, gracias por vuestra ayuda y paciencia, un trocito de esto es vuestro.

Quiero agradecer a Juan, mi profe, por haberme guiado durante muchos años, por haberme apoyado desde el principio en seguir este camino y ver su felicidad cuando nos encontramos en el INA o incluso en congresos, porque te debo mucho de lo que he conseguido. Gracias!

A mis Señoras (Rocío, Esther y Mape), a Paulita, a Blanqui, a Esteff, a Agus y a Vane, os quiero y os adoro, este libro también es para vosotras, por todos los momentos que me ha quitado de poder estar juntas y por todo el apoyo que me habéis dado durante todo este tiempo. Os quiero con locura.

Y ahora, mi familia. Esta tesis va dedicada a mis padres, que siempre me han inculcado una educación basada en el respeto y en la perseverancia. Si de algo podéis estar orgullosos es de que lo habéis conseguido con los tres. Os debo muchas cosas, pero entre ellas, que haya llegado hasta aquí. Gracias.

A Breik, mi perro, con él he crecido y con él se fue un trocito de mí en este último año. Porque él también es parte de esto, por su compañía y amistad durante todos estos años. Porque ahora me doy cuenta de que madrugar con tus buenos días era mucho más fácil.

A mis tíos, en especial a mi tía Mari y a mi tío Álex, ejemplos en mi vida. Sois fundamentales para mí y os tengo que agradecer que siempre me hayáis apoyado incondicionalmente. Esto es para vosotros.

A mi abuelo, porque no existe en el mundo un abuelo mejor que tú. Eres fundamental en nuestras vidas y tengo que darte las gracias por todo el apoyo y la dedicación que has tenido conmigo. Te quiero.

Agradecimientos

Mi abuela, porque sin ella nada de esto hubiera sido posible. Porque gracias a ella todo esto comenzó. Nadie en el mundo ha sentido tanto orgullo por mí como ella y le debo tanto que rendirse nunca será opción. Sin duda, esto va por ella, porque sus recuerdos me dan la fuerza todos los días para seguir sumando.

A Álvaro. Mi compañero de viaje, gracias a ti esto está siendo posible. Gracias por tus consejos, paciencia y amor. Tú le has dado la luz que necesitaba a esto, has sabido cómo animarme en los momentos más duros y celebrar los momentos más dulces. Gracias a ti he sacado sonrisas para repartir todos los días, de donde pensaba que ya no quedaban. Te debo muchísimo más de lo que puedes imaginar. Gracias también a tu familia por hacerme sentir una más de vosotros. Os quiero.

A mi madre por ser el ejemplo de mi vida, la persona más inteligente y luchadora que conozco. Hoy soy lo que soy gracias a ti, y sí, mi madre es la mejor madre del Universo. Podría agradecerte muchísimas cosas, pero quiero agradecerte especialmente la paciencia que tienes conmigo, tu amor incondicional y el orgullo que sientes por nosotros. Somos como somos gracias a ti. Te quiero.

A mis hermanos, mis estrellas, porque sin ellos mi vida no tendría sentido. Al Tete, al que todo el mundo adora, porque te lo mereces, eres la persona más buena que conozco. Hemos pasado casi todos los momentos de nuestra vida juntos, los buenos y los malos, y hemos aprendido a seguir subiendo poco a poco. Ojalá la vida te brinde todo lo bueno que te mereces. A María, porque es mi persona favorita, mi suerte, mi hermana pequeña. Por nuestra telepatía, nuestros gustos tan diferentes y tan idénticos a la vez, nuestra forma de hablar, de cantar, de gruñir... y sobre todo, nuestras risas infinitas, de esas de llorar hasta deshidratarnos, eso nos hace especiales. Os adoro, y sé que llegaréis donde os propongáis y yo siempre estaré cerca para animaros a llegar más y más lejos. A vosotros dedico este libro.

Y si habéis leído hasta aquí, ahora sabréis lo afortunada que me siento, y aunque esta etapa ha sido muy dura, he podido llegar hasta aquí gracias a vosotros. Así que sólo puedo agradeceros una vez más por hacer de mi vida un sitio precioso.

GRACIAS

A mis hermanos



INDEX

ABREVIATIONS.....	3
ABSTRACT/RESUMEN	9
INTRODUCTION	15
1. ORGANIZATION OF THE THALAMUS.....	16
1.1 Origin	16
1.2 Emergence of the distinct thalamic sensory nuclei.....	17
2. THALAMOCORTICAL AND CORTICOTHALAMIC PATHWAY DEVELOPMENT.....	19
2.1 Development of thalamocortical projections.....	19
2.2 Development of corticothalamic projections	21
2.3 The first thalamo-cortical interactions.....	22
3. DEVELOPMENT OF SENSORY SYSTEMS	23
3.1 General Organization	23
3.2 The Visual System	26
3.3 The Somatosensory System	29
3.4 The Auditory System.....	32
4. ACTIVITY-DEPENDENT MECHANISMS IN THE THALAMOCORTICAL DEVELOPMENT.....	33
4.1 Role of spontaneous activity in the development of the visual system.....	34
4.2 Role of spontaneous activity in the somatosensory system development.....	35
4.3 Role of spontaneous activity in the auditory system development	37
5. SENSORY SYSTEM CROSS-TALK: THE CROSS-MODAL PLASTICITY.....	39
5.1 Experience-independence of cross-modal plasticity.....	40
OBJECTIVES:.....	47
RESULTS.....	51
CHAPTER I: PRENATAL THALAMIC WAVES REGULATE CORTICAL AREA SIZE PRIOR TO SENSORY PROCESSING	51
CHAPTER II: COMMON MECHANISMS INVOLVED IN CROSS-MODAL PLASTICITY OF SENSORY SYSTEMS.	111
<i>Auditory embryonic deprivation leads to an experience-independent expansion of the barrel-field</i>	113
<i>Auditory embryonic cochleation does not trigger major thalamocortical and subthalamic rewiring.....</i>	115
<i>Embryonic ablation of the auditory input triggers changes in gene expression in the somatosensory thalamus.....</i>	117
CHAPTER III: SPONTANEOUS THALAMIC WAVES REGULATE CORTICO-THALAMIC INNERVATION IN THE VISUAL SYSTEM.....	119
<i>Embryonic bilateral enucleation triggers changes in corticothalamic innervation</i>	120
<i>Ablation of retinal input embryonically alters the pattern of wave activity in the dLGN </i>	120
<i>Embryonic bilateral enucleation induces changes in gene expression in the dLGN.....</i>	121
<i>Blocking the thalamic waves alters the innervation pattern of corticothalamic axons in the dLGN.....</i>	123
<i>The absence of thalamic calcium waves does not affect thalamocortical axonal topography</i>	124
<i>The absence of thalamic waves does not change retinothalamic innervation.....</i>	125
MATERIALS AND METHODS	131

DISCUSSION	139
CONCLUSIONS/CONCLUSIONES	151
REFERENCES.....	159



Abbreviations

5-HT	Serotonin Receptor	MGN	Medial Geniculate Nucleus
A1	Primary Auditory Cortex	NaChBac	bacterial voltage-gated sodium channel
AC1	Adenylyl Cyclase 1	NBT	nitro-blue tetrazolium chloride
aCSF	Artificial Cerebrospinal Fluid	NF-κB	Nuclear Factor Kappa-Light-Chain-Enhancer of Activated B cells
AP-1	Activator Protein 1	Ngn	Neurogenin
BCIP	5-bromo-4-chloro-3'-indoly phosphate p-toluidine salt	NMDA	N-Methyl-D-Aspartate
CICR	Calcium-induced calcium release	NMDAR	NMDA Receptor
CN	Cochlear Nucleus	NR1	Glutamate Receptor, Ionotropic, NMDA1 (zeta 1)
CoupTF-1	Nuclear Receptor Subfamily 2, Group F, Member 1	NR2b	Glutamate Receptor, Ionotropic, NMDA2B (epsilon 2)
CREB	cAMP Responsive Element Binding Protein	OC	Organ of Corti
CTAs	Corticothalamic Axons	OD	Ocular Dominance
CTB	Choleratoxin Subunit B	OHCs	Outer Hair Cells
DCC	Deleted in Colorectal Carcinoma	Olig3	Oligodendrocyte Transcription Factor 3
DiA	4-[4-(dihexadecylamino)styryl]-N-methylpyridinium iodide	Otx2	Orthodenticle Homeobox 2
DIG	Digoxigenin	P	Prosomere

Abbreviations

DiI	1,1'-dioctadecyl 3,3,3',3'-tetramethylindocarbocyanine perchlorate	Pax6	Paired Box 6
dLGN	Dorsal Lateral Geniculate Nucleus	Pom	Posterior Medial Nucleus
Dlx	Distal-Less Homeobox	Prv	Principal Trigeminal Nucleus
DMG	Dorsal Medial Geniculate Nucleus	PSPB	Pallial-Subpallial Boundary
DTB	Diencephalon-Telencephalon boundary	RGCs	Retinal Ganglion Cells
embBC	Embryonic Bicochleation	RNA	Ribonucleic Acid
embBE	Embryonic Bienucleation	Rorb	RAR-Related Orphan Receptor Beta
Emx	Empty Spiracles Homeobox	RT	Room Temperature
Fgf	Fibroblast Growth Factor	RYR	Ryanodine Receptors
FO	First Order	S1	Primary Somatosensory Cortex
GABA	Gamma-Aminobutyric Acid	SC	Superior Colliculus
Gbx2	Gastrulation Brain Homeobox 2	SOC	Superior Olivary Complex
GFP	Green Fluorescent Protein	Sox14	Sex Determining region Y-box 14
HO	Higher Order	Sox3	Sex Determining region Y-box 3
IC	Inferior Colliculus	Sp8	Trans-Acting Transcription Factor 8
IHCs	Inner Hair Cells	SPGNs	Spiral Ganglion Neurons
ION	Infraorbital Nerve	TCAs	Thalamocortical Axons
IP3	Inositol Triphosphate	TRN	Thalamic Reticular Nucleus
LGE	Lateral Ganglionic Eminence	TTX	Tetrodotoxin
LL	Lateral Lemniscus	V1	Primary Visual Cortex
LP	Lateral Posterior Nucleus	VB	Ventrobasal complex

Mash1	Achaete-scute Family bHLH Transcription Factor 1	vGlut	Vesicular Glutamate Transporter
MD	Monocular Deprivation	VPM	Ventral Posterior Medial Nucleus
MGE	Medial Ganglionic Eminence	Wnt	Wingless-type MMTV Integration Site Family
mGluR	Metabotropic Glutamate Receptor	ZLI	Zona limitans intrathalamica



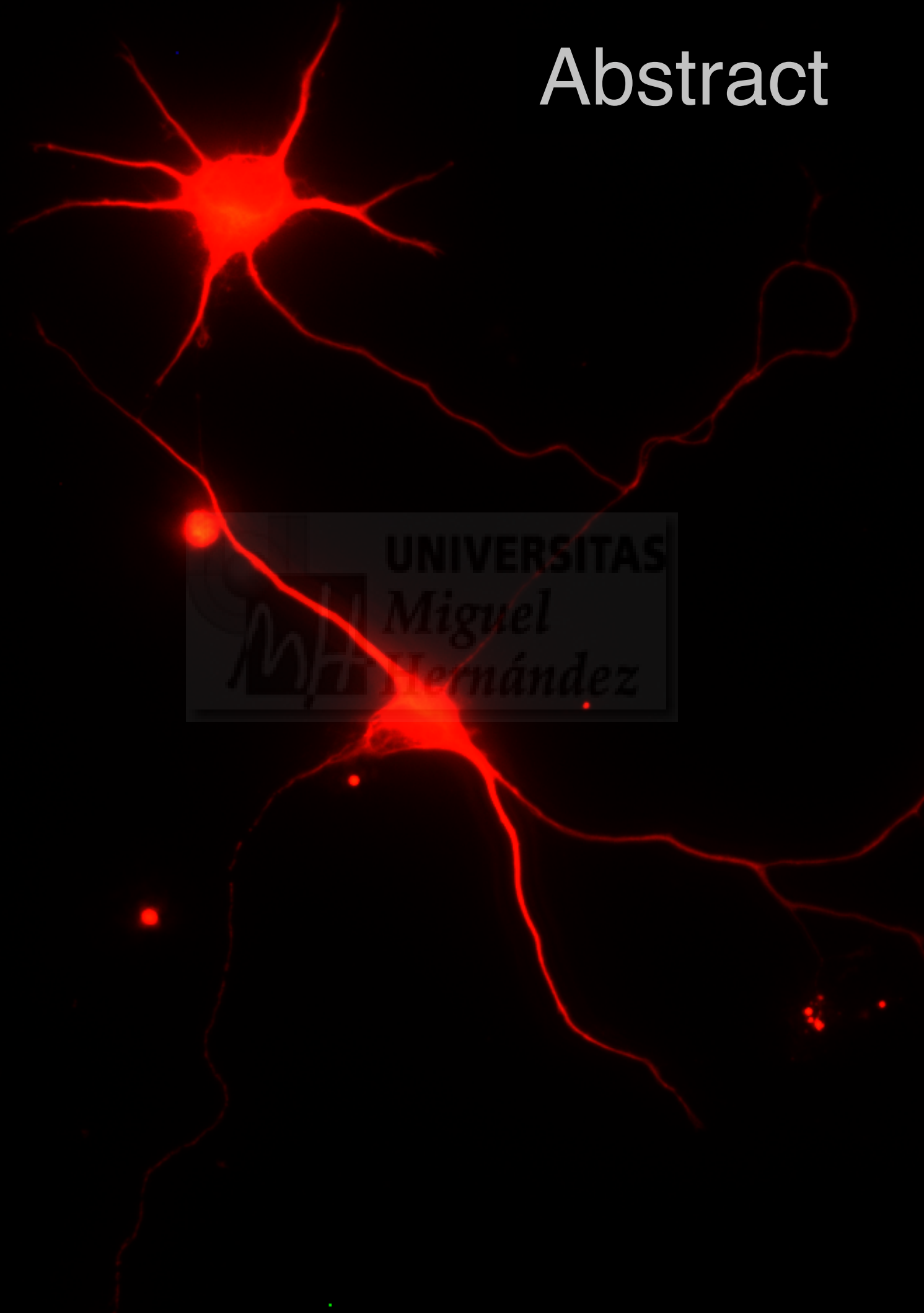


UNIVERSITAS

Miguel

Hernández

Abstract



Abstract

Understanding how the brain adapts to the sensory lost might help us to better decipher the role of intrinsic and extrinsic mechanisms involved in cortical development. A paradigm extensively used to unravel the role of the afferent input in the development of the cortex, is the deprivation of one sensory modality. The deprivation of one sensory modality leads to an adaptive reorganization of the deprived and non-deprived sensory circuits. In this Thesis I used different animal models in which visual or auditory input is impaired during embryonic stages. A recent publication from our laboratory, and the core of this Thesis, has shown that when visual input is removed embryonically, the thalamus triggers a profound reorganization of the somatosensory cortex through changes in thalamic gene expression and thalamocortical axonal branching (Moreno-Juan et al, 2017). We have demonstrated the existence of a prenatal subcortical mechanism that regulates cortical areas size in mice. This mechanism is mediated by the presence of thalamic spontaneous calcium waves that provides a means of communication between different sensory systems. Thus, changes in thalamic calcium waves lead to changes in the genetic profile of thalamic neurons, more specifically the upregulation of *Rorβ* in VPM neurons that predates the enlargement of the barrel-field. We have elucidated that common mechanisms are present in visual and auditory deprived animals as the upregulation of *Rorβ* takes place in the VPM neurons of the embryonic auditory cochleated animals precluding the enlargement of the barrel-field. Moreover, we have found a previously unknown role of thalamic spontaneous activity in disrupting the shape of the corticothalamic axons development. These findings reveal that embryonic thalamic calcium waves coordinate the development and shape of the cortex and the plasticity prior to sensory information processing. Our results will help to better understand how the brain adapts to sensory injury and to investigate possible therapeutic targets promoting behavioural gains and eliminating those connections that may be maladaptive.

Resumen

Una de las cuestiones más interesantes del campo de la neurobiología es intentar descifrar el rol de los mecanismos intrínsecos y extrínsecos implicados en el desarrollo de la corteza cerebral. La privación de una modalidad sensorial se ha utilizado durante mucho tiempo para desvelar el rol de los inputs aferentes en el desarrollo de la corteza cerebral. La privación de una modalidad sensorial provoca adaptaciones en la reorganización de los circuitos afectados y en los intactos. En la memoria de Tesis doctoral aquí presentada se han utilizado diferentes modelos animales en los que se han dañado los inputs visuales o auditivos en estadios embrionarios. Recientemente hemos mostrado en una publicación de nuestro laboratorio, y el tema central de esta Tesis, que al abolir la entrada de información visual durante estadios embrionarios, el tálamo coordina reorganizaciones en la corteza somatosensorial mediante cambios en la expresión genes en el tálamo y cambios en en las ramificaciones de los axones talamocorticales (Moreno-Juan et al., 2017). Hemos demostrado la existencia de un mecanismo subcortical que regula el tamaño de las áreas corticales en ratones. Este mecanismo está mediado por la presencia de ondas de actividad espontánea de calcio lo que proporciona un método de comunicación entre diferentes sistemas sensoriales. Por lo tanto, cambios en las ondas de calcio conlleva a cambios en el perfil genético de las neuronas talámicas, específicamente el incremento de ondas en el núcleo talámico somatosensorial provoca una sobreexpresión de *Rorb* en las neuronas de este núcleo lo que promueve un aumento en el tamaño de la corteza de barriles. Además, hemos encontrado un rol previamente desconocido de la actividad espontánea talámica en el correcto desarrollo de los axones corticotalámicos. Estos resultados revelan que las ondas de calcio talámicas embrionarias coordinan el desarrollo y la forma de la corteza cerebral y la plasticidad antes de que la información sensorial sea procesada. Nuestros resultados ayudarán a entender mejor cómo el cerebro se adapta tras sufrir daños sensoriales y a investigar posibles dianas terapéuticas que promuevan beneficios y poder eliminar las conexiones que podrían no ser productivas.

UNIVERSITÄT
SALZBURG
SALZBURGER
UNIVERSITÄT

Introduction



Introduction

The extreme complexity of the brain is influenced by the cooperation among genetic programs, cellular interactions and external cues. One of the most challenging questions in the field of neuroscience is to determine how sensory inputs influence the functional architecture of the brain. The sensory information from the external environment is received by the receptor organs that are activated at the peripheral site, and subsequently, is transmitted to proper cortical sensory areas in order to be integrated and processed. The transmission of this sensory information occurs via parallel sensory pathways that convey in the thalamic subcortical region.

As aforementioned, before reaching specific sensory cortical territories, all sensory information (except the olfactory) reaches the thalamus. Thus, the thalamus is the first station along the sensory pathways where inputs from the distinct sensory modalities converge. The thalamus is comprised by distinct modality-specific nuclei with a fine-tuned topographical connectivity (Petersen, 2007; Huberman et al., 2008; Tsukano et al., 2017). This topographical organization emerges at embryonic stages as thalamocortical connectivity develops and is the responsible for the highly functional organization of the thalamo-cortical loop (Jhaveri et al., 1991; Schlaggar and O'Leary, 1994). Until embryonic day 15 in mice, the cortex and the thalamus are mutually disconnected but follow a similar temporal pattern of specification of their territories. In both structures, molecular determinants pre-pattern sensory cortical areas and thalamic nuclei (Mallamaci and Stoykova, 2006; Rash and Grove, 2006; O'Leary and Sahara, 2008; Greig et al., 2016). Postnatally, cortical areas are refined by activity-dependent mechanisms through the sensory inputs (spontaneous and evoked) to form primary sensory cortical maps. Thus, although primary cortical areas are highly specialized prenatally, they can be malleable later in life, varying their position and size in function of peripheral inputs.

The aim of this Thesis work is to determine the rules by which sensory cortical territories and areas are adapted following sensory input deprivation and the re-specification events that take place in the brain, especially in the thalamus and in the cortex, when sensory inputs are lost early in life.

1. Organization of the thalamus

1.1 Origin

The thalamus was first described by Galen, who had studied at the great school of anatomy at Alexandria. Galen used the Greek word *thalamos*, comparing the human brain with the ground plan of a Greek house, with the bridal chamber at its heart. Anatomists, who first began to describe the brain in detail during the 14th century, identified the thalamus as a part of the diencephalon. Today we know that contrary to what was thought, the thalamus does not act just as a mere relay station, but has important functions in brain processing in general. The thalamus is an essential area involved in higher-order brain processing, and the regulation of states of sleep and wakefulness.

The diencephalon is divided in three areas along the longitudinal axis of the neural tube that are called prosomers (p) 1-3 (Bulfone et al., 1993; Rubenstein et al., 1994). The p3 is located in the most rostral part of the diencephalon and will rise to the prethalamus (previously known as the ventral thalamus). The p2 is the origin of the thalamus (previously known as the dorsal thalamus). Between these two prosomeres is the zona limitans intrathalamica (ZLI), which makes a boundary between the p2 and p3 (Rubenstein et al., 1994). The p1 is located more caudally to the p2 and will form the pretectum (**Figure 1**).

During the embryonic development, the process of patterning of the different brain regions requires instructive cell populations that are known as 'local organizers'. These organizers are located in the boundaries between different areas of the neural primordium and express gradients of morphogenetic signals in the adjacent tissues. The ZLI has been suggested to function as a secondary organizer for the development of the thalamus via the expression of secreted factors such as *Shh*, *Wnts* and *Fgfs* (Zeltser, 2005). The thalamus expresses *Gbx2*, *Olig3*, *Sox2*, *Ngn1* and *Ngn2* along its antero-posterior axis of the ventricular zone (VZ), which will give rise to the glutamatergic thalamic neurons (Jones and Rubenstein, 2004; Vue et al., 2007; Price, 2012). Once born, these cells migrate from the VZ towards their corresponding thalamic mantle area in order to conform the different nuclei. In the rodent, the number of GABAergic interneurons is less than 5% of the total neuronal population in each of the primary thalamic nuclei, except in the dLGN where the percentage increases up to 20-25% (Jones, 2007; Çavdar et al., 2014).

Furthermore, the origin of these dLGN GABAergic interneurons remains controversial, and at least two different origins have been suggested. One is the VZ of the prethalamus where *Otx2*-positive and *Sox14*-negative GABAergic interneurons have been localized (Jones, 2002; Golding et al., 2014). A second possible origin is the tectum, where interneurons *Gata2* and *Sox14* positive are found (Jager et al., 2016). In any case, most of the inhibition present in the thalamus is coming from the thalamic reticular nucleus (TRN) which is located in a key locus along the thalamocortical pathway. Interestingly, the TRN is composed by different sensory sectors topographically organized that convey different type of information such as auditory, gustatory, somatosensory, visceral, visual, motor and limbic. The TRN develops from the prethalamus and its development is regulated by the expression of *Mash1* and *Dlx* (Jones, 2002; Hayes et al., 2003; Jones and Rubenstein, 2004; Jones and Rubenstein, 2004; Vue et al., 2007).

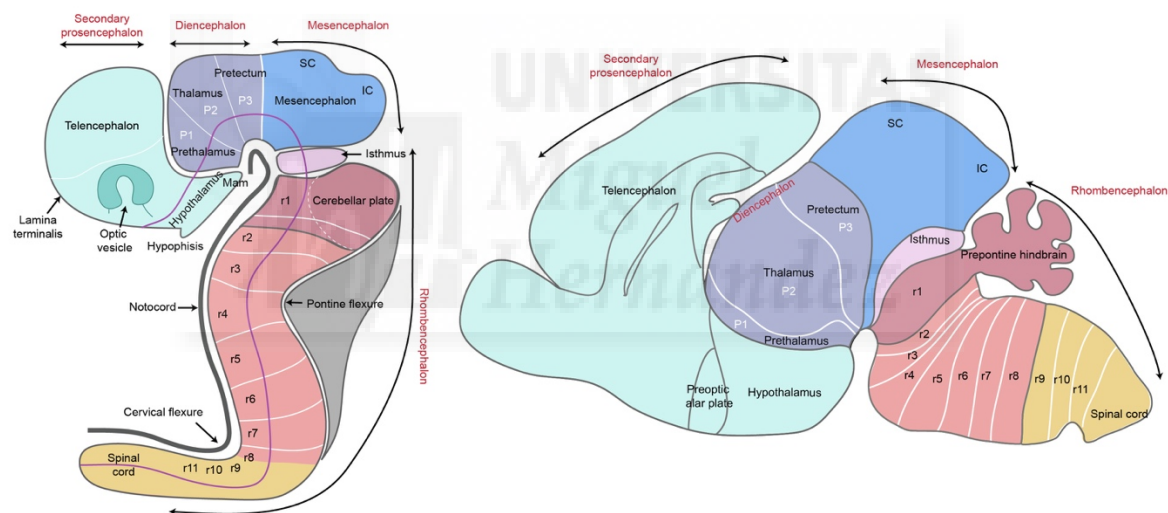


Figure 1 | A schematic diagram of the prosomeric model in an E10.5 mouse neural tube (left image) and in a P4 mouse brain (right image) in which the primary and secondary brain vesicle limits can be distinguished and the major future neural structures originated from each neuromere (Adapted from Watson et al., 2011 and from Allen Brain Atlas).

1.2 Emergence of the distinct thalamic sensory nuclei

The thalamic mantle is formed by several nuclei that are grouped in three main classes: relay, association and non-specific. Relay nuclei receive sensory and motor inputs from the periphery and project to primary sensory cortical areas. The association nuclei receive

Introduction

most of their input from primary and secondary cortical areas and project back to the cerebral cortex in the association areas where they appear to regulate neural activity. The nonspecific nuclei, project throughout the cerebral cortex, and are involved in general functions such as alerting. Sets of regulatory genes distinguish these subdivisions in the developing and adult rodent and primate thalamus (Nakagawa and O'Leary, 2001; Jones and Rubenstein, 2004), but expression occurs across multiple nuclei, in a regional rather than nucleus-specific pattern (Murray et al., 2007).

The relay nuclei of the thalamus can be divided into two orders. The first order (FO) nuclei receive input from subcortical afferents. In this thesis, I will focus on the study of visual, somatosensory and auditory FO nuclei of the thalamus. The visual thalamus, the dorsal lateral geniculate nucleus (dLGN) receive direct input from the retina, specifically from the retinal ganglion cells (RGCs) (Valverde, 1968; Godement et al., 1984; Reichova, 2004) and from the dLGN, axons go towards the primary visual cortex (V1). The somatosensory thalamus, the ventral posterior medial nucleus (VPM) receives input from the trigeminal pathway (Ralston, 1969) and from this structure, neurons target the primary somatosensory cortex (S1). The auditory thalamus, the ventral medial geniculate nucleus (MGv), receives input from the inferior colliculus (IC) (Jones and Rockel, 1971; Lee and Sherman, 2010) and targets the primary auditory cortex (A1). These three modality-specific thalamic nuclei send their axons to the Layer 4 of their corresponding cortical area (Clark, 1932; Sherman and Guillery, 2002; Guillery and Sherman, 2002) but they also project to almost all the cortical layers (Frost and Caviness, 1980). The higher order (HO) nuclei also show modality-specific segregation of their axons but their main driver input is from the cortex instead from the periphery. They form the cortico-thalamo-cortical loop of information (Sherman and Guillery, 2002; Guillery and Sherman, 2002).

Although there is an increasing knowledge about transcription factors that specify the fate of thalamic projection neurons (Nakagawa and Shimogori, 2012; Price, 2012; Song et al., 2015), the identification of specific genes that influence the emergence of the distinct thalamic structures and regions has not been addressed systematically. In a study published by our laboratory, we unravelled key transcription factors and networks that likely underlie the specification of individual sensory-modality thalamocortical connections. In this study, several genes that had a restricted expression pattern in the

principal thalamic nuclei were identified suggesting their possible role in specifying thalamocortical topographical targeting and organization (Gezelius and López-Bendito, 2016; Gezelius et al., 2017). Interestingly, a recent study has also provided evidences of the ontogenic development of the thalamic nuclei. In this study, the authors demonstrated that the progenitors from the VZ of the thalamus are divided to produce a specific cohort of neuronal cells that are already fated to a specific territory. Clones generated in the medial ventral posterior region of the thalamic VZ contributed mostly to colonize FO sensory- and motor-related nuclei, whereas clones in the anterior and medial dorsal regions contributed predominantly to HO cognitive and HO sensory- and motor-related nuclei (Shi et al., 2017). Moreover, the authors described a clonal segregation between the FO and HO sensory- and motor-related nuclei across different modalities, suggesting that the lineage relationship influences functional organization in the thalamus (Shi et al., 2017).

2. Thalamocortical and corticothalamic pathway development

During the second and third weeks of embryonic development in mice, the neocortex and the thalamus start to extend their axons to establish reciprocal connections. Thalamocortical cells start to project their axons ventrally at E12.5, before the axons from the periphery reach the thalamus, and turn laterally crossing the boundary between the diencephalon and the telencephalon (DTB) (Molnár, 1998). In the subpallium, TCAs already show a specific topographical organization (Molnár, 2012) that requires the presence and function of several molecules such as Semaphorins/Plexin, ephrins/Eph, or netrins/DCC (Molnár et al., 2012; Garel and López-Bendito, 2014; Braisted, 1999; Braisted et al., 2009).

2.1 Development of thalamocortical projections

The subpallium develops a specific group of cells named as ‘corridor cells’ that are necessary for the navigation of thalamocortical axons (TCAs) along this structure (López-Bendito et al., 2006; Uemura et al., 2007). Corridor cells are GABAergic neurons that are originated at the VZ of the lateral ganglionic eminence (LGE) and temporally allocate at the mantle of the medial ganglionic eminence (MGE) forming a passage (**Figure 2**). These

Introduction

cells form a permissive environment for the navigation of the TCAs to the cortex (López-Bendito et al., 2006) and provide gradients of axon guidance cues that are important for the topographical sorting of the TCAs (Bielle et al., 2011; Leyva-Díaz et al., 2014).

At E13.5, TCAs go through the internal capsule (IC) and corridor to arrive to the pallial-subpallial boundary (PSPB) at the entrance of the cortex. Corticothalamic axons (CTAs) leave the cortical plate and meet with the TCAs in this structure around E14.5 (Stoykova and Gruss 1994; Puelles et al., 2000; Jacobs et al., 2007; Mandai et al., 2014). The TCAs reach their proper target in their cortical region before layer 4 neurons from the primary cortices are born, and wait in the subplate compartment where they transiently connect with these cells before invading the cortical plate and it has been demonstrated that this communication is important for the correct topographic innervation of TCAs to layer 4 (Friauf and Shatz, 1991; Allendoerfer and Shatz, 1994; Catalano and Shatz, 1998; Zhou et al., 1999; Molnar and Hannan, 2000; McQuillen et al., 2002; Higashi et al., 2002; López-Bendito and Molnár, 2003; Shimogori, 2005; Hull et al., 2009; Kanold and Luhmann, 2010; Bagnall et al., 2011; Constantinople and Bruno, 2013).

Once TCAs reach the subplate, they have to enter in their appropriate cortical layer, which is progressively differentiating, to establish their final pattern of innervation. First, TCAs start to invade the lower layers of the cortex at birth, and reach the layer 4 during the first postnatal week. After this period, the axons from the thalamus start to refine to form specialized structures such as the barrels in S1 (Agmon et al., 1995; López-Bendito and Molnár, 2003; Garel and Rubenstein, 2004).

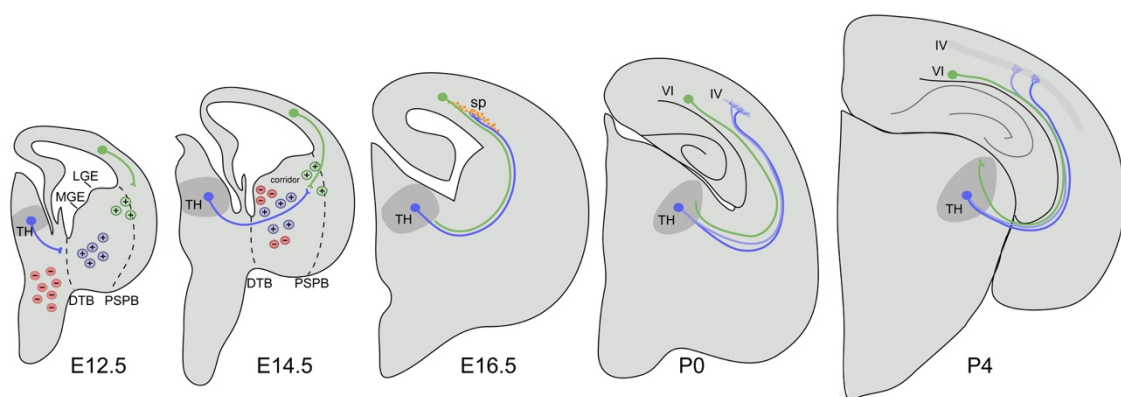


Figure 2| Thalamocortical pathway development and organization. Schematic drawing of the development of the TCA at different time points. At E12.5 the TCAs and the CTAs start to grow

towards their targets following specific pathways guided by the expression of attractive and repellent molecules. At E14.5 the TCAs have crossed the DTB and the CTAs have crossed the PSPB. The axons meet in the IC at this time point. At E16.5 the TCAs reach the subplate of the cortex and start their waiting period in this layer. At P0 the TCAs are in the layer 4 of the cortex with their terminals expanded while the CTAs are reaching the thalamus. At P4 the TCAs start to refine their terminals and the CTAs are invading the nuclei of the thalamus.

2.2 Development of corticothalamic projections

CTAs are originated from corticofugal pyramidal neurons located in cortical layer 6 and 5 (Auladell et al., 2000; Price et al., 2006; Molyneaux et al., 2007). The postmitotic cortical neurons start to migrate towards the preplate at E10.5 and to extend neurites (Bicknese et al., 1994; Noctor et al., 2004; Lickiss et al., 2012). The corticofugal neurons project ventro-laterally and reach the PSPB around E13.5 (Erzurumlu and Jhaveri, 1992; Jacobs et al., 2007). In the PSPB the CTAs wait for one day before progressing towards the thalamus through the subpallium (De Carlos and O'Leary, 1992; Molnar and Cordery, 1999) and enter the IC at E15.5 (Richards et al., 1997). This waiting period is crucial for the normal development cortico-thalamic axons (Deck et al., 2013a). Next, the CTAs arrive to the TRN where it occurs a second waiting period (Molnar and Cordery, 1999) which has still an unknown function. After reaching the reticular nucleus, these axons start to invade the thalamus at E17.5 but it will not be until postnatal stages where the CTA fully invade their proper thalamic nuclei (Miller et al., 1993; Molnar and Cordery, 1999; Jacobs et al., 2007).

Corticothalamic neurons from layer 6 project towards the FO thalamic nuclei from which they receive modality-specific input, V1 to dLGN; S1 to VPM and A1 to MGv (Guillery, 1967; Jones and Powell, 1968; Diamond et al., 1969; Hoogland et al., 1987). These CTAs form glutamatergic synapses with distal dendrites of the relay cells (Guillery, 1995; Sherman and Guillery, 1998; Rouiller and Welker, 2000; Jones, 2002) and also contact TRN cells generating an inhibitory circuit that modulates the thalamic neural activity (Jones, 2002; Guillery et al., 2003).

Layer 5 corticothalamic axons project towards the HO thalamic nuclei that receive most of their inputs from corticobulbar and corticospinal layer 5 neurons (Sherman and Guillery, 2002). Furthermore, HO neurons project to upper and lower layers of different

cortical areas allowing the cortico-cortical flux of information and integrating different cortical areas into a global network.

2.3 The first thalamo-cortical interactions

The correct development of the cortical maps requires the balanced interaction between intrinsic (gene expression) and extrinsic (input/activity-dependent signals generated spontaneously or triggered from the environment) factors. It was last century when two hypotheses were proposed to explain the process of cortical arealization and the precise innervation of TCAs to the developing cortical areas. One was the protomap hypothesis basically leaded by PasKo Rakic (Rakic, 1988) that claimed that cortical progenitor cells were specified with positional information during neurogenesis. The second hypothesis, the protocortex model, followed by Dennis O'Leary, claimed that the areal identity of cortical cells was conferred by signals extrinsic to the cortex, mainly the input from the TCAs (Van der Loos and Woolsey, 1973; O'Leary, 1989). Today it is accepted that both theories were right as the cortical arealization process is pre-patterned by the function of genetic areal determinants and secondly influenced by the arrival of input through the TCAs. Thus, TCAs would regulate the maturation and the maintenance of areal identity later prenatal and postnatally (Grove and Fukuchi-Shimogori, 2003; Arai and Pierani, 2014).

There are many studies supporting the idea that both i) intrinsic information to the cortex and ii) information from the TCAs, are necessary for the correct cortical map formation. For example, genetic manipulations of cortical determinants as deletion of *Coup-TF1*, *Emx2* or *Emx1* in the cortex, showed the aberrant development of cortical maps but the correct cortical area targeting of TCAs (Mallamaci et al., 2000; Bishop et al., 2003; Hamasaki et al., 2004; Armentano et al., 2007; Stocker and O'Leary, 2016) and the loss of *Pax6* and *Sp8* led to the expansion of the caudal V1 and the reduction of the anterior territories (Bishop et al., 2003; Zembrzycki et al., 2007; O'Leary et al., 2007). These results suggest that the specification of neocortical areas is controlled by intrinsic information in the protocortex. Moreover, several studies have shown that the TCAs have a high impact on the cortical arealization, on the size, position and molecular identity of the cortical areas during embryogenesis (Miyashita-Lin et al., 1999; Nakagawa et al., 1999; Vue et al., 2013; Garel, 2002). In these studies, the alteration of the thalamocortical

innervation did not result on early regionalization defects in the cortex, suggesting that at early stages intrinsic mechanisms are involved in the regionalization of developing cortex. Nevertheless, as the majority of these mouse models are not able to survive until postnatal stages, it remained less understood what is the impact of the TCAs in the final arrangement of the cortical areas territories and map formation. However, other studies have shown that the early manipulation of specific genes that are important for cortical arealization can cause an abnormal organization of the TCAS, indicating that TCAs also use intracortical positional information (Shimogori, 2005; Zembrzycki et al., 2013; Stocker and O'Leary, 2016). Moreover, recent evidence has shown that embryonic alterations in the development of the thalamic nuclei (such as decreased size of dLGN or ablation of VPM nucleus) results in a postnatal defect in the cortical areas size and specification of primary versus secondary sensory areas (Vue et al., 2013; Chou et al., 2013; Pouchelon et al., 2014). These results demonstrate that thalamocortical neurons have cell-intrinsic differentiation programs that initially define neuronal permissiveness to distinct inputs to then reciprocally instruct gene expression programs in their targets.

In summary, many studies have shown that cortical arealization requires multiple steps initiated during embryogenesis by morphogen release from central organizers, that postnatally will be fine-tuned by the TCAs input. Additionally, recent studies have revealed that postmitotic cortical neurons are more plastic than thought and that thalamocortical input can influence the development of cortical maps later in the postnatal life (Wimmer et al., 2010; Oberlaender et al., 2011; Yu et al., 2012; Li et al., 2013).

3. Development of Sensory Systems

3.1 General Organization

As mentioned, the cerebral cortex is parcelled into distinct anatomical and functional areas that are connected with specific thalamic nuclei (**Figure 3**). The basic structure of the sensory pathways is the following: i) the stimulus is captured by the sensory receptors located in the periphery, and ii) the information travels through specific sensory paths to the thalamus and from there to the cortex. In the visual, somatosensory and auditory cortices there is a topographical representation of the sensory periphery called retinotopy in V1, somatotopy in S1 and tonotopy in A1.

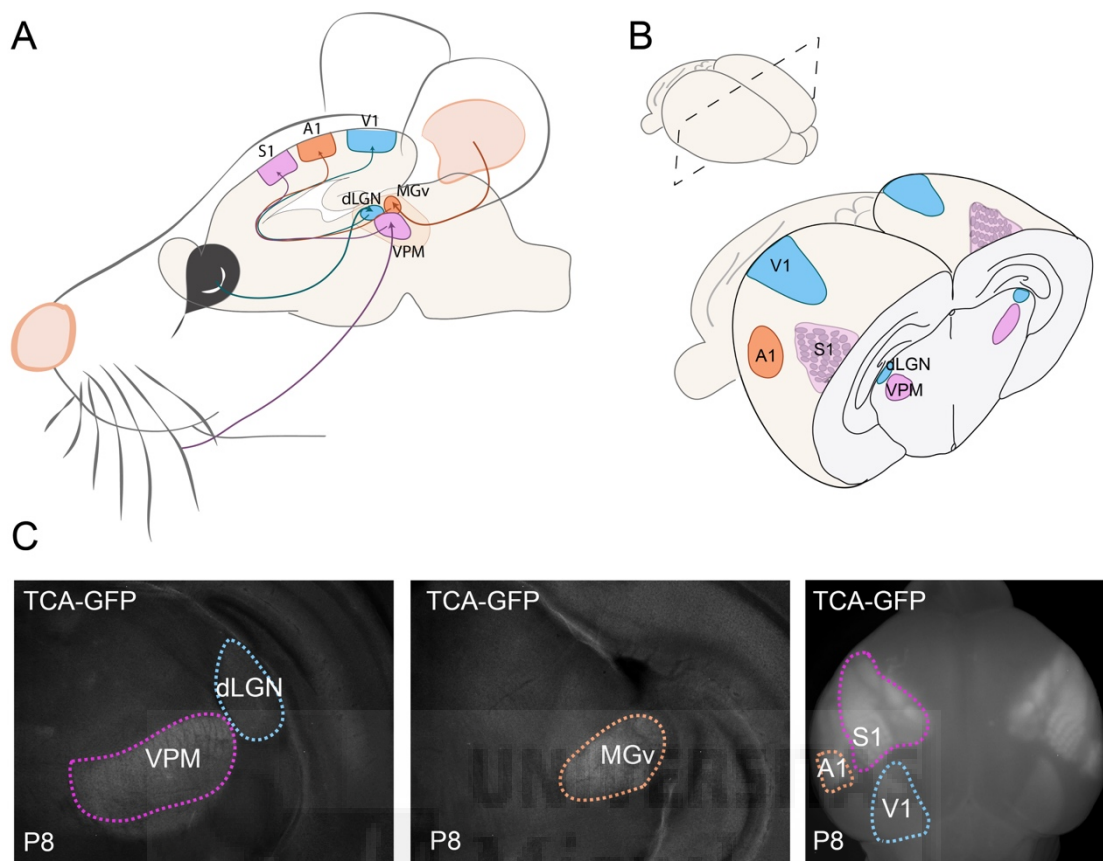


Figure 3 | Organization of the primary sensory pathways. (A) Diagram showing the organization of the peripheral axons from whiskers (violet), eyes (blue) and ear (brown) to their corresponding thalamic nuclei, VPM, dLGN and MGv, respectively. From the thalamus the axons go to cortical areas S1, V1 and A1, respectively. (B) Schema showing the rostro-caudal level at which thalamic dLGN and VPM are present and the cortical areas S1, V1 and A1. Note that MGv is not present at this level because it is found caudally. (C) TCA-GFP mouse in coronal sections (two pictures of the left) showing the dLGN, VPM and MGv. The right image is a whole brain picture of the TCA-GFP mouse showing the cortical areas V1, S1 and A1 thanks to the expression of SERT-GFP in the terminals of the TCAs.

In the thalamus, the sensory information will reach specific FO nuclei. The neurons located in each of these FO nuclei will connect layer 4 of their proper primary cortical areas. From this layer two main pathways develop. First, the intracortical communication that goes from the layer 4 to the layer 2/3 of the primary and secondary sensory areas and primary motor area. Second, the cortico-thalamo-cortical loop where

axons from the layer 4 of primary sensory areas connect to the layer 5b neurons that send axons to contact HO thalamic neurons, namely the lateral posterior (LP) for visual, the posteromedial (POm) for somatosensory and the dorsal medial geniculate (dMG) for auditory. Then, the HO nuclei project back to layer 4 neurons of the secondary areas (**Figure 4**).

This is a general but simplified version of the connectivity present across sensory systems. However, there are more pathways from the sensory cortices to other subcortical structures such layer 6a axons are sent to the FO nuclei (cortico-thalamic axons) and FO thalamic nuclei are also projecting to the layer 5b and 6 and HO towards the layer 6 (Crandall et al., 2015).

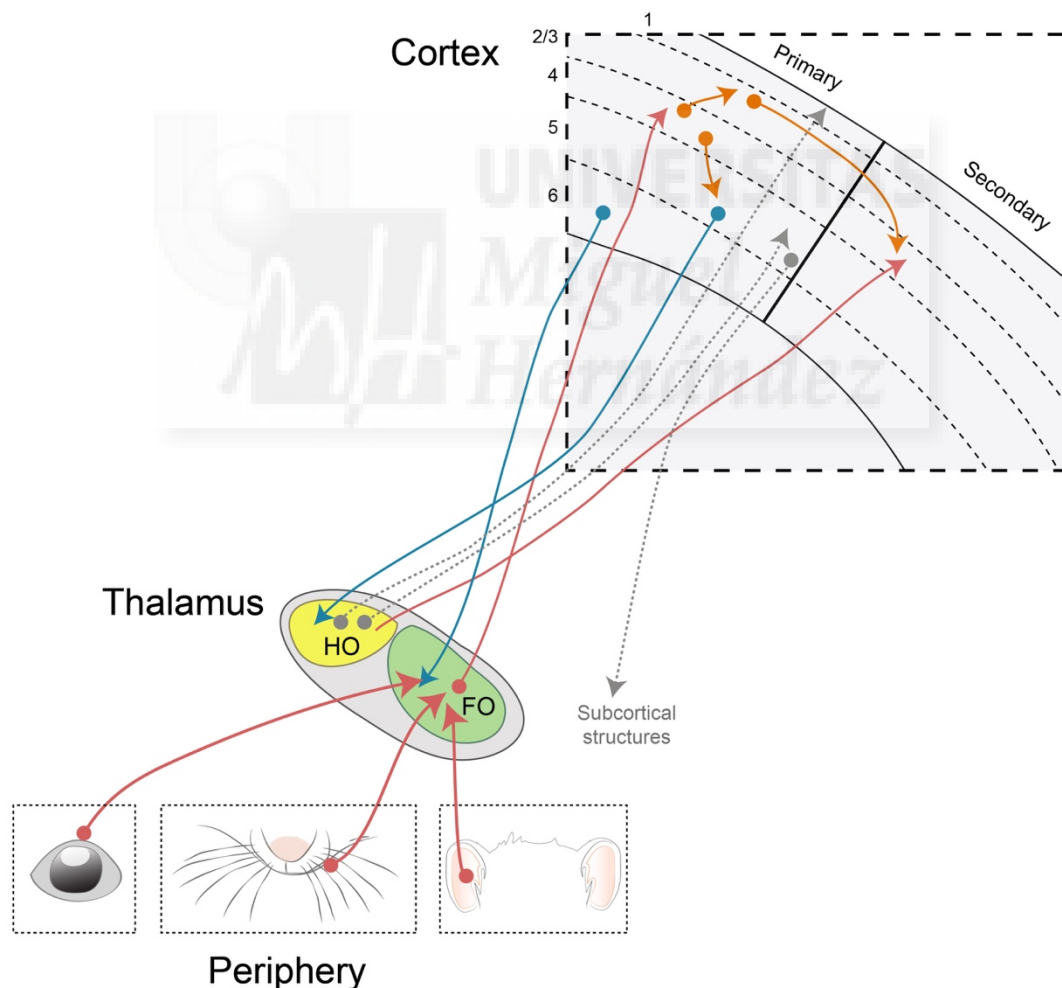


Figure 4 | Sensory pathways. Three main pathways allow the information flow in the thalamocortical connectivity. Ascending pathway from the periphery towards the FO thalamus

Introduction

and from there to the layer 4 of the cortex (in red). Intracortical pathway from layer 4 towards layer 2/3 of the primary and secondary cortical areas (orange). Cortico-thalamo-cortical loop (in blue), from layer 4 to layer 5b and from here towards HO thalamic nuclei that will project to the layer 4 of secondary areas. The cortico-thalamic projection from layer 6a towards FO nuclei in the thalamus (in blue). Other connections are present between HO nuclei to layer 1 and 5 and from layer 5 neurons towards other non-thalamic subcortical structures.

In the next section, the anatomical connectivity and developmental pattern for each sensory system will be recapitulated.

3.2 The Visual System

The retina is the peripheral structure that collects the visual information. The retina has three layers of nerve cell bodies separated by two layers of synapses. The photoreceptors, the rods and cones, are present in the back of the retina. The medial laminar layer of the retina is composed by three types of cells, the bipolar, horizontal and amacrine cells that filter, shape and transmit the signals towards the RGCs. The RGCs occupy the top of the retina and their axons pass across the surface of the retina and form the optic nerve. These neurons transmit the visual information to the central nervous system. There are among 33 types of RGCs and each of them responds to a specific aspect of the visual field. Although RGCs connect to numerous structures in the central nervous system, the dLGN and superior colliculus (SC) are their main targets. The dLGN is conveying the visual information for the image-forming pathway to the V1 and the SC is involved in the control of the head and movement of the eyes.

In mice, the RGCs start to extend their axons towards the optic chiasm at E12.5 where axons have the choice to cross or not the midline. Studies in mice with retrograde labelling injections in the eyes have shown that the contralateral and ipsilateral axons from RGCs do not overlap in the dLGN neither in the SC. This topographic organization, called eye specific segregation, is crucial for the correct representation of a binocular vision (**Figure 5**) (Godement et al., 1984; Reese, 1998; Muir-Robinson et al., 2002; Jaubert-Miazza et al., 2005). The ipsilateral RGCs are present in the ventrotemporal retina and are around 3-5% of the total amount of RGCs in rodents (Petros et al., 2008). The RGCs reach the dLGN at E15.5 and the SC at E18.5 but the ipsilateral axons arrive before

to the optic chiasm and they do not innervate dLGN until P0, suggesting the existence of a waiting period or a lower rate axonal growth compared to contralateral axons. Before P4, ipsilateral and contralateral axons overlap in the dLGN, starting to segregate and occupy their specific space, with ipsilateral projections forming a patch surrounded by contralateral axons.

Despite the eye-specific segregation in subcortical targets, the RGCs show a specific retinotopy where axons are topographically distributed (**Figure 5B**). This organization is determined by gradients of molecules, mainly from the ephrin family, that are expressed along visual pathway and indicate positional information. Retinotopic maps in retinorecipient targets are formed by two processes: i) First, axons are confined to a specific position due to the function of Eph/ephrins in their target as presented in a gradient of expression, ii) Second, RGC axons refine with the retraction of collaterals and increased branches in the correct target location.

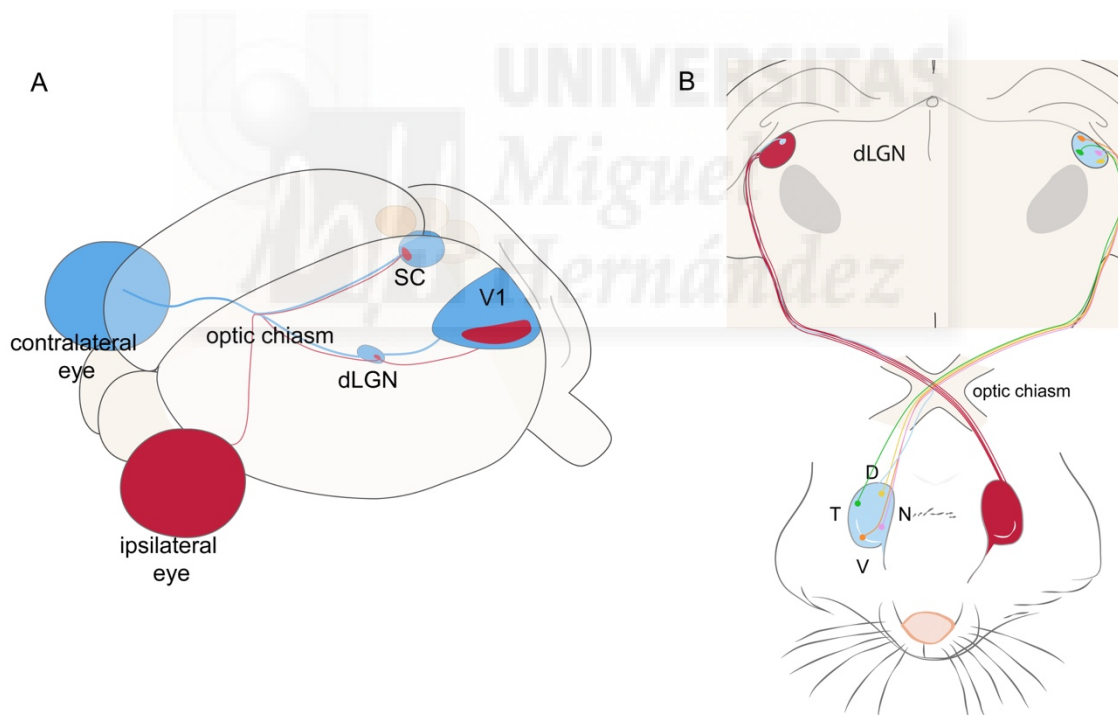


Figure 5 | Organization of the visual sensory pathway. (A). Diagram showing the organization of the peripheral axons from the contralateral eye (blue) and ipsilateral eye (red). The axons go to the optic chiasm where the contralateral axons cross towards the contralateral hemisphere and the ipsilateral axons stay in their hemisphere. Some of the axons go towards the SC and some of them are going to the dLGN that will project to the V1. Note the specific retinal segregation in all the stations. (B). Scheme showing the direction of the retinal axons towards the dLGN. The majority of the axons will cross in the optic chiasm but some persist in the same hemisphere. Note

Introduction

the specific retinotopy of the organization of the retinal axons in the dLGN. (A is adapted from Tenelle et al., 2013).

The connectivity from the RGCs to dLGN is being elucidated. At first, it was thought that one relay neuron in the dLGN receive input from 1-5 RGCs (Chen and Regehr, 2000). However, recent studies with more advanced techniques have demonstrated that there is a heterogeneous circuitry where some relay neurons in the dLGN receive inputs from 1-2 RGCs and others receive contacts from 12 up to 30 RGCs (Cruz-Martín et al., 2014; Hammer et al., 2015; Morgan et al., 2016; Litvina and Chen, 2017; Rompani et al., 2017). The novel genetic strategies to label specific RGCs populations in mice have opened new avenues to understand the retinal output pathways (Dhande et al., 2015; Roska and Meister, 2014). It has been shown by retrograde labelling from V1, that the visual primary cortex is connected with at least 8 extrastriate cortical regions (Wang and Burkhalter, 2007).

The embryonic retina develops a patterned of synchronous spontaneous activity called retinal calcium waves that have a crucial role in the development of the visual circuit and that will be extensively reviewed in the section 4.1 below.

The visual system has been widely used to unravel the mechanisms behind the experience-dependent neuronal plasticity. Many types of visual manipulations have been done in order to study the role of experience during brain development. In one hand, invasive manipulations such as eyelid suture, splitting the optic chiasm, intraocular injection of tetrodotoxin (TTX) and the complete enucleation but also non-invasive manipulations such as dark rearing from birth, dark exposure with different periods or dark-light, eye patching, exposure to specific stimulus of light, etc. The use of these different methods of visual impairment has allowed the characterization of the timing of the critical periods for ocular dominance (OD) and has helped to unravel the mechanisms behind the cortical adaptations after visual deprivation. The OD is fundamental for the correct development of the binocular vision and when it is impaired it can cause amblyopia. The monocular deprivation of one eye (MD) during the critical period, that conveys in mice from P20 –P35, produces loss of the response in the cortex connected with the deprived eye and a gain in cortical response connected with the open eye (Shatz and Stryker, 1978). These shifts in the OD are followed by changes in the thalamocortical

connections, the TCAs from to the deprived eye disappear and the axons from the intact eye are expanded (Hubel et al., 1977; Shatz and Stryker, 1978; Antonini and Stryker, 1996; Antonini et al., 1999). A normal balance between excitatory/inhibitory activities in the cortex is needed for the plasticity and the critical period onset is triggered by the maturation of cortical inhibitory circuits (del Rio et al., 1994; Hensch, 2005; Fagiolini and Hensch, 2000; Fu et al., 2015; Cichon and Gan, 2015).

As aforementioned, the layer 6 corticothalamic axons from V1 project to the dLGN and although they reach the thalamus at P0 they do not invade this structure until P6 (Grant et al., 2012; Seabrook et al., 2013). In a recent publication, it has been shown that when retinal input is lost in mice at P0, these corticothalamic axons innervate the dLGN earlier. Moreover, in this model, layer 5b axons that normally project to HO nuclei of the thalamus, they invade FO nuclei. Furthermore, blocking the spontaneous retinal waves with epibatidine leads to similar results indicating that activity feeds a forward mechanism that controls the identity towards a FO in the presence of activity or towards HO in its absence (Grant et al., 2016). However, the role of the thalamic spontaneous activity in driving these changes has not been tested yet.

3.3 The Somatosensory System

The somatosensory system is one of the most behaviourally important sensory systems in rodents. The majority of the somatosensory information in mice comes from the facial whiskers on the snout. The sensory input from the whiskers goes through the trigeminal nerve to reach the trigeminal nucleus. Each whisker has a specific representation in the ipsilateral principal trigeminal nucleus in the brainstem (PrV) named barrelete (Ma and Woolsey, 1984). Then, these axons cross the midline around E11.5 and elongate rostrally towards the contralateral thalamus reaching the VPM nucleus at E17.5. At this structure, trigeminal axon terminals arborize and refine to form the specific organization of the barreloids around P2-P3 in mice (Kivrak and Erzurumlu, 2012). Finally, the TCAs from the VPM will form the barrels in the layer 4 of S1 around P4-P5 (**Figure 6**) (Van der Loos and Woolsey, 1973). Functionally, the stimulation of a single whisker leads to an activation of a single barrel.

The barrel cortex is composed by five rows of barrels and each barrel is comprised by two main components: i) the TCAs terminals from VPM neurons that occupy the

centre or the “hollow” of the barrels, and ii) the layer 4 granule cells that form the “walls” of the barrels by orienting their dendrites towards the hollow (Killackey HP, 1973; Jensen KF, Killackey HP, 1987; Pasternak and Woolsey, 1975; Simons et al., 1984). Barrels in layer 4 of S1 start to be present around P4 as TCAs start to refine and the terminals that are not confined to one barrel are eliminated. At the same time the neurons from the layer 4 of the S1 start to surround the barrels (Rice et al., 1985).

As mentioned above, during perinatal stages TCAs establish functional contacts with subplate neurons and these interactions seem to be crucial for topographic sorting of the TCAs (Hull et al., 2009; Bagnall et al., 2011; Garel and López-Bendito, 2014; Friauf and Shatz, 1991; Higashi et al., 2002; Kanold and Luhmann, 2010; Constantinople and Bruno, 2013). However, there are evidences that specific genes in the subplate and in the cortical plate such as *Fgf8* (Fukuchi-Shimogori, 2001; Shimogori, 2005) or layer 4/VPM gene gradients such as Ephrins can regulate the specific topographic map of the TCAs in S1.

The barrel cortex has been widely used to study the mechanisms involved in the development and plasticity of cortical maps. Sectioning the infraorbital nerve (ION) or removing a row of whiskers during the first postnatal week impairs the clustering of TCAs in layer 4 and the loss of barrels (Van der Loos and Woolsey, 1973; Weller and Johnson, 1975; Killackey et al., 1976). Moreover, the activity from the TCAs and/or the periphery is also necessary to generate a correct barrel-field in S1 (Jensen and Killackey, 1987; Fox et al., 1996). Along this line, in the study published by our laboratory that is the core of this thesis, we have characterized a mechanism important for the development of the barrel cortex that is also present in plasticity processes in the barrel-field that occur after early enucleations. This mechanism involves spontaneous thalamic activity, in terms of calcium waves, and trigger an experience-independent expansion of the barrel field in the blind mice (Moreno-Juan et al., 2017). Other activity-dependent molecules have been implicated in the development of the somatosensory map in S1, as the correct function of the NMDA receptors (NMDAR) (Fox et al., 1996; Mitrovic et al., 1996), that will also be reviewed in detailed in the section 4.2 below.

The impact of the correct targeting of TCAs to specify the development of the sensory-related pattern and underlying circuitry in S1 has begun to be understood. Recently, a study in which the VPM nucleus of the thalamus was ablated from embryonic

life has shown a remarkable rewiring capabilities within the S1 circuitry. The axons from the HO somatosensory thalamic nucleus, the POM, rewire and project to layer 4 neurons in S1 which change their transcriptional programs toward a layer 4 identity of the S2 (Pouchelon et al., 2014). The results suggest that afferent input can define the target fate identity which is in turn malleable. This is also the case for other subcortical stations, such as the thalamus. After ION section, the VPM somatosensory nucleus transcriptionally switches to resemble a HO POM nucleus (Frangeul et al., 2016).

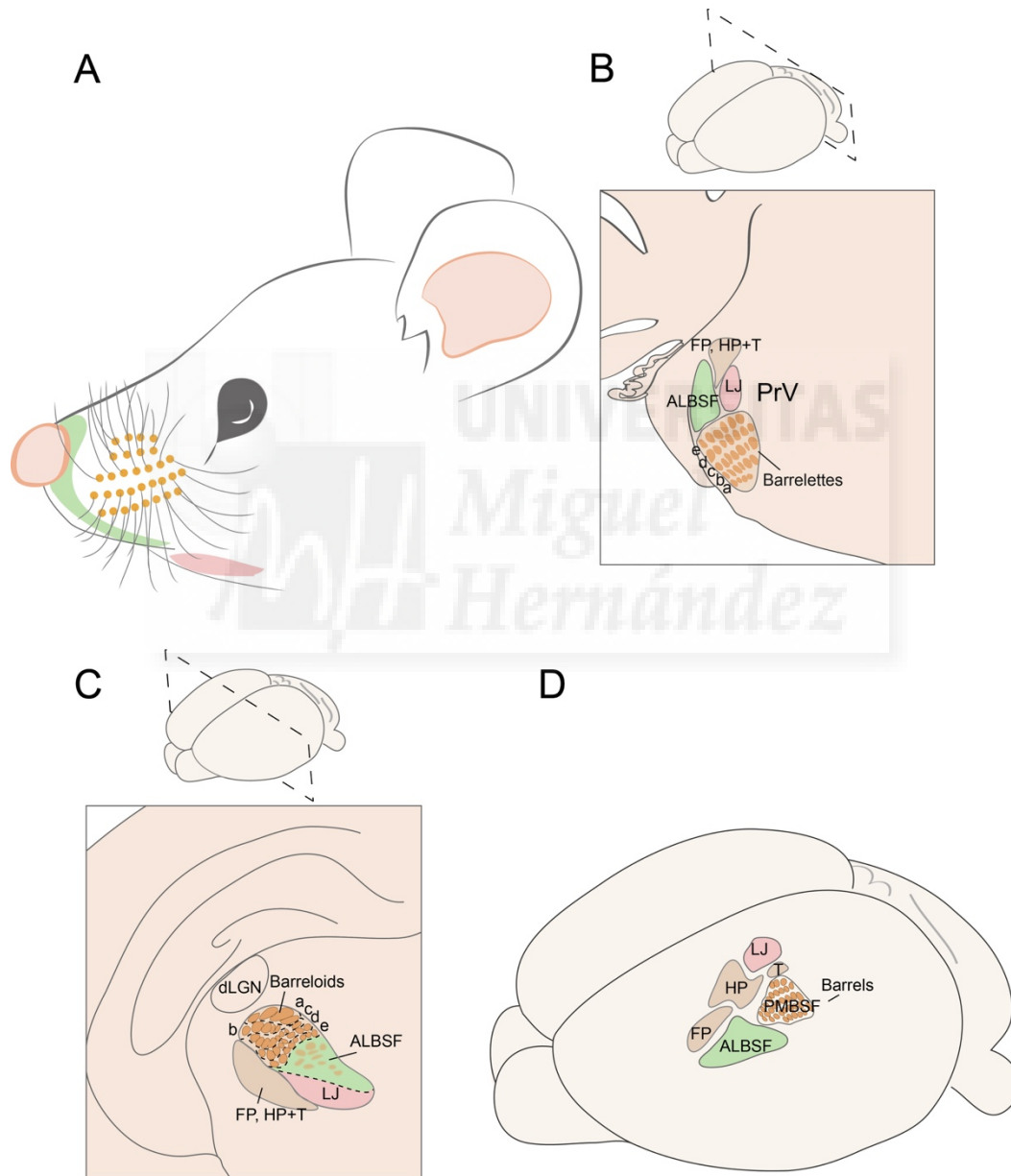


Figure 6 | Organization of the somatosensory sensory pathway. Diagram showing the somatosensory mouse pathway, which transfers information from the whiskers to the S1. (A)

Whiskers located on the face surface of the mouse organized into five rows. Along the pathway the whiskers are represented in a topographic manner in the PrV nucleus of the brainstem (**B**), in the VPM nucleus of the thalamus (**C**) and finally in the S1 (**D**).

3.4 The Auditory System

The auditory system is composed by a complex circuitry that starts from the middle ear where the collection of the sound occurs at the auricle. The middle ear contains the small ossicles, the malleus, the incus and the stapes. The vibrations produced by the sound in the middle ear are transmitted to the cochlea. The cochlea is located in the inner ear and generates fluid movements that activate sensory cells that transduce the mechanical energy of sound into electrical signals. Hearing involves the epithelium, known as organ of Corti (OC) which is located in the cochlea. The cochlea is composed by the inner hair cells (IHCs) that detect the auditory stimuli and the outer hair cells (OHCs) that amplify the low-level sounds by increasing the amplitude and the frequency selectivity of basilar membrane vibrations (Ashmore et al., 2010). The auditory signal is detected by the hair cells which receive afferent innervation from spiral ganglion neurons (SGNs) (Kiang et al., 1982) and efferent innervation from the superior olivary complex (SOC) (Strutz, 1981; Liberman and Brown, 1986). In the adult organ of Corti, the IHCs are the principal encoder of the auditory signal and one IHC is connected by multiple type I SGNs (Meyer et al., 2009). Although there are more OHCs than IHCs, their connectivity is much more restricted. Type II of SGNs connect with OHCs and these connections are thought to modulate cochlear sensitivity and drive the olivocochlear efferent reflex, which is important for the adjustment of hearing sensitivity and frequency selectivity (Berglund and Ryugo, 1987; Jagger, 2003; Thiers et al., 2008; Froud et al., 2015).

The cochlea shows a topographically organization along its longitudinal axis. The cells located in the basal portion of the cochlea respond to high frequency sounds, while the cells located in the apex respond to low frequencies. This topographic organization is present in the entire auditory pathway and it is called tonotopy (Mann and Kelley, 2011). It has been proposed that gradients of signal molecules might be under the regulation of the establishment of the tonotopy in the hair cells.

In mice, the cochlear duct starts to form at E11.5 and elongates to over two complete turns at P15. The organ of Corti can be distinguished at E16.5, the postnatal

maturation which allow the opening of the tunnel of the Corti organ and the distance between the IHCs and the OHCs increase (Lim and Anniko, 1985; Kelley et al., 1995; Lim and Kalinec, 1998; Kopecky et al., 2012). At E18.5 the IHCs and OHCs are differentiating and use lateral inhibition by notch signalling to prevent neighbouring precursor cells to become hair cells. In mice, at P0 the cochlea has the entire number of turns but is still not mature. Mice can hear around P12 when the cochlear nerve fibers innervate single IHCs preserving the tonotopic map of the cochlear duct (Yu et al., 2014).

The auditory information goes through the vestibulocochlear 8th cranial nerve to the cochlear nucleus (CN) in the brainstem. Then, the auditory information travels through the main auditory pathway to the lateral lemniscus (LL), the inferior colliculus (IC) in the midbrain, the medial geniculate nucleus (MGN) in the thalamus and to the auditory cortex (Willott, 2001). Moreover, there is other pathway from the CN that goes to the SOC and is important for the correct spatial sound localization.

4. Activity-dependent mechanisms in the thalamocortical development

The presence of spontaneous activity has been described in different sensory systems as visual, auditory, somatosensory and olfactory circuits. Prior to sensory experience, genetic factors act together with spontaneous activity in order to build correct functional networks. However, the relationship between these two factors is just started to be determined. Moreover, and thanks to the development of new technical approaches, the role of spontaneous neuronal activity *in vivo* can, for the first time, be accurately measured and studied. For example, calcium imaging in the mouse visual system *in vivo*, recording in the SC and in V1 simultaneously, has shown that the properties of the calcium waves in these two structures are similar, demonstrating that spontaneous calcium waves can convey information about the spatial properties from the retina to the visual cortex (Ackman et al., 2012). Moreover, *in vivo* experiments in ferrets have shown that increasing the frequency of spontaneous activity in the retina by pharmacological approaches between P15 and P25 animals, accelerates the normal refinement of the dLGN receptive fields (Davis et al., 2015).

However, it is still not known how thalamic and cortical neurons communicate during early stages. As was mentioned above, there are evidences suggesting that subplate neurons are implicated in the generation of cortical oscillatory patterns before the onset

of the sensory experience (Myers, 2003; Kanold and Luhmann, 2010; Hoerder-Suabedissen and Molnár, 2015). These studies suggest that spontaneous electrical activity might function as a messenger carrying topographic information and facilitating the formation of sensory maps. Furthermore, during TCA development, the spontaneous activity of thalamic neurons also contributes to control axonal growth rate. Studies by our group have shown that somatic spontaneous calcium spikes in the thalamic neurons regulate the speed of growth of TCAs. This regulation is mediated by activity-dependent gene regulation of receptors such as *Robo1* or *Dcc* that act as a brake or as an accelerator, respectively (Mire et al., 2012; Castillo-Paterna et al., 2015). These publications demonstrate that spontaneous thalamic activity intrinsically modulates the rate of axons extension in the thalamocortical system and thus contribute to show another example of a wider function of spontaneous activity in early brain development.

Subcortical neuronal activity can also influence the proper formation of cortical maps. A paradigm for investigating the role of afferent input and their pattern of electrical activity in the development of cortical circuitry and function is to perform sensory deprivation that provokes a rewiring of the afferents that carry information about one sensory modality to central targets and pathways that normally process a different sensory modality. These manipulations causes adaptive reorganization of neurons to integrate the function of two or more sensory systems. Such a neuroplastic phenomenon is called “**cross-modal plasticity**” which I will describe more in detail.

4.1 Role of spontaneous activity in the development of the visual system

In the retina, spontaneous neural activity is present before visual experience, predominantly in the form of calcium waves and this activity is propagated towards the subsequent visual relay stations: dLGN, SC and V1 (Ackman et al., 2012; Siegel et al., 2012). It has been demonstrated that this activity is important for the final refinement of the visual circuits as contains retinal spatial and temporal information (Ackman et al., 2012). There are three forms of spontaneous calcium waves in the retina. The embryonic stage I is mediated by the presence of gap-junction coupled waves. These waves mature towards the stage II from P0 where they are mediated by cholinergic transmission and it is present. The last stage, the stage III is mediated by glutamatergic transmission (Firth et al., 2005).

Different experimental approaches have demonstrated the role of the retinal waves in the development of the visual system, such as disturbing the eye-specific segregation in the dLGN of cats by blocking retinal waves *in vitro* by TTX administration that inhibits the firing action potentials and their propagation (Shatz and Stryker, 1988). Other experiments have narrowed the specificity of the blockage of retinal waves by the administration of epibatidine which inhibits a nicotinic receptor or the use of a transgenic mice lacking the beta2-acetylcholine receptor (β 2-AChR). In both cases the specific-eye segregation in the dLGN of ferrets and mice is severely impaired (Penn et al., 1998; Rossi et al., 2001; Rebsam et al., 2009). Interestingly, these defects can be rescued by the developmental program of the calcium waves that switches from type to type (Huberman et al., 2002; Grubb et al., 2003). Thus, retinal waves are crucial phenomenon indispensable for the normal specific-eye segregation, specific map formation and specific retinotopy.

4.2 Role of spontaneous activity in the somatosensory system development

As mentioned above, in each of the somatosensory station, the somatosensory information is drawn in a precise anatomical organization of the whisker map (Killackey et al., 1995; Sehara and Kawasaki, 2011). Early manipulations of the periphery before the presence of the barrels have been widely used to determine the mechanisms involved in barrel-map formation. Pioneer studies in the '70s through the sectioning of the ION or damaging the whiskers follicles demonstrated that peripheral input is needed to cluster thalamocortical axon terminals in layer 4 (Van der Loos and Woolsey, 1973; Weller and Johnson, 1975; Killackey et al., 1976). Many studies have then shown that spontaneous activity regulates many physiological processes that include the formation and refinement of cortical topographic maps (Spitzer, 2006; Luhmann, 2017). However, it has remained controversial to understand whether the peripheral input or the spontaneous neural activity is the important regulator in the barrel map formation. During the development of the somatosensory thalamocortical system, the role of early spontaneous activity has been demonstrated and it is more evident that synchronous activity is regulating different processes during early stages of sensory system development (Hanganu-Opatz, 2010; Kilb et al., 2011; Luhmann et al., 2016). Moreover, during early postnatal development spontaneous cortical activity is necessary for the formation of functional pre-columns (Golshani et al., 2009; Yang et al., 2013) and this activity depends on an intact subplate

Introduction

(Dupont et al., 2005; Hanganu et al., 2009). The elimination of the spontaneous and sensory-evoked spindle bursts in the subplate cells disrupts the correct barrel map formation, indicating that spontaneous activity involving the subplate circuitry influence the development of the cortical maps (Tolner et al., 2012).

The majority of the somatosensory spontaneous cortical spindle bursts are not generated within S1. *In vivo* simultaneous recording of S1 and VPM in P0-P1 rats have shown that when a VPM lesion is performed, the response in the S1 by whisker stimulation is blocked and the cortical spontaneous events are remarkably reduced (Yang et al., 2013). Furthermore, silencing the whisker pad with lidocaine, has a great impact in the spontaneous spindle burst activity in S1 which is severely reduced, suggesting that during this period, cortical spontaneous activity in the somatosensory cortex is related to the sensory periphery (Yang et al., 2013).

In the last decades, several studies have been done trying to identify the presynaptic vs postsynaptic activity-dependent mechanisms involved in barrel-map formation. The manipulation of genes such as adenylyl cyclase 1 (AC1), NMDAR1, metabotropic glutamate receptor 5, phospholipase C- beta1, cAMP-dependent protein kinase type II regulatory subunit, monoamine oxidase A or sodium-dependent 5-HT transporter cause aberrant barrel map organization (Li et al., 1994; Cases et al., 1996; Iwasato et al., 1997; Abdel-Majid et al., 1998; Hannan et al., 2001; Persico et al., 2001; Salichon et al., 2001; Lu et al., 2003; Rudhard et al., 2003; Gheorghita et al., 2006; Inan, 2006; Lu, 2006; Watson, 2006; Wijetunge et al., 2008; She et al., 2009). Although these studies identified genes important for barrel map formation, the somatosensory topography is not just restricted to the cortex and aberrant maps in subcortical structures can also lead to defects in cortical barrel map formation.

Selective ablation of genes in specific compartments of the somatosensory structures can better contribute to determine the place of action of these proteins in barrel map formation. In mice mutants for NR1 or NR2B subunit of NMDARs or mGluR5 in layer 4 neurons, or loss of AC1 in the cortex, revealed that postsynaptic defects have cell-autonomous regulation in the barrel cortex (Iwasato et al., 2008; Espinosa et al., 2009; Mizuno et al., 2014; Ballester-Rosado et al., 2016). On the other hand, perturbations of the presynaptic activity, such as ablating the vesicular glutamate transporter 1 and 2 (vGlut1 and vGlut2) in the TCAs, have stronger phenotypes in barrel map formation (Li

et al., 2013). Our group has recently published a publication reviewing the state of the art and current knowledge on the thalamocortical pre- and postsynaptic elements involved in the organization of the barrel cortex, including activity-dependent mechanisms. Altogether, the results recapitulated in this review clearly support a central role of neural activity on barrel map formation (Martini et al., 2017).

Concluding, the emergence of the somatotopy barrel map formation in S1 involves intrinsic and extrinsic features. It has been widely studied the role of the input influence in the barrel map formation by the use of specific manipulation of gene expression and neuronal activity. However, the role of the subcortical regions in the somatosensory development such as the thalamus is still not well defined.

4.3 Role of spontaneous activity in the auditory system development

The auditory system establishes initial connections early in development and can convey information from the periphery well before the auditory sensory onset. During the first postnatal weeks, before the auditory sensory onset in mice, IHCs can be depolarized and triggers bursts of calcium spikes that induce glutamate release in SGNs. These calcium spikes triggers bursts of action potentials in the SGNs that are transmitted to the auditory pathway and can promote neuronal survival, synapses maturation and the refinement of the connections (Sanes et al., 1992; Sanes and Takacs, 1993; Gabriele et al., 2000; Leake et al., 2002; Kim and Kandler, 2003) that can modulate the tonotopic segregation (Friauf and Lohmann, 1999; Rubel and Fritzsche, 2002; Kandler et al., 2009). However, the role of spontaneous activity in auditory development is still unclear due to the limitation of the existence of models that allow the specific manipulation of the spontaneous activity in the cochlea and more *in vivo*.

Studies done by cochlear ablation, injection of ototoxic drugs and using transgenic models of deafness, have been used to study the role of peripheral damage in the auditory pathway development. However, these models also produce a degeneration of the afferent fibers and the level of spontaneous activity before the auditory onset has not been examined (Youssoufian et al., 2008) so, phenotypes found in later stages are not clearly due by the loss of sound-evoked activity and/or the loss of previous spontaneous activity. Furthermore, mutant models without auditory input mimicking the deafness, may affect also brainstem cells (Schug et al., 2006; Noh et al., 2010; Hirtz et al., 2011). Elegant studies

Introduction

with deprivation of excitatory input in SGNs, cochlear removal, degeneration of the IHCs or using transgenic models with impaired calcium-dependent glutamate release in the IHCs, lead to degeneration of the SGNs and neurons in the cochlear nuclei (Hashisaki and Rubel, 1989; Mostafapour et al., 2000; Hirtz et al., 2011). In the auditory system there is also a critical period for IHCs degeneration, when manipulation of the cochlea is done after the hearing onset, no degeneration is present in the IHCs whereas when the cochlear ablation is done before the auditory experience, severe neuronal loss is present (Hashisaki and Rubel, 1989; Tierney et al., 1997; Mostafapour et al., 2000). Cochlea ablation before the onset of hearing impairs the developmental decrease of intracellular Cl⁻ in auditory neurons (Shibata et al., 2004). This misbalance disrupts inhibition of neurons in lateral superior olive and in the IC (Kotak and Sanes, 1996; Vale and Sanes, 2000; 2002; Vale et al., 2003). In a transgenic mouse model congenitally deaf, *dn/dn*, the firing properties and channel expression of lateral superior olive neurons is also altered (Couchman et al., 2011; Hirtz et al., 2011). These results suggest that lack of peripheral activity disrupts the physiological maturation of auditory system.

Moreover, it has been shown that spontaneous activity in the auditory system during development is responsible of refine synapses in brainstem neurons. In congenitally deaf mice *dn/dn*, the synaptic strength is enhanced, suggesting that spontaneous activity promote functional elimination of synapses in physiological conditions (Oleskevich and Walmsley, 2002; Oleskevich et al., 2004; McKay and Oleskevich, 2007).

There are evidences claiming that spontaneous activity in the auditory system before the hearing onset helps to the correct development of the auditory pathway. It has been shown in cochlear-ablated gerbils, that the loss of the peripheral input triggers anatomical changes in the pathway as it leads to ectopic connections between cochlear nucleus to superior olive and IC (Russell and Moore, 1995). Moreover, cochlear ablation in rats during early postnatal stages leads to an impaired formation of innervation from the dorsal nucleus of lateral lemniscus to the IC (Gabriele et al., 2000; Franklin et al., 2006; 2008). Additionally, it has been shown in mice that lack cholinergic inhibition of IHCs that changes in burst firing patterns provoke defects in the axonal pruning and tonotopic refinement (Clause et al., 2014), suggesting that the precise patterns of activity can influence the segregation of auditory inputs.

5. Sensory system cross-talk: the cross-modal plasticity

The functional architecture of the brain is strongly influenced by sensory inputs. The changes in the patterns of stimuli provoke adaptive responses of neural networks giving rise to the emergence of plasticity. As we mentioned in the last sections, a paradigm extensively used to unravel the role of the afferent input in the development of the cortical maps, is the deprivation of one sensory modality. This deprivation has strong effects not only in the development of its own architecture but also in the development of the rest of the sensory modalities. This neuroplastic phenomenon is known as “cross-modal plasticity”. The study of the cross-modal plasticity and the deciphering of the functional rearrangement that occurs in the brain after sensory deprivation has widely used over the past 30 years to understand the role of intrinsic and extrinsic mechanisms involved in cortical development. However, the identity of the brain regions that are changed, the exact mechanisms that underlie cross-modal plasticity and the neural basis of behavioural compensation remain largely unknown.

Schneider and Frost originally developed the cross-modal plasticity paradigm in the ‘70s. In their work, the authors showed that neonatal lesions of specific subcortical structures in hamsters could cause the ectopic innervation of retinal axons of targets that they do not normally innervate (Schneider, 1973; Frost and Schneider, 1979). Since then, cross-modal plasticity has been investigated in several animal models. For example, it was published that in frogs, cutting the optic nerve and regenerating into the telencephalon results in a functional retinal projection into the olfactory lobe (Rebillard et al., 1977; Scalia et al., 1995). Moreover, in previous studies it has been reported that the primary auditory cortex can be driven by visual stimuli in congenitally deaf cats (Rebillard et al., 1977).

One of the most useful animal models to study the cross-modal plasticity is the ferret. The ferret presents highly organized visual pathway and interestingly, is born at a very premature stage of development, thus, sensory-manipulations can be done postnatally while circuits are still immature and developing, mimicking an embryonic manipulation in other animal models. Studies performed by bilateral and unilateral lesion of the IC and SC in ferret (Sur et al., 1990; Angelucci et al., 1997; 1998) provoke the deafferentiation of the MGN and the visual information is provided indirectly to the

auditory cortex. This new visual projection from MGN to A1 is functional and carries visual information (Roe et al., 1990; Sur et al., 1990). A hypothesis formulated to explain such a phenomenon of rewiring connectivity, is that visual input is relayed from the MGN to the A1 via TCAs whose physical identity is unchanged but that provide spatiotemporal patterns of electrical activity to auditory cortex that are very different from normal. Thus, if A1 receives visual input during development, it acquires visual organization and specific changes in cortical circuits.

In humans, it has been reported the presence of the cross-modal plasticity among different sensory modalities following sensory input loss. For example, in individuals with cochlear implants, visual cortical areas are recruited by auditory learning processing. This result indicates that there must be a link between the adaptations in the intact modality and the deprived one. Also, studies in deaf and blind humans showed compensatory adaptations among the spared and the affected sensory systems. In fact, in congenitally blind individuals showed auditory and olfactory-enhanced capabilities compared with sight people (Lessard et al., 1998; Roder et al., 1999; Leclerc et al., 2000; Voss et al., 2004; Araneda et al., 2017). Moreover, the posterior visual areas can be activated by somatosensory inputs in the blind and in the deaf, the auditory cortex can be activated by somatosensory or visual inputs (Levanen and Hamdorf, 2001; Bavelier and Neville, 2002). Interestingly, a few studies have shown that training or spatial attention can produce the recruitment of the areas that are adapted cross-modally in blind or deaf individuals. The reorganization in these cases is produced in the multimodal areas that can be malleable even without a sensory loss (Buchel et al., 1998; Calvert, 2001; Macaluso et al., 2001; Shams et al., 2001).

5.1 Experience-independence of cross-modal plasticity

Despite the fact that the barrel cortex shows intramodal plasticity (when one whisker is removed, the barrel decreases or disappear and the spared barrels are enlarged), it can be cross-modally expanded when visual deprivation is produced early in life. The classical studies on cross-modal plasticity have hypothesized that these cortical adaptations after sensory loss are due by the increased experience-dependent neural activity of the intact sensory systems during the postnatal life (Bronchti et al., 1992; Rauschecker et al., 1992; Toldi et al., 1994; Zheng and Purves, 1995; Toldi et al., 1996).

Nevertheless, the findings of an experience-dependent mechanism for cross-modal plasticity cannot explain the cross-modal adaptations found before the onset of sensory experience.

Deprivation of the visual periphery causes a decrease in the size of V1 and any map representations. Recent studies have shown some of these plastic adaptations are present well before the sensory active experience. For example, in enucleated mice at P0, the expression pattern of genes that are involved in cortical arealization occurs before the mice start to use actively the senses (Dye et al., 2012). Furthermore, in rats enucleated at birth there is a cross-modal increase in the barrel-field size before the active sensory whisking (Fetter-Pruneda et al., 2013; Abbott et al., 2015). These sensory-independent mechanisms of plasticity might require forms of spontaneous activity as aforementioned, as it can modulate the formation of cortical maps before sensory experience starts (Espinosa and Stryker, 2012; Huberman et al., 2006). Along this line, our group has recently found that the thalamus influences sensory cortical areas size prior to sensory experience (Moreno-Juan et al., 2017). Thus, the peripheral and central brain structures have an important role on modulating the size of cortical areas and territories within a given or across several sensory systems before sensory experience. Altogether these studies open the hypothesis that the changes in the somatosensory cortex after visual deprivation are due by shifts in the developmental programs of sensory systems development and are fully due to increased levels of experience-dependent neuronal activity. However, the mechanisms underlying the possible communication among different sensory systems are still poorly explored.

It is clear that the cross-modal plasticity requires cross-talk among different sensory modalities and a putative scenario for this inter-modality communication is the thalamus – as it is where sensory input converge before reaching the cortex. In the work presented in this thesis, we have found that embryonic enucleations in mice provoke an increase of the barrel size at P4, along with changes in the spontaneous activity of different thalamic nuclei and changes in gene expression in the thalamus (Moreno-Juan et al., 2017). Thalamic calcium waves are coordinating input-specific gene expression patterns influencing the size of primary cortical areas during development prior to sensory experience. With this work, the thalamus emerges as a key brain structure to play a pivotal

Introduction

role in this early cortical plasticity and therefore, as a potential target for therapeutic interventions.

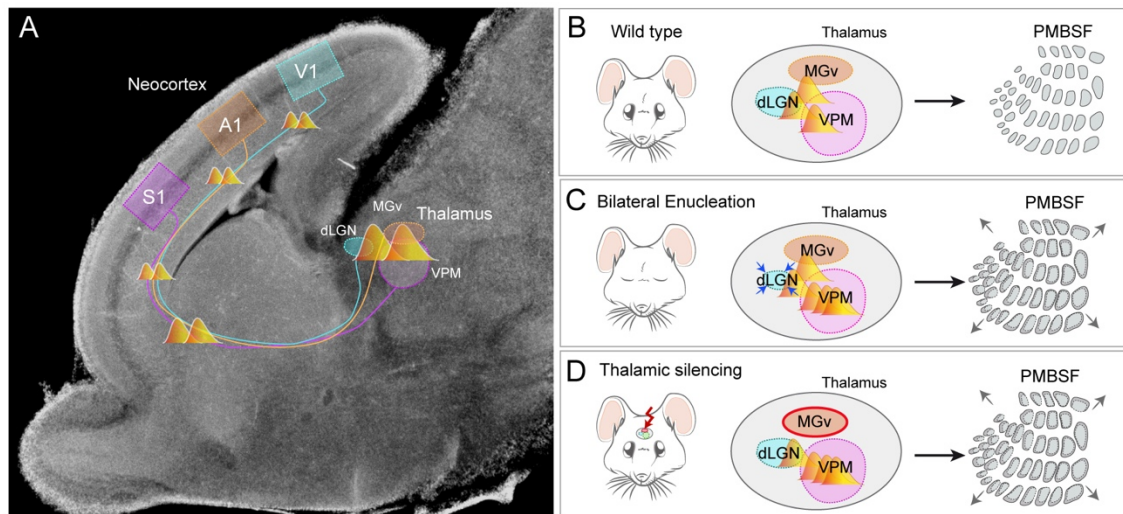
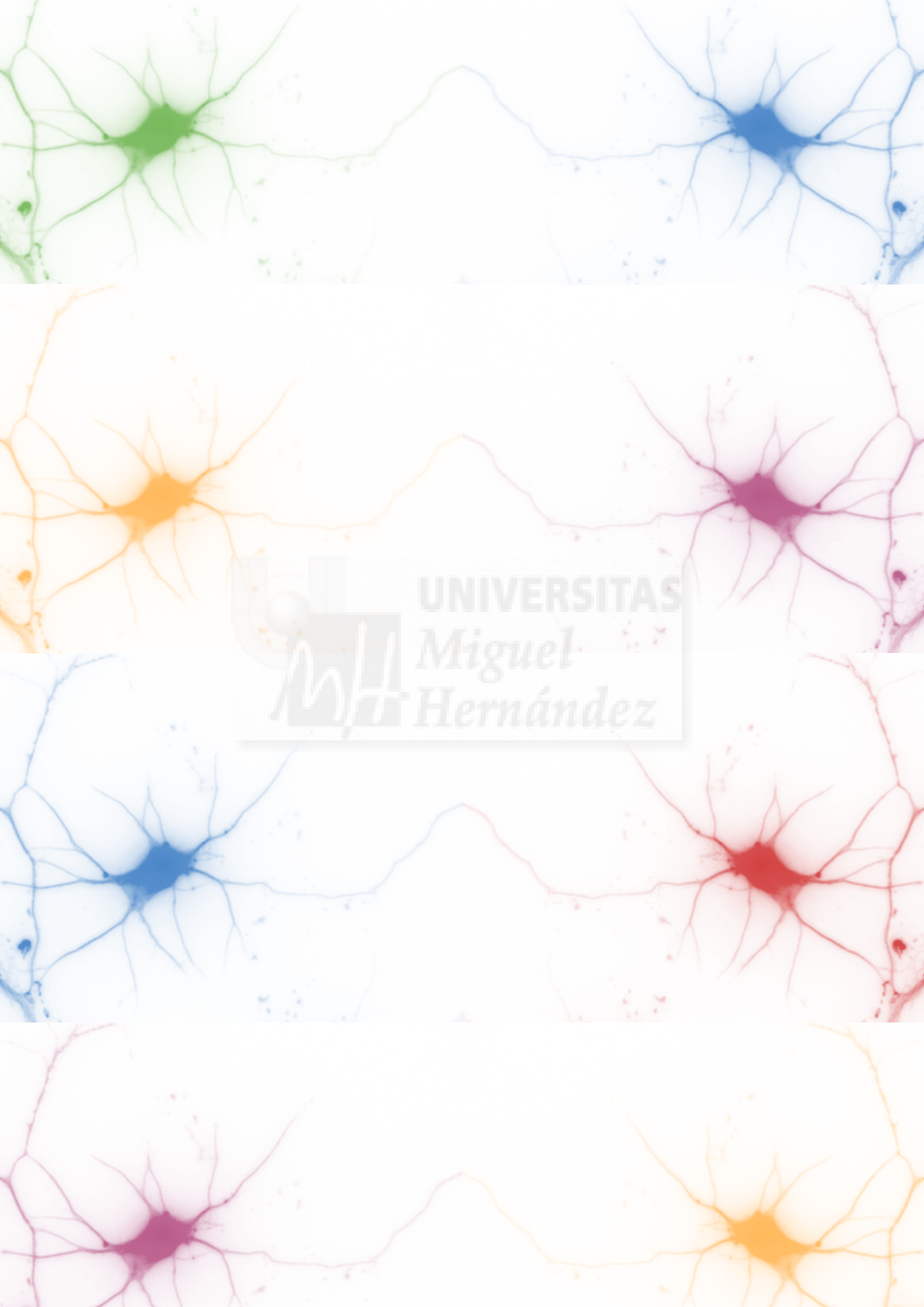


Figure 7 | Thalamic calcium waves communicate sensory modalities and regulate S1 barrels formation. (A) Embryonic Ca^{2+} waves propagate among principal thalamic sensory nuclei and reach the neocortex through thalamocortical axons at E16.5 in mice. (B) Bilateral embryonic enucleation at E14.5 triggers more Ca^{2+} waves in VPM and dLGN, eventually leading to an increment in barrel size and PMBSF area. (C) Silencing Ca^{2+} waves in the MGv increases Ca^{2+} waves frequency in the VPM. This change precedes barrel and PMBSF area enlargement. (Extracted from (Martini et al., 2017)).



UNIVERSITAS
Miguel
Hernández



Objectives

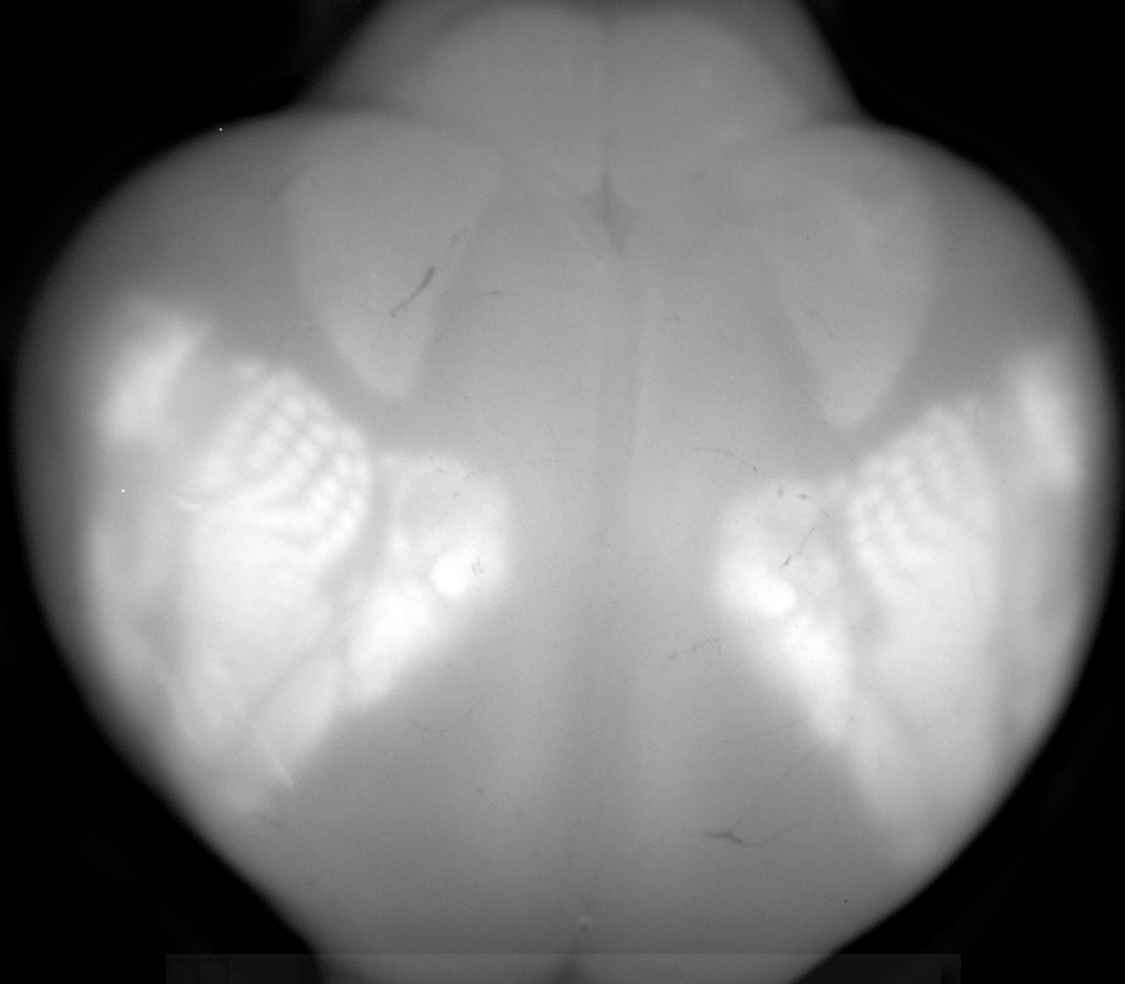


Objectives:

The main objective of this PhD Thesis work was to understand the thalamic role in the control of cortical plasticity after input deprivation. The specific aims were the following:

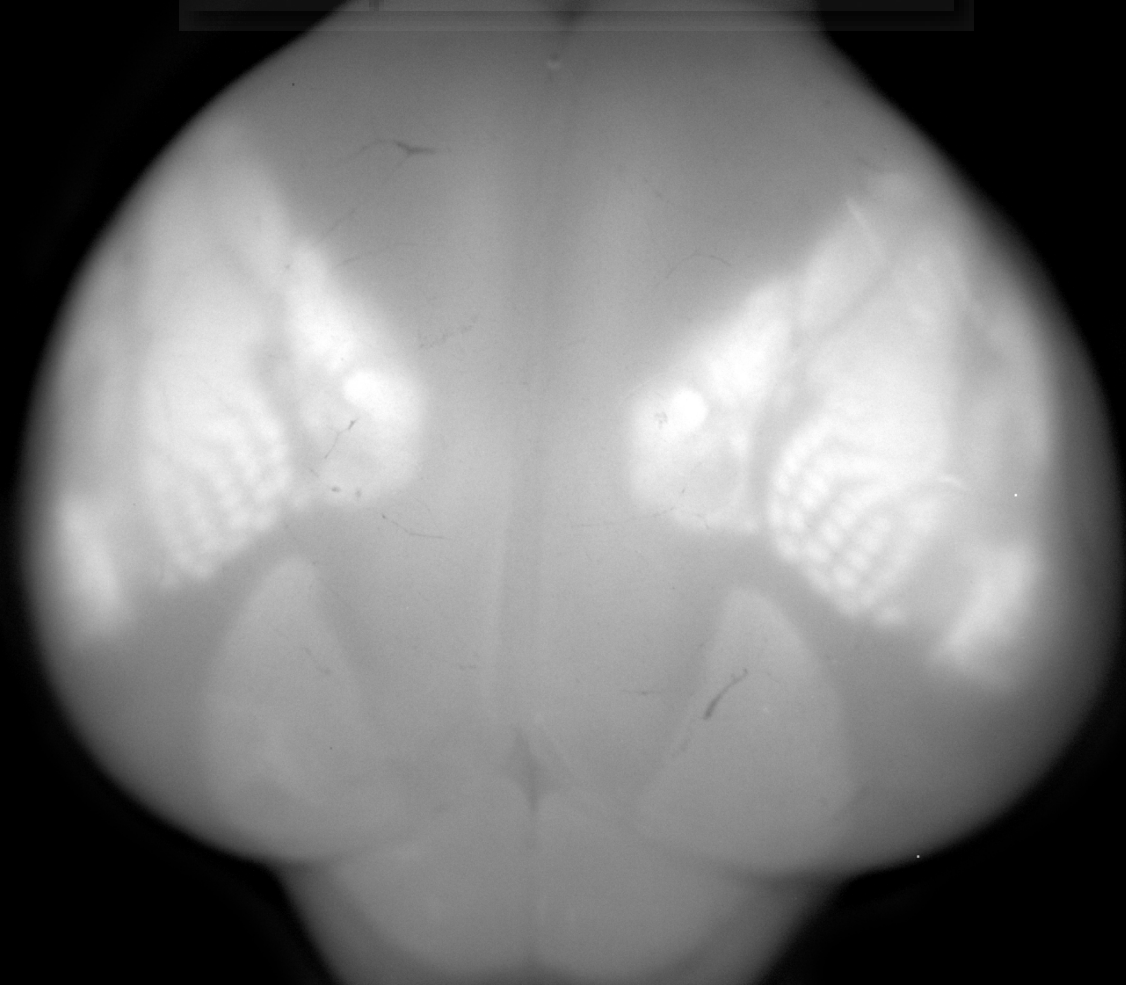
- To investigate where and when the first neuroplastic brain adaptations occur upon sensory input loss.
- To understand the role of the thalamus in cortical neuroplasticity after input deprivation.
- To identify common mechanisms involved in cross-modal plasticity.
- To unravel the role of thalamic spontaneous activity on the corticothalamic projections.





 UNIVERSITAS
Miguel
Hernández

Results



Results

Chapter I: Prenatal thalamic waves regulate cortical area size prior to sensory processing

This work has been published by three first co-authors and in collaboration with members of my laboratory and with researchers from other institutions that are co-authors of the article. Here I described the author contribution for each of the co-authors: Guillermina López-Bendito conceived the idea. Verónica Moreno-Juan performed the experiments related to the embryonic enucleation mouse model, analysis of analysis of *Brn3b^{Cre};R26^{tdTomato}*, *Rorb* knockout and and *Nestin^{Cre};Rorb^{fl}* mice, and performed the dissociated thalamic cultures. Noelia Antón-Bolaños, performed the experiments related to the spontaneous activity in the MGv silenced mouse model. Antón Filipchuk performed the Ca²⁺ imaging experiments. Cecilia Mezzera and Verónica Moreno-Juan performed the microarray assay. Henrik Gezelius, Sebastien Ducret and Filippo Rijli generated the *R26^{Kir2.1-mCherry}* mouse line. Belén Andrés and Verónica Moreno-Juan performed the *in utero* electroporations. Luis Rodríguez-Malmierca performed mice perfusions and the *in situ* hybridization experiments. Rafael Susín genotyped the mouse colonies, generated the *in situ* probes and plasmids for electroporation and performed the quantitative PCRs. Olivier Schaad analyzed the microarray data. Takuji Iwasato provided the TCA-GFP Tg mouse line. Roland Schüle provided the *Rorb* conditional mouse. Michael Rutlin and Sacha Nelson provided the *Rorb* full knockout brains. Verónica Moreno-Juan, Anton Filipchuk and Noelia Antón-Bolaños conducted the data analysis and Miguel Valdeolmillos, Filippo Rijli and Guillermina López-Bendito wrote the paper.

The article presented here contain supplementary movies that are available online in this link: <https://www.nature.com/articles/ncomms14172> and will be attached to the digital format in CD of this Thesis.

Results

Prenatal thalamic waves regulate cortical area size prior to sensory processing

Verónica Moreno-Juan^{1,9}, Anton Filipchuk^{1,9}, Noelia Antón-Bolaños^{1,9}, Cecilia Mezzera^{1,2}, Henrik Gezelius¹, Belen Andrés¹, Luis Rodriguez-Malmierca¹, Rafael Susín¹, Olivier Schaad^{3,4}, Michael Rutlin^{5,6}, Sacha Nelson⁵, Sebastien Ducret⁷, Miguel Valdeolmillos^{1,8}, Filippo M. Rijli^{7,8} and Guillermina López-Bendito^{1,*}

¹Instituto de Neurociencias de Alicante, Universidad Miguel Hernández-Consejo Superior de Investigaciones Científicas (UMH-CSIC), Sant Joan d'Alacant, Spain

²Champalimaud Neuroscience Programme, Champalimaud Centre for the Unknown, 1400-038 Lisbon, Portugal

³NCCR frontiers in Genetics, University of Geneva, Geneva, Switzerland

⁴Department of Biochemistry, Sciences II, University of Geneva, Geneva, Switzerland

⁵Department of Biology and National Center for Behavioral Genomics, Brandeis University, Waltham, MA 02454, USA

⁶Department of Biochemistry and Molecular Biophysics, HHMI, Columbia University Medical Center, New York, NY 10032, USA

⁷Friedrich Miescher Institute for Biomedical Research, Maulbeerstrasse 66, 4058 Basel, Switzerland

⁸These authors contributed equally to this work

⁹Co-first author

*Correspondence to: g.lbendito@umh.es

Nature Communications 2017, 8:14172 Feb 3. Doi: 10.1038/ncomms14172

Published article available at this link:

<https://www.nature.com/articles/ncomms14172>

Here is presented the final version prepared for its publication following the University rules.

Prenatal thalamic waves regulate cortical area size prior to sensory processing

Verónica Moreno-Juan^{1,14}, Anton Filipchuk^{1,14}, Noelia Antón-Bolaños^{1,14}, Cecilia Mezzera^{1,2}, Henrik Gezelius¹, Belen Andrés¹, Luis Rodríguez-Malmierca¹, Rafael Susín¹, Olivier Schaad^{3,4}, Takuji Iwasato^{5,6}, Roland Schüele^{7,8,9}, Michael Rutlin^{10,11}, Sacha Nelson¹⁰, Sebastien Ducret¹², Miguel Valdeolmillos^{1,13}, Filippo M. Rijli^{12,13} and Guillermina López-Bendito^{1,*}

¹Instituto de Neurociencias de Alicante, Universidad Miguel Hernández-Consejo Superior de Investigaciones Científicas (UMH-CSIC), Sant Joan d'Alacant, Spain

²Champalimaud Neuroscience Programme, Champalimaud Centre for the Unknown, 1400-038 Lisbon, Portugal

³NCCR frontiers in Genetics, University of Geneva, Geneva, Switzerland

⁴Department of Biochemistry, Sciences II, University of Geneva, Geneva, Switzerland

⁵Division of Neurogenetics, National Institute of Genetics (NIG), Mishima, 411-8540, JAPAN

⁶Department of Genetics, SOKENDAI (The Graduate University for Advanced Studies), Mishima, 411-8540, JAPAN

⁷Urologische Klinik und Zentrale Klinische Forschung, Klinikum der Universität Freiburg, Breisacherstrasse 66, 79106 Freiburg, Germany.

⁸BIOSS Centre of Biological Signalling Studies, Albert Ludwigs University, 79106 Freiburg, Germany.

⁹Deutsches Konsortium für Translationale Krebsforschung (DKTK), Standort Freiburg, 79108 Freiburg, Germany

¹⁰Department of Biology and National Center for Behavioral Genomics, Brandeis University, Waltham, MA 02454, USA

¹¹Department of Biochemistry and Molecular Biophysics, HHMI, Columbia University Medical Center, New York, NY 10032, USA

¹²Friedrich Miescher Institute for Biomedical Research, Maulbeerstrasse 66, 4058 Basel, Switzerland

¹³These authors contributed equally to this work

¹⁴Co-first author

*Correspondence to: g.lbendito@umh.es

ABSTRACT

The cerebral cortex is organized into specialized sensory areas, whose initial territory is determined by intracortical molecular determinants. Yet, sensory cortical area size appears to be fine tuned during development to respond to functional adaptations. Here we demonstrate the existence of a prenatal sub-cortical mechanism that regulates the cortical areas size in mice. This mechanism is mediated by spontaneous thalamic calcium waves that propagate among sensory-modality thalamic nuclei up to the cortex and that provide a means of communication among sensory systems. Wave pattern alterations in one nucleus lead to changes in the pattern of the remaining ones, triggering changes in thalamic gene expression and cortical area size. Thus, silencing calcium waves in the auditory thalamus induces *Rorb* upregulation in a neighboring somatosensory nucleus precluding the enlargement of the barrel-field. These findings reveal that embryonic thalamic calcium waves coordinate cortical sensory area patterning and plasticity prior to sensory information processing.

Results

Sensory systems are represented in the primary sensory areas of the brain in organized maps. In the embryo, these territories are pre-patterned by restricted gene expression independently of external inputs¹⁻⁵. However, sensory cortical areas are malleable later in life as their position and size varies in function of peripheral stimuli. For example, deprivation or the loss of sensory stimuli in the visual or somatosensory systems leads to a reduction in the size of the corresponding primary cortical area and altered map representations⁶⁻⁹. Moreover, spontaneous network activity from sensory peripheral neurons also modulates the formation of cortical maps prior to sensory experience^{10,11}. This is the case of retinal waves that direct map refinement in the superior colliculus and visual cortex through spatiotemporal patterns of peripheral activity¹²⁻¹⁴. Thus, this bottom-up plasticity, peripheral-to-central, is a well-defined mechanism that modulates cortical maps within a given sensory system.

Conversely, central structures such as the thalamus, can also influence intramodally sensory cortical areas prior to sensory experience. Genetic manipulation of visual or somatosensory thalamocortical axons (TCAs) during embryogenesis perturbs the formation of the corresponding cortical sensory map^{15,16}. Yet when a sensory input is lost early in life, thalamocortical circuits can reorganize and this change is correlated with adaptations in the size of the sensory cortical area related to the lost input¹⁷⁻¹⁹. Furthermore, top-down plasticity for the somatosensory system has also been demonstrated recently, whereby the size of the cortical barrel-field modifies its representation in subcortical sensory nuclei²⁰. Thus, it is clear that both peripheral and central structures play a key role in modulating the size of cortical areas and territories within a given sensory system.

Intriguingly, the plastic changes that occur in the cortex of sensory deprived animals involve both the deprived and spared cortical areas. For example, removal of the eyes at birth leads to a reduction of the primary visual cortex and an expansion of the somatosensory cortical barrel-field in blind adult rodents²¹⁻²³. Thus, there would appear to be some communication among distinct sensory systems and cortical areas, although the mechanisms that underlie such effects remain unexplored.

Here we describe the existence of thalamic spontaneous calcium waves that have a specific pattern of propagation among distinct sensory-modality nuclei. We hypothesize that thalamic waves may play a pivotal role in regulating the development of cortical representations from different sensory modalities. Abolishing spontaneous calcium waves in the auditory nucleus of the thalamus alters the pattern of spontaneous waves in

the neighboring somatosensory ventral posterior medial (VPM) nucleus, and equivalent changes were also observed in embryonically enucleated mice. The increased frequency of waves in the VPM precedes an enlargement of the cortical barrel-field in S1. Mechanistically, we found activity-dependent regulation of the nuclear orphan receptor *Rorβ* in the VPM, which produced an increase in the complexity of thalamocortical axon (TCA) terminals. Gain- and loss-of-function experiments offer further support to the hypothesis that *Rorβ* expression in the thalamus is a key regulator of sensory cortical area adaptation.

In summary, our findings reveal a novel mode of communication between distinct sensory-modality thalamic nuclei, whereby spontaneous calcium waves control gene expression and trigger cortical size adaptations prior to the onset of sensory information processing.



RESULTS

Visual embryonic deprivation expands the barrel-field

It is well known that eye enucleation at early postnatal stages triggers a profound reorganization of deprived and non-deprived sensory cortical areas^{8,24}. For instance, the somatosensory cortical area size is expanded in blind animals^{8,25} while the visual primary area is reduced^{8,24,26}. To determine if the development of sensory cortical territories is coordinated among distinct sensory systems already at prenatal stages, we performed bilateral eye enucleation at embryonic day (E) 14.5 (embBE), before retinal axons reach the thalamus. Experiments were done in wild type or in a transgenic mouse line that expressed the membrane-bound enhanced green fluorescent protein (GFP) from the sensory thalamus (TCA-GFP mouse²⁷). The absence of retinal axons was verified using dye tracing or a retinal ganglion cell specific transgenic mouse, *Brn3b*^{Cre/+}, crossed with a *R26*^{tdTomato} reporter line (**Supplementary Fig. 1a** and **Fig. 1a**). We then assessed the development of the visual, somatosensory and auditory cortical areas size at early postnatal stages. Measurements of the primary cortical areas size showed a 33.3% decrease in V1 (control: $100 \pm 3.11\%$, $n = 13$; embBE: $66.7 \pm 1.88\%$, $n = 12$) and a 13.6% expansion of S1 (control: $100 \pm 1.73\%$, $n = 13$; embBE: $113.7 \pm 2.28\%$, $n = 12$; **Fig. 1b** and **1c**). The A1 area did not change after embBE. The decrease in the V1 area in the embBE mice was accompanied by a similar 39.8% reduction in the dorsal lateral geniculate nucleus (dLGN) size (**Supplementary Fig. 1b-1d**). This reduction has been reported before in early postnatal enucleated mice²⁶. Interestingly, the size of the VPM did not change after embBE (**Supplementary Fig. 1b-1d**) suggesting that the expansion of S1 might be triggered by changes in the axonal arborization of VPM thalamic neurons. To test this, we closely look at the developmental progression of the primary somatosensory cortex (S1) that displays a topographical representation of the whisker pad along the feed-forward pathway from the brainstem to the barrel field in S1 (refs 6, 28, 29). Immunostaining for the vesicular glutamate transporter 2 (vGlut2) that specifically labels TCA terminals in cortical layer IV, revealed a 10.7% increase in the total posteromedial barrel subfield (PMBSF) area of embBE mice at P4 (control: $100 \pm 2.63\%$, $n = 10$; embBE: $110.7 \pm 3.58\%$, $n = 14$; **Fig. 1d** and **1e**) and a 12.4% increase at P8 (**Supplementary Figs. 2a** and **2b**). The size of each individual barrel was also greater in the embBE mice than in their control littermates at both P4 (17.7% mean increase; control: $100 \pm 2.75\%$, $n = 10$; embBE: $117.7 \pm 5.07\%$, $n = 14$; **Fig. 1f**) and P8 (18.7%

mean increase; **Supplementary Figs. 2a** and **2b**). Moreover, these changes persisted in the adult (P30) embBE mice, where the PMBSF was increased by 11.25% as compared to control animals (**Supplementary Figs. 2c** and **2d**).

Although active whisking is not performed until P10-P13 in mice³⁰, to unequivocally demonstrate that the barrel enlargement is independent of an increase in passive whisker flickering in young pups, we trimmed the whiskers of embBE mice daily from birth until P4. At P4, the increase in the size of the barrel area in embBE animals whose whiskers were trimmed (dewhiskered) was similar to that of embBE mice with untrimmed whiskers (control: $100 \pm 3\%$, $n = 13$; control dewhiskered P0-P4: $103 \pm 2.8\%$, $n = 16$; embBE: $113.6 \pm 3.5\%$, $n = 13$; embBE dewhiskered P0-P4: $118.6 \pm 4.2\%$, $n = 13$; **Fig. 1g**). Moreover, the size of barrelettes in the brainstem spinal sensory (SpV) and principal sensory (PrV) trigeminal nuclei (**Supplementary Fig. 3**), and of barreloids in the somatosensory VPM thalamic nucleus (**Fig. 1h**) was normal in early postnatal embBE animals. This strongly suggested that the enlargement of the S1 cortical area in embBE animals is not due to changes occurring at the level of either brainstem somatosensory nuclei or their presynaptic input to the thalamus. The adaptation in S1, however, might rather depend on reorganization of thalamocortical input, well before visual sensory experience.

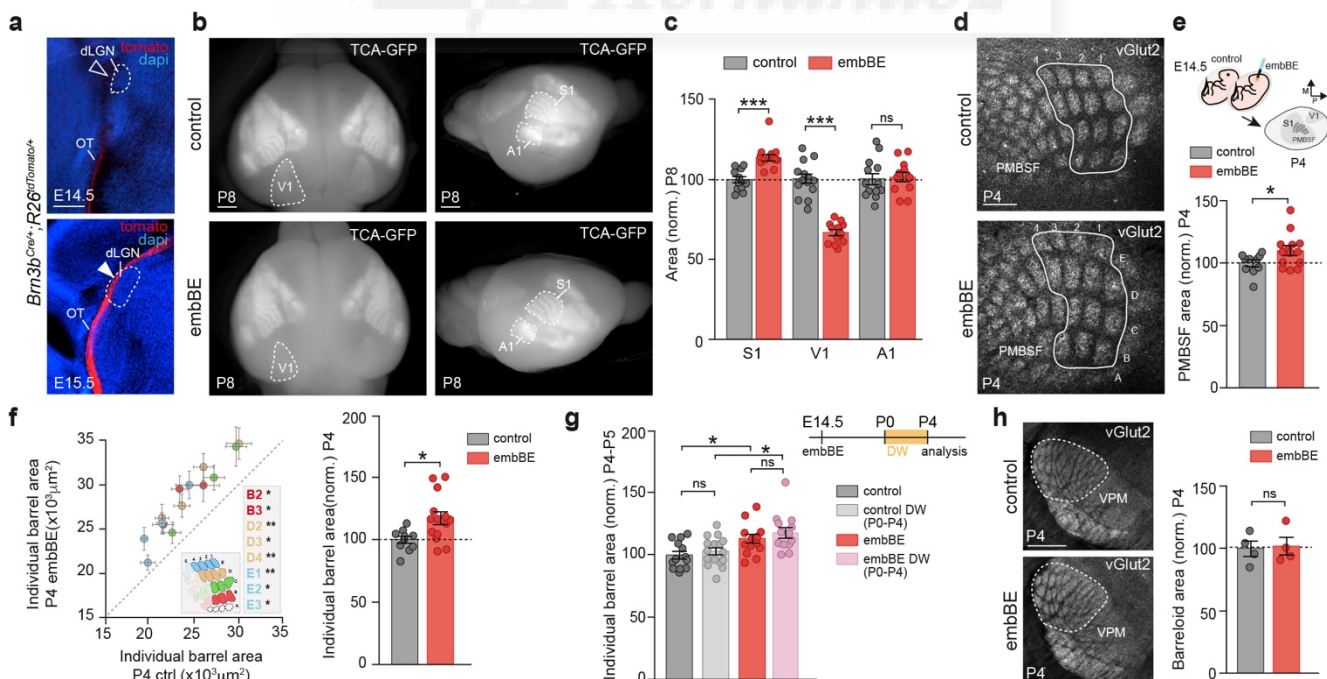


Figure 1 Embryonic eye removal triggers experience-independent cross-modal changes in S1 somatosensory cortex. **(a)** *Brn3b^{Cre/+};R26^{tdTomato}* mouse shows the absence of retinal axons in the

Results

dLGN at E14.5 and their presence at E15.5. **(b)** Labeling of principal sensory cortical areas at P8 in a control TCA-GFP transgenic mouse or in a TCA-GFP mouse in which bilateral enucleation has been performed embryonically. **(c)** Quantification of the areas of S1, V1 and A1 shown in **b** (** $P < 0.001$ for S1 and V1; not significant (ns): $P = 0.76$ for A1; Two-tailed Student's t-test). **(d)** vGlut2-immunostaining in the posteromedial barrel subfield (PMBSF) of S1 in control ($n = 10$) and embBE ($n = 14$) mice at P4. **(e)** Experimental design and quantification of the total PMBSF area shown in **d** ($*P = 0.03$; Two-tailed Student's t-test). The expansion of the PMBSF in the embBE was proportional along the medio-lateral axis (630.30 ± 39.04 pixels in control and 670.71 ± 38.79 pixels in embBE) and the antero-posterior axis (326.60 ± 18.66 in control and 337.93 ± 26.35 in embBE mice). **(f)** Plot of the area of each individual barrel (left) and quantification of the mean individual barrel area (right) in control and embBE brains at P4 ($*P = 0.011$; Two-tailed Student's t-test). Inset describes the barrels that are significantly expanded in the embBE mice compared to controls. **(g)** Design of the experiment and quantification of the individual barrel area of control ($n = 13$), control dewhiskered ($n = 16$), embBE ($n = 12$) and embBE dewhiskered ($n = 13$) mice at P4 ($*P < 0.05$; ns, not significant; Two-way ANOVA test with Tukey's post hoc analysis). Interaction between dewhiskering and embBE was not significant ($P = 0.77$). **(h)** vGlut2-immunostaining in the VPM nucleus of the thalamus in control and embBE mice at P4, quantification of the total barreloid area (control $100 \pm 6.23\%$, $n = 4$; embBE: $102.1 \pm 7.11\%$, $n = 4$; $P > 0.99$; Mann-Whitney U-Test). Graphs represent mean \pm SEM. Scale bars, 1mm in **b** and $300\mu\text{m}$ in **a**, **d** and **h**.

Thalamic calcium waves communicate sensory thalamic nuclei

In subcortical structures, spontaneous network activity within a given sensory modality has been shown to shape the spatial and functional organization of the corresponding sensory cortical area^{12,31,32}. The thalamus is the first sub-cortical structure where the peripheral and sub-cortical inputs of visual, auditory and somatosensory circuits converge. Moreover, the results in embBE mice suggested that communication in the thalamus among distinct sensory-modality thalamocortical afferent nuclei might take place to regulate inter-areal cortical size before sensory experience. Spontaneous activity could be a promising candidate to provide such inter-nuclear communication.

We took advantage of the $Gbx2^{CreER}; R26^{tdTomato}$ mice to analyze Ca^{2+} signaling in thalamocortical slices in which the thalamic sensory nuclei are labeled (**Fig. 2a**). We found a consistent pattern of activity characterized by the emergence of thalamic Ca^{2+} waves in the principal sensory nuclei (VPM, dLGN, and ventro medial geniculate (MGv)) lasting from E14.5 up to P2 (**Supplementary Figs. 4a-4d**). Thalamic waves also involve

higher-order nuclei at perinatal stages. This pattern of activity was clearly distinct from the asynchronous Ca^{2+} transients recorded in single cells and the synchronous activity seen in small clusters (**Fig. 2b** and **Supplementary Figs. 4e** and **4f**). Waves propagated with a mean front speed of $141.93 \pm 29.3 \mu\text{m}$ per second, leading to a delay in the onset of the Ca^{2+} transient in cells located progressively distant to the wave origin (**Fig. 2c**). Spatially, thalamic waves propagated across distinct sensory-modality thalamic nuclei, from one nucleus to another (VPM-dLGN, VPM-MGv and vice versa; **Fig. 2d** and **Supplementary Movies 1-3**) with a frequency of 0.20 ± 0.04 waves per minute and a duration of 7.45 ± 0.26 seconds (**Supplementary Fig. 4g**). The analysis of inter-wave intervals showed a wide distribution, ranging from 15 to more than 400 seconds, concentrated in the 0-3 minutes interval but without a defined peak of occurrence (**Supplementary Fig. 4h**). In order to test whether this thalamic form of activity is transmitted to the cortex, we performed calcium imaging in transgenic mice that specifically expresses the calcium indicator protein GCaMP6 in the sensory thalamic neurons (**Fig. 2e**). Remarkably, analysis of the activity pattern at E16.5 showed that thalamic waves are propagated through the TCAs reaching cortical areas (**Figs. 2f** and **2g**; **Supplementary Movie 4**).

Results

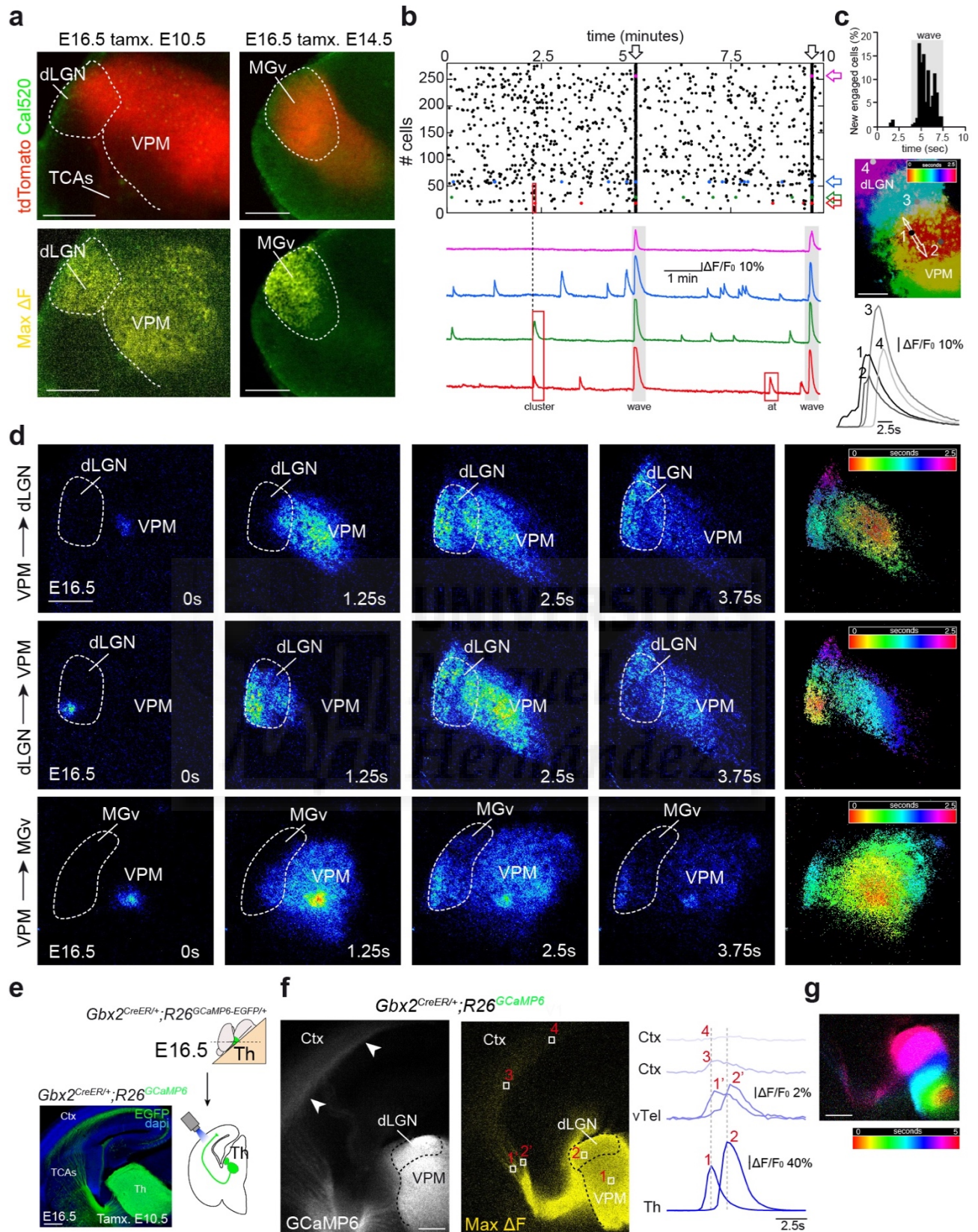


Figure 2 Thalamic spontaneous waves drive the communication between distinct thalamic nuclei.

(a) Fluorescence images of E16.5 $Gbx2^{CreER/+};R26^{tdTomato}$ 45 degrees thalamocortical acute slices

loaded with the calcium indicator Cal520. Areas corresponding to the dLGN, VPM and MGv nuclei express tomato in function of the time of tamoxifen administration (upper panels). Maximum projection of Ca^{2+} waves (yellow) covering the three principal thalamic nuclei (lower panels). **(b)** Raster plot of the activity recorded in more than 250 individual cells in the dLGN-VPM during 10 minutes. The arrows label synchronous Ca^{2+} transients corresponding to Ca^{2+} waves. The lower panel shows examples of Ca^{2+} activity traces in four individual thalamic neurons (indicated by color arrows in the raster plot) illustrating the three patterns of Ca^{2+} transients: asynchronous scattered, synchronous clusters and waves. **(c)** Cell-by-cell wave propagation. Upper panel: Percentage of neurons (over both dLGN and VPM nuclei) that are activated at every time point during wave propagation. Middle panel: Temporal spread of a wave front (color coded). Lower panel: Examples of Ca^{2+} transients in 4 cells during a wave indicated in the middle panel (cell 1 initiated the wave). **(d)** Propagation of thalamic waves at E16.5 in acute slices: from the VPM into the dLGN (upper panels); from the dLGN into the VPM (middle panels); and from the VPM into the MGv nuclei (lower panels). The calcium signal intensity is coded in pseudocolor. Right panels for each wave show the temporal color coded spread of the wave front from its origin (red zone) up to the borders of the nuclei. **(e)** Expression of GCaMP6-EGFP in embryonic acute thalamocortical slice from $Gbx2^{CreER/+};R26^{GCaMP6-EGFP/+}$ mice with tamoxifen administrated at E10.5. **(f)** Acute slice showing GCaMP6 in the thalamocortical projections at E16.5 (left). Maximum projection of a Ca^{2+} wave from the same slice (right, yellow) showing the propagation of the thalamic waves to the cortex. Traces showing the progression of a wave from VPM (1) to dLGN (2) that propagated along the TCAs (1' and 2') up to distinct medio-lateral cortical territories (3 and 4). **(g)** Temporal color-coded spread of the wave shown in **f**. Scale bars, 200 μm in **a**, 100 μm in **c** and 200 μm in **d-g**.

Thalamic waves are propagated via gap junctions

Next, we further investigated the properties and underlying mechanisms of waves initiation and propagation. At E16.5, thalamic waves were originated from the three principal sensory thalamic nuclei with a higher frequency of origin at the VPM (**Fig. 3a** and **3b**). Irrespective of their origin, the maximum area of propagation was constant for successive waves that consistently travelled across the same territory (**Fig. 3a**). Within a given nucleus, the origins of waves were randomly distributed, without a regular trigger zone (**Fig. 3c**). To determine the possible mechanisms involved in the waves initiation, we checked the effect of the voltage-sensitive Na channel blocker tetrodotoxin (TTX). The application of 1 μM of TTX (**Fig. 3d, 3e**) led to the abolition of the calcium waves. These results suggest that wave's initiation/propagation requires the activation of voltage-

Results

dependent Na-channels. Consistently with this, the gradual depolarization of the cells by step increases in the concentration of extracellular potassium, leads to a gradual increase in the frequency of the waves (**Fig. 3f**).

The function of gap-junctions has been implicated in the propagation of cortical waves in the developing neocortex³³⁻³⁵. Thus, we wondered whether gap-junctions might also participate in the mechanism of thalamic waves propagation. Notably, treatment of thalamic slices with the general gap junction blocker Carbenoxolone eliminated the propagation of the Ca^{2+} waves, while preserving, although reduced, single cell and cluster activity (**Fig. 3g, 3h**). Whereas connexin-36 is expressed in developing brain areas and has been implicated in developmental processes³⁶, treatment with the Cx36 specific gap-junction blocker Mefloquine only decreased the frequency of the Ca^{2+} waves without blocking them (**Supplementary Fig. 4i**), suggesting that additional connexins might be involved in this process.

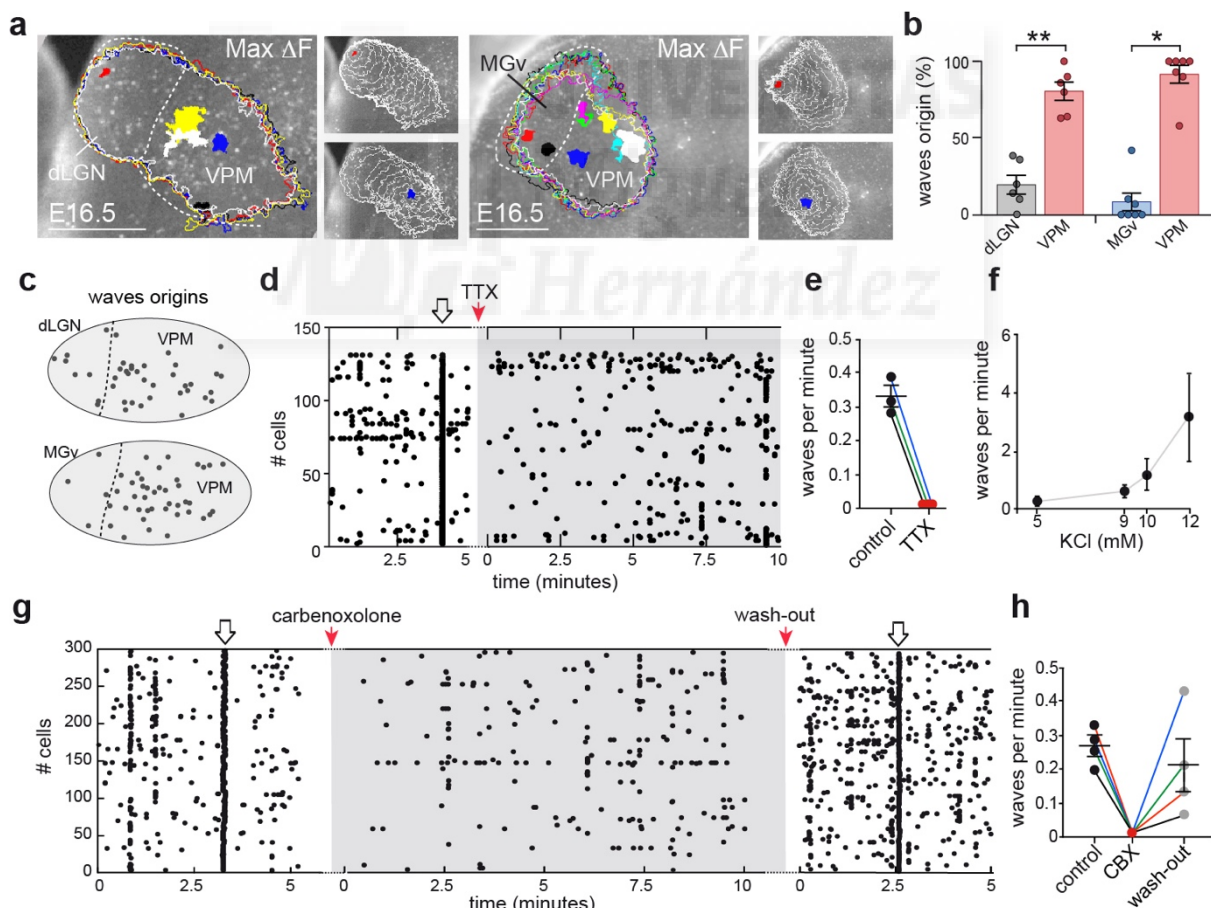


Figure 3 Origin and propagation properties of thalamic waves. (**a**) Site of origin (color-coded filled contours) and corresponding maximum spread (color outlines) of five successive waves

originated in the dLGN–VPM and eight waves in the MGv–VPM nuclei. The area covered by the waves in the dLGN–VPM example was $149.728\mu\text{m}^2 \pm 5.873\mu\text{m}^2$ and in the MGv–VPM example was $188.715\mu\text{m}^2 \pm 16.722\mu\text{m}^2$. Insets represent examples of the propagation of wave 1 (red) and wave 2 (blue) for each pair. The white contours show the pattern of spread of the wave front measured at 250msec intervals. **(b)** Quantification of the percentage of waves depending on the origin at E16.5. The vast majority of waves are originated in the VPM (** $P = 0.004$; Paired t-test; * $P = 0.016$; Wilcoxon matched-pairs signed rank test). **(c)** Schemas representing the stochastic nature of the thalamic waves origins for each pair of nuclei (dLGN–VPM; $n = 40$ sites in 5 independent experiments; MGv–VPM, $n = 67$ sites in 5 independent experiments). **(d)** Effect of bath application of the voltage-dependent sodium channels blocker tetrodotoxin (TTX, $1\mu\text{M}$) on the Ca^{2+} activity. TTX completely abolished the thalamic waves without substantially affecting the asynchronous activity or the clusters. **(e)** Quantification of Ca^{2+} dLGN–VPM waves frequency before and during TTX administration. **(f)** Dose-dependent response in waves per minute, after increasing the extracellular potassium concentration from 5mM (control) to 12mM. **(g)** Effect of bath application of the gap junction blocker carbenoxolone ($50\mu\text{M}$) on the Ca^{2+} activity. The most noticeable effect is the reversible abolition of the synchronous waves. **(h)** Quantification of Ca^{2+} dLGN–VPM waves frequency before, during and after carbenoxolone administration. Graphs represent mean \pm SEM. Scale bars $250\mu\text{m}$.

Blockage of thalamic waves affects the size of cortical areas

We have shown that spontaneous calcium waves of activity emerge in thalamic neurons from early stages of embryonic development and propagate among distinct sensory thalamic nuclei prior to the formation of cortical maps. We next investigated whether thalamic Ca^{2+} waves might coordinate the size of cortical areas during prenatal development. We generated a transgenic mouse that conditionally expressed the Kir2.1 (Kir) inward rectifier potassium channel fused to the mCherry protein (referred to as $R26^{Kir}$). When crossed to the $Gbx2^{CreER}$ line, the $R26^{Kir}$ mouse allows thalamic activity to be manipulated *in vivo*. When tamoxifen was administered at E14.5, *Kir* was specifically overexpressed in MGv thalamic neurons in a mosaic fashion (**Supplementary Figs. 5a** and **5b**; referred to as the MGv^{Kir} mouse) resulting in the blockade of the waves that originated in this structure (**Fig. 4a**). Individual cell activity remained in the inter-wave periods, although in fewer cells (**Supplementary Figs. 5c** and **5d**). Therefore, this model provides a means to address a specific role of thalamic Ca^{2+} waves in influencing cortical area size.

Results

The abolition of waves from the MGv resulted in an altered wave pattern in the VPM nucleus at E16.5. While the frequency of wave spreading between the dLGN and VPM nuclei remained unchanged, numerous *de novo* waves appeared in the VPM that remained restricted to this territory, significantly increasing the mean wave activity in this nucleus (control: 0.20 ± 0.04 waves per minute VPM, $n = 6$; MGv^{Kir} : 0.34 ± 0.04 waves per minute VPM, $n = 11$; **Fig. 4b** and **4c** and **Supplementary Movie 5**). Despite the increase of wave frequency, the average number of calcium transients per neuron did not change in the VPM of the MGv^{Kir} mouse compared to control (**Supplementary Figs. 5e** and **5f**), indicating that it is the synchronization of Ca^{2+} activity what was altered and not the extent of asynchronous activity. Interestingly, silencing thalamic waves in the MGv caused a 12.3% increase in the size of the S1 area (**Supplementary Figs. 6a** and **6b**) with an 8% enlargement of the total PMBSF area (control: $100 \pm 1.74\%$, $n = 11$; MGv^{Kir} : $108 \pm 2\%$, $n = 12$; **Fig. 4d**). Individual barrels were also increased in size by 10.1% at P7 (control: $100 \pm 3.07\%$, $n = 11$; MGv^{Kir} : $110.1 \pm 2.85\%$, $n = 13$). We also found a significant decrease of 51.9% in the A1 area in the MGv^{Kir} mouse (**Supplementary Figs. 6a** and **6b**), suggesting that silencing thalamic waves within a thalamic sensory nucleus leads to a decrease in the size of its corresponding cortical area. No changes in the size of either barreloids in the VPM or the area of the dLGN and MGv nuclei were observed in the MGv^{Kir} mice (**Supplementary Figs. 6c-6g**).

These findings suggest that the expansion of the barrel-field in S1 might be triggered by the increased frequency of waves in VPM, rather than being a direct consequence of MGv silencing. To test the general validity of this assumption, we recorded Ca^{2+} wave activity in the VPM of embBE mice at E17. As in the MGv^{Kir} model, we found an increase in the frequency of waves in the VPM in the embBE mice (control: 0.16 ± 0.03 waves per minute VPM, $n = 5$; embBE: 0.29 ± 0.03 waves per minute VPM, $n = 5$; **Fig. 4e** and **4f** and **Supplementary Movie 6**). Altogether these results strongly suggest that prenatal thalamic waves are key regulators of sensory cortical area size and

that prenatal alteration in inter-thalamic sensory nuclei communication may trigger size adaptation in cortical territories.

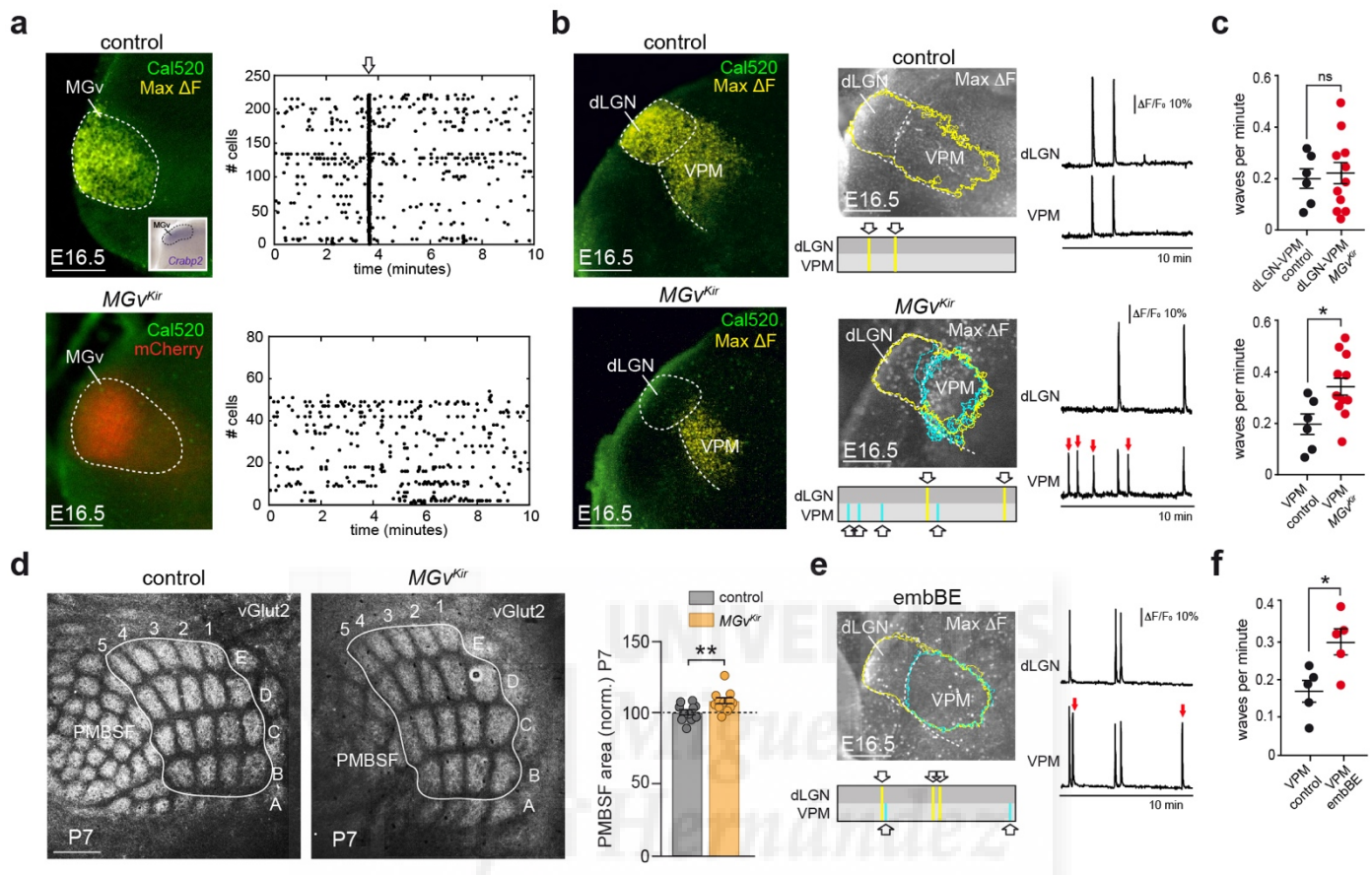


Figure 4 Blocking the waves in the auditory nucleus alters the pattern of wave activity in the VPM and triggers an enlargement of the barrel-field in S1. **(a)** Maximum projection of a Ca^{2+} wave (yellow) at the level of the MGv in an E16.5 control (upper panel, inset *post hoc in situ* hybridization of the auditory thalamic marker *Crabp2*) and in a *MGv^{Kir}* (lower panel) littermate. No waves are observed in the territory were Kir2.1 is overexpressed (mCherry). Raster plot of individual cells activity recorded during 10 minutes in the MGv of control (upper panel) and *MGv^{Kir}* (lower panel) mice. The Ca^{2+} transient labelled by the open arrow in the control reflects a Ca^{2+} wave. **(b)** Maximum projections of Ca^{2+} waves (yellow) propagating between the dLGN and VPM in an E16.5 control mouse (upper panels) and in a *MGv^{Kir}* littermate (lower panels). Additional waves (red arrows) remain restricted to the VPM in the *MGv^{Kir}* mouse (blue contours). **(c)** Upper panel shows the quantification of Ca^{2+} waves that propagate between dLGN–VPM in the control ($n = 6$) and *MGv^{Kir}* ($n = 11$) mice showing no significant change (dLGN–VPM: 0.20 ± 0.04 waves per minute control; 0.21 ± 0.04 waves per minute *MGv^{Kir}*, $P = 0.84$). Lower panel shows the significant increase of *de novo* waves in the VPM in the *MGv^{Kir}* mouse (VPM: $0.20 \pm$

Results

0.04 waves per minute control; 0.34 ± 0.04 waves per minute MGv^{Kir} , $*P = 0.028$; Two-tailed Student's t-test). **(d)** vGlut2-immunostaining in tangential sections of the PMBSF in the S1 of P7 control ($n = 11$) and MGv^{Kir} mice ($n = 12$). Quantification of the PMBSF area in P7 MGv^{Kir} mice relative to the controls ($**P = 0.007$; Two-tailed Student's t-test). **(e)** Maximum projections of Ca^{2+} waves in the embBE mouse at E17. Waves propagating between the dLGN and VPM (yellow) and *de novo* VPM waves (blue). **(f)** Quantification of the frequency of waves in the VPM in the embBE mouse (VPM: 0.16 ± 0.03 waves per minute control; 0.29 ± 0.03 waves per minute embBE, $*P = 0.019$; Two-tailed Student's t-test). Graphs represent mean \pm SEM. Scale bars, $200\mu\text{m}$ in **a**, **b**, **e** and **f**, and $300\mu\text{m}$ in **d**.

Correlated activity modulates thalamic *Rorβ* gene expression

Next, we addressed the molecular mechanism by which VPM thalamic neurons drive size adaptation of the cortical somatosensory area. In embBE mice, the enlargement of the barrel-field occurs in the first postnatal week suggesting that changes in gene expression in the perinatal VPM thalamic neurons might underlie these cortical adaptations. Hence, we compared the VPM gene expression profiles in control and embBE animals at P0 and P4 (i.e. before and at the time of barrel formation) (**Fig. 5a**). A microarray analysis identified 106 genes, whose expression changed significantly in the VPM of embBE mice at P0 (**Fig. 5b**). Moreover, most of the VPM genes that changed significantly were upregulated at P0 and P4 (**Fig. 5b**). These results demonstrate that peripheral deprivation from a given sensory-modality (e.g. visual) triggers changes in gene expression in the non-deprived thalamic somatosensory VPM nucleus. These cross-modal gene expression changes could not be explained by either TCA rewiring or major sub-thalamic reorganization of thalamic afferents (**Supplementary Fig. 7**).

Among the genes differentially expressed in the VPM, the RAR-related orphan receptor B (*Rorβ*)³⁷ was within the top ten genes significantly upregulated in the VPM (1.9-fold) in embBE mice at P0 (**Fig. 5b** and **5c**). *Rorβ* was shown to be implicated in somatosensory cortical development³⁸ and in the postnatal cortex, *Rorβ* expression is layer-specific, with strong expression in layer IV neurons of primary cortical areas³⁹. In the thalamus, *Rorβ* is expressed in dLGN, VPM and auditory medial geniculate body (MGB) neurons³⁹. Between P0 and P4, *Rorβ* expression was enhanced in the VPM of control (2.4-fold) and embBE (1.6-fold) mice (**Fig. 5c**). *In situ* hybridization at P0 and P4 confirmed the upregulation of *Rorβ* expression in the VPM nucleus of embBE mice, mainly in its most dorsal lateral portion, the region where barreloids develop (**Fig. 5d**).

The expression of cholecystokinin (*Cck*), a gene enriched in the VPM⁴⁰, was unaffected in the VPM of the embBE mouse at P0 (**Supplementary Fig. 8a**). The expression of *Rorβ* in other principal thalamic nuclei, as the MGv, did not change in the embBE mouse (**Supplementary Fig. 8b**). Thus, the increase of *Rorβ* expression in the somatosensory thalamic neurons predates the enlargement of the PMBSF in embBE mice.

We next tested whether spontaneous activity might regulate *Rorβ* expression in VPM, as it is shown to modulate changes in gene expression in thalamic neurons⁴¹. We first analyzed the levels of *Rorβ* expression in VPM neurons when thalamic spontaneous activity has been artificially increased by incubation of slices with a high concentration of extracellular potassium (KCl). The increase of activity leads to a significant increase in *Rorβ* expression levels as shown by quantitative PCR (**Fig. 5e**) strongly suggesting an activity-dependent regulation of *Rorβ* expression. Then, we tested whether in the *MGv^{Kir}* mouse in which there is a prenatal increase in the frequency of Ca²⁺ waves in the VPM, without overall increase of Ca²⁺ spontaneous activity (**Supplementary Figs. 5f**), the *Rorβ* expression levels are also upregulated. Indeed, analysis of *Rorβ* expression in the *MGv^{Kir}* mouse demonstrated the upregulation of mRNA levels in VPM neurons both by quantitative PCR at E16.5 and by *in situ* hybridization at P0 (**Figs. 5f** and **5g**). Thus, prenatal *Rorβ* expression in VPM neurons might be regulated by synchronous spontaneous thalamic activity. Moreover, we found that the expression of *Rorβ* in the MGv of the *MGv^{Kir}* mouse is decreased at P0 (**Supplementary Figs. 8c** and **8d**), which is correlated with the decrease of A1 size. Altogether, these results indicate that *Rorβ* expression is positively regulated by correlated spontaneous activity.

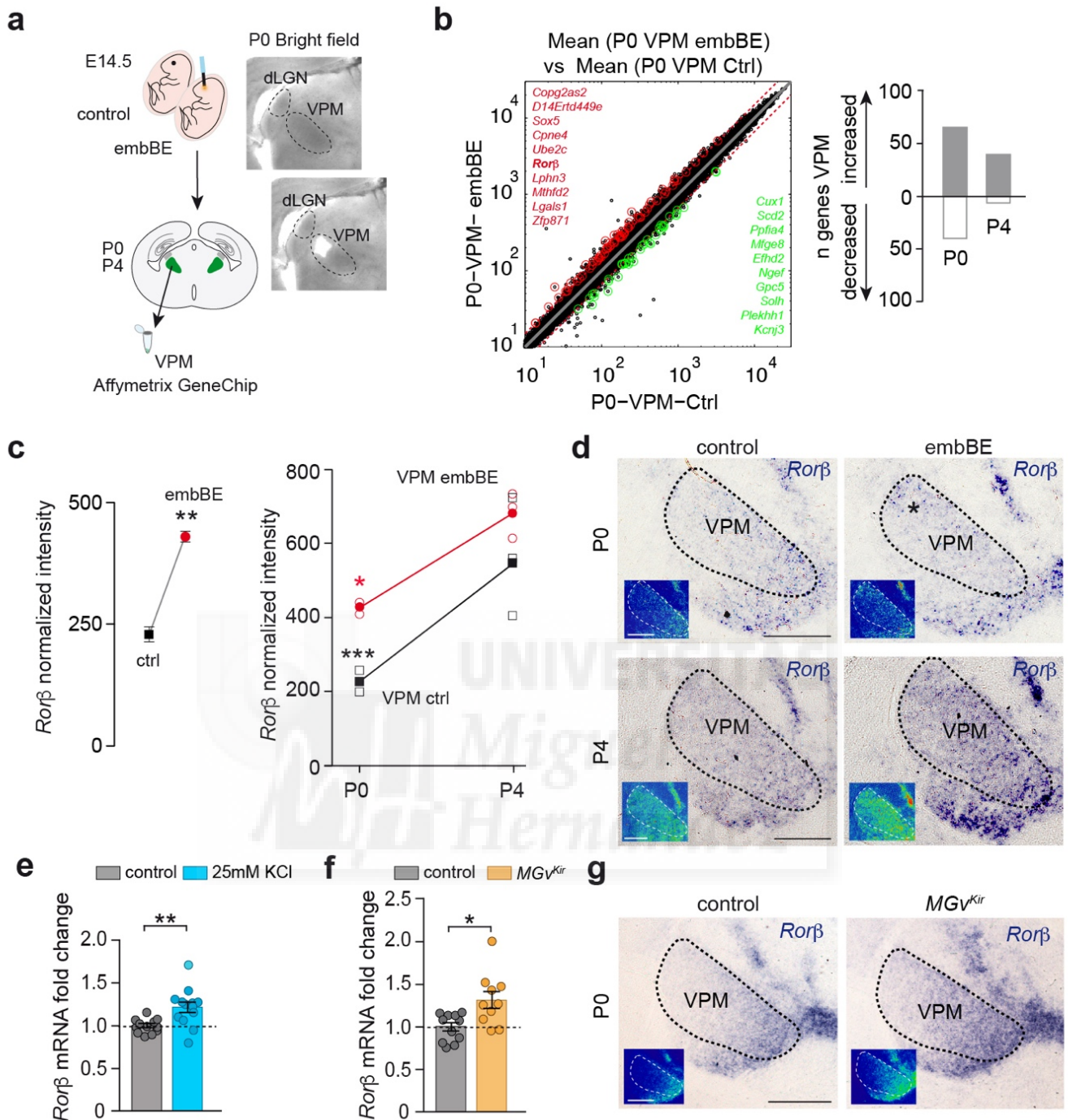


Figure 5 Both embBE and abolition of MGv waves induce changes in gene expression in the VPM thalamic nucleus. **(a)** Scheme representing the microarray experiment. VPM nuclei were collected at P0 and P4, and the RNA was extracted and processed according to the Affymetrix GeneChip protocol. Bright field image showing a coronal slice after dissection of the VPM nucleus. **(b)** Scatter-plots showing significantly upregulated or downregulated transcripts (red and green circles, respectively) with a change of ≥ 1.5 or ≤ -1.5 -fold and a P value of ≤ 0.05 at P0 and P4. In the VPM, 106 transcripts were significantly regulated at P0 and 47 at P4, with an overall

tendency towards upregulation. The top ten significantly upregulated or downregulated transcripts in the VPM are listed in red or green, respectively. (c) The expression of the *Rorβ* gene in VPM nucleus is upregulated by 1.9-fold at P0 in embBE mice (** $P = 0.008$; Two-tailed Student's t-test). Between P0 and P4, *Rorβ* expression is upregulated in the VPM 2.4-fold in control mice (** $P < 0.001$; Two-tailed Student's t-test) and 1.6-fold in embBE mice (* $p = 0.04$; Two-tailed Student's t-test). (d) *In situ* hybridization for *Rorβ* in coronal sections from control and embBE animals at P0 and P4. Note the stronger expression of *Rorβ* in the VPM area (asterisk) of embBE animals compared to the controls. (e) Quantitative real-time PCR for *Rorβ* transcripts in VPM neurons, in control media ($n = 12$) or after treatment with 25mM of KCl ($n = 13$) in acute slices at E16.5 (** $P = 0.0042$, Two-tailed Student's t-test). (f) Quantitative real-time PCR for *Rorβ* in the VPM nucleus in control ($n = 11$) and *MGv^{Kir}* ($n = 10$) mice at E16.5 (* $P = 0.01$, Mann-Whitney U-Test). (g) *In situ* hybridization for *Rorβ* in coronal sections from control ($n = 5$) and *MGv^{Kir}* ($n = 5$) animals at P0. Graphs represent mean \pm SEM. Scale bars, 300 μ m.

***Rorβ* enhances TCA branching and controls barrel-field size**

The fact that *Rorβ* is expressed more strongly in VPM neurons after enucleation and *MGv* silencing, prompted us to hypothesize that thalamic *Rorβ* might be an important element in the control of the somatosensory system developmental program. To address the role of *Rorβ*, we first examined the size of the barrel-field territory in a conditional *Nestin^{Cre/+};Rorβ^{fl/fl}* mice at P8 (**Fig. 6a**), and found that in the absence of *Rorβ* the total PMBSF area was 18.1% smaller (*Nestin^{+/+};Rorβ^{fl/fl}*: $100 \pm 3.33\%$, $n = 7$; *Nestin^{Cre/+};Rorβ^{fl/fl}*: $81.9 \pm 2.93\%$, $n = 5$; **Fig. 6b**) compared with their control littermates. Furthermore, a 21.8% decrease in the size of individual barrels was also evident at this stage at P8 (*Nestin^{+/+};Rorβ^{fl/fl}*: $100 \pm 3.49\%$, $n = 8$; *Nestin^{Cre/+};Rorβ^{fl/fl}*: $78.2\% \pm 2.19\%$, $n = 7$; **Fig. 6c**). A similar reduction was observed in *Rorβ^{-/-}* mice at P4 (**Supplementary Fig. 9**).

We next examined the effect of *Rorβ* gain of function on thalamic axon growth and branching in dissociated thalamic neurons *in vitro*. *Rorβ* overexpression in thalamic neurons provoked an increase in axon complexity and neurite length (*i-Gfp*: $880.3 \pm 68.9 \mu$ m, $n = 33$ neurons from three independent experiments; *Rorβ-i-Gfp*: $1,727 \pm 130.7 \mu$ m, $n = 29$ neurons from 3 independent experiments), as compared to control neurons (**Figs. 6d** and **6e**). To assess whether the size of the PMBSF area might be controlled by thalamic *Rorβ* expression, we induced *Rorβ* overexpression *in vivo* by *in utero* electroporation of

Results

VPM neurons at E11.5 (**Fig. 6f** and **Supplementary Fig. 10**). First we analyzed the size of *Rorβ*-overexpressing TCA terminals defining individual barrels and found that the individual barrel size was 26.8% larger in *Rorβ*-overexpressing hemispheres as compared to *i-Gfp*-electroporated control (*i-Gfp*: $100 \pm 4.4\%$, $n = 4$; *Rorβ-i-Gfp*: $126.8 \pm 5.4\%$, $n = 5$; **Fig. 6g**). Moreover, single axon reconstructions of VPM neurons showed that overexpression of *Rorβ* leads to an increased axonal terminal length (*i-Gfp*: $453.6 \pm 53.55\mu\text{m}$, $n = 12$; *Rorβ-i-Gfp*: $727.8 \pm 62.96\mu\text{m}$, $n = 11$; **Figs. 6h** and **6i**) and a larger axonal terminal area in S1 (*i-Gfp*: $100 \pm 14.57\%$, $n = 12$; *Rorβ-i-Gfp*: $193 \pm 29.3\%$, $n = 12$; **Figs. 6h** and **6i**). Thus, expression of *Rorβ* in VPM neurons influences the total PMBSF area by modifying thalamocortical axonal branching *in vivo*.



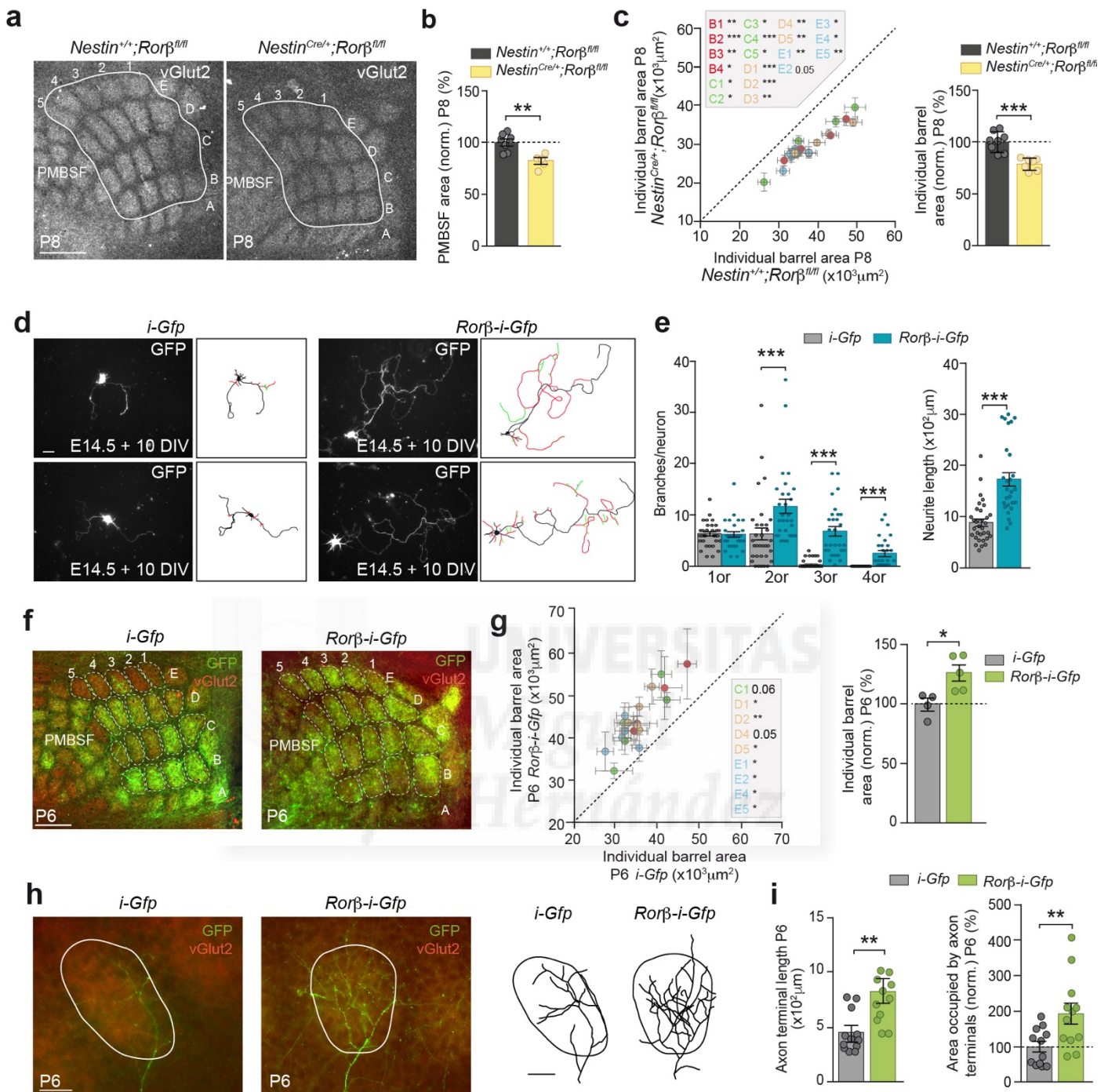


Figure 6 Thalamic *Rorβ* modulates the development of the somatosensory system and axonal branching. **(a)** vGlut2-immunostaining in tangential sections of the PMBSF from control *Nestin^{+/+};Rorβ^{fl/fl}* ($n = 8$) and *Nestin^{Cre/+};Rorβ^{fl/fl}* ($n = 7$) mice at P8. **(b)** Quantification of the total PMBSF area shown in **a** (** $P = 0.0031$; Two-tailed Student's t-test). **(c)** Plot of each individual barrel area and quantification of individual barrel area in control *Nestin^{+/+};Rorβ^{fl/fl}* ($n = 8$) and *Nestin^{Cre/+};Rorβ^{fl/fl}* ($n = 7$) brains (** $P < 0.001$; Two-tailed Student's t-test). Insert describes the barrels that are significantly reduced in the double mutant mice. **(d)** Fluorescence

Results

images and representative drawings of thalamic neurons from E14.5 mice transfected with *i-Gfp* ($n = 33$ neurons from 3 independent cultures) or *Rorβ-i-Gfp* ($n = 29$ neurons from 3 independent cultures) and analyzed at 10 days *in vitro* (DIV). **(e)** Quantification of branches per neuron at increasing branch orders ($***P < 0.001$ for 2nd, 3rd and 4th branch orders; Mann-Whitney U-Test). Quantification of the total neurite length per neuron ($***P < 0.001$; Mann-Whitney U-Test). **(f)** Flattened tangential sections showing vGlut2-immunostaining in S1 at P6 after *Rorβ-i-Gfp* ($n = 5$) electroporation compared to control *i-Gfp* electroporated brains ($n = 4$) at E11.5. Thalamic *Rorβ* overexpression induces the increase on the size of the individual barrel area. **(g)** Quantification of the individual barrel area at P6 in *i-Gfp*-electroporated and *Rorβ-i-Gfp* electroporated brains ($*P = 0.02$; Mann-Whitney U-Test). Insert describes the barrels that are significantly expanded after *Rorβ-i-Gfp* electroporation. **(h)** Coronal sections showing the axonal arborization of individual VPM neurons in a single barrel (immunolabeled with vGlut2) after electroporation with *i-Gfp* ($n = 12$ neurons from 4 brains) or *Rorβ-i-Gfp* ($n = 12$ neurons from 9 brains). Right panel: example of single axons reconstruction under the two conditions. **(i)** Quantification of the axon terminal length and the area occupied by the axon terminals shown in **h** ($**P = 0.003$ and $**P = 0.009$; Two-tailed Student's t-test). Graphs represent mean \pm SEM. Scale bars, 300 μ m for **a** and **f**, 100 μ m for **d** and 20 μ m for **h**.

DISCUSSION

Elucidating the mechanisms that control the developmental programs of the distinct sensory cortical areas is critical to understand area-specific sensory circuits and function. We report here a previously unrecognized prenatal role for the thalamus, which depends on propagation of spontaneous calcium waves among distinct sensory-modality nuclei (**Fig. 7**). These thalamic waves allow developing sensory nuclei to interact and coordinate input-specific gene expression, in turn influencing the size of primary cortical areas during development prior to sensory experience. In addition, modulating the frequency

of these waves provides a means to induce adaptations in cortical territories, as seen by the increased barrel area size in embBE and MGv^{Kir} mice.

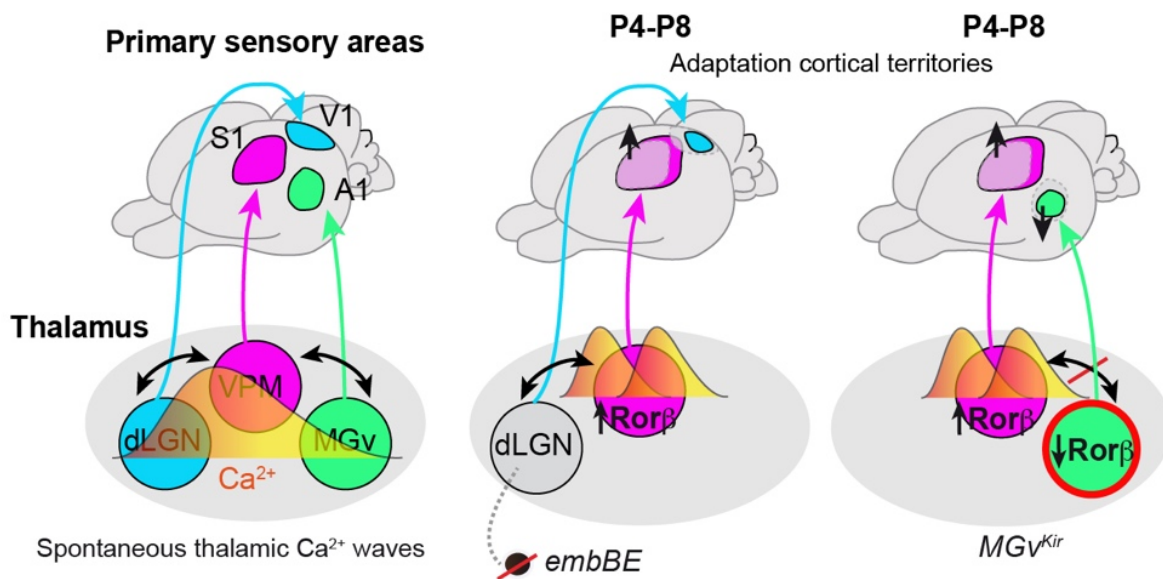


Figure 7 Thalamic mechanism of coordinating sensory cortical areas territories mediated by the existence of spontaneous calcium waves. Embryonically visual input deprived mice (embBE) show an expansion of the primary somatosensory cortex (S1) prior to sensory experience. This expansion of the barrel-field is triggered by activity-dependent gene regulation in the VPM. Both the embryonic abolishment on peripheral input or silencing thalamic waves in the auditory nucleus of the thalamus (MGv) leads to an increase wave activity in the VPM, which triggers *Rorβ* expression and an expansion of the barrel-field in S1. When the MGv auditory thalamic waves are silenced, the expression of *Rorβ* is decreased and this effect predates the reduction of the A1 area.

To define the sub-cortical mechanisms involved in the prenatal control of cortical area size, we used embBE in which the visual cortical area does not receive any input from its respective sensory modality, the eyes being removed before thalamocortical afferents reach the cortex^{42,43}. We found that the expansion of the PMBSF area and individual barrels in the adult embBE mouse is set during the first postnatal week, before the animal experiences any sensory input. These results are in line with recent observations in rodents enucleated at birth, where changes in gene expression and in the size of cortical areas were detected postnatally^{23,44}. The fact that the enlargement of S1 and the reduction of A1 described in the MGv^{Kir} mice are not correlated with a

Results

modification in the size of the respective thalamic nuclei supports a thalamo-cortical rather than a top-down⁴⁵ mechanism for plasticity. However, whether a cortico-cortical mechanism might also contribute to the cross-modal experience independent phenomenon described here remains to be tested.

Our finding that thalamic waves emerge before peripheral input reaches the thalamus (see also⁴⁶) indicates that they might be intrinsically generated in this structure. Indeed, spontaneous calcium waves persist in the absence of retinal input, although their pattern and frequency is altered if no axons from this organ are received. In sensory systems, spontaneous peripheral activity appears before the onset of natural sensory transduction and it is thought to play a key role in pattern formation^{13,32}. Thus, it is likely that spontaneous activity generated peripherally will eventually override intrinsically generated thalamic waves, as suggested by the correlated activity of successive visual relay stations recorded at early postnatal stages^{47,48}. It has been shown that silencing peripheral input postnatally⁴⁹, or in adulthood⁵⁰, does not eliminate synchronous thalamic sensory activity, suggesting that intrinsic and peripherally transmitted activity can co-exist.

Early neuronal activity can play a merely permissive role in neural circuit formation or an instructive role through specific spatiotemporal patterns of neuronal activity^{51,52}. Our results show a correlation between the increase of the frequency of the waves in the VPM, in both embBE and the *MGv^{Kir}* mice, and the enlargement of the PMBSF size. This increase in wave activity is not accompanied by a change in the total activity in individual cells in the VPM, suggesting that the patterned thalamic waves are instructive for barrel field development. Moreover, the abolishment of the calcium waves specifically in the MGv triggered a decrease of the A1 area size, again without changing the overall single cell activity, and thus supporting an instructive role of the thalamic waves in the developmental program of cortical areas.

Waves of calcium activity have been recorded in thalamic astrocytes at early postnatal stages in rat⁵³. However, it is unlikely that astrocytes contribute to the prenatal waves described here, as astrogenesis in the rodent brain takes place postnatally⁵⁴. Spontaneous thalamic waves precisely delineate thalamic nuclei, suggesting that this activity may play a role in the early definition of these territories. Moreover, we found that waves propagate from one sensory-modality thalamic nucleus to another, with robust specificity, and that they engage a large proportion of the neurons in each structure. Hence, asynchronous activity generated by individual neurons and then amplified by

connectivity through gap junctions, may recruit sufficient number of thalamic neurons to periodically initiate synchronous waves. The results from the MGv^{Kir} mouse seem to support this notion, given that conditional overexpression of *Kir2.1* in the MGv provokes the disappearance of thalamic waves. However, it remains to be tested whether sensory-modality thalamic nuclei might have a specific connexins expression patterns or stronger gap junction connectivity than adjacent thalamic regions, preventing the Ca^{2+} waves from surpassing their borders. Our results with TTX and Carbenoxolone that block thalamic calcium waves, suggest similar mechanisms of generation and propagation of thalamic and neocortical spontaneous synchronous activity^{33,34}.

Selective silencing of the waves in the auditory nucleus produces changes in the frequency of thalamic waves and in the expression of *Rorβ* in the neighboring VPM nucleus (without affecting its size), eventually provoking an enlargement of the PMBSF. Our data suggest that prenatal thalamic *Rorβ* expression is a regulator of the size of the barrel cortex representation and they show that in the VPM, *Rorβ* is upregulated embryonically in a spontaneous activity-dependent manner. Increasing the frequency of calcium waves in the VPM, either by embryonic eye enucleation or by MGv wave silencing in MGv^{Kir} mice, enhances *Rorβ* expression in the somatosensory thalamic nucleus, an event that precedes the enlargement of the PMBSF area in the S1 region. Conversely, *Rorβ* expression is downregulated in the MGv nucleus of MGv^{Kir} mice where A1 area is significantly decreased, implying a more general role of *Rorβ* in modifying cortical areas size across sensory modalities.

Our data shows that the enlargements in the S1 area size shown in the embBE and MGv^{Kir} mice are accompanied by an expansion of individual barrels, and thus they are probably caused by an increase in the complexity of the TCA branches that form the barrels. Indeed, increasing *Rorβ* levels in dissociated thalamic neurons *in vitro* or in the VPM neurons *in vivo*, lead to an increased length and complexity of TCAs. Altogether these results suggest a mechanism in which an activity-dependent regulation of *Rorβ* might control the expansion and plasticity of cortical areas by modulating TCA branching. Interestingly, an analysis of the *Rorβ* promoter identified several motifs that are putative targets for Ca^{2+} sensitive transcription factors like CREB, AP-1 and NF-κB binding sites^{41,55,56}. In addition to the effects on *Rorβ* expression, calcium waves are

Results

transmitted to the thalamocortical terminals providing a patterned form of activity that may also contribute to shape different sensory cortical territories.

In conclusion, our results highlight how spontaneous activity-dependent mechanisms play a prominent role in the early stages of development^{41,57}. We show that highly synchronized spontaneous activity in the form of Ca^{2+} waves provides a means of communication among distinct sensory systems that regulates gene expression programs and that drives cross-modal adaptation of cortical sensory area size. Moreover, such a network of communication establishes the thalamus as an important sub-cortical hub of coordination between prenatal sensory systems. This information provides novel clues to understand the compensatory cortical expansion and increased capabilities observed in congenitally blind and deaf humans⁵⁸⁻⁶⁰.



Methods

Mouse strains

Wild type mice maintained on a C57BL/6 background were used for the microarray expression profiling, whereas wild type mice maintained on an ICR/CD-1 background were used for the *in vivo* experiments, tracing studies, Ca²⁺ imaging, organotypic and primary neuronal cultures. The day on which the vaginal plug was detected was designated as E0.5. The *R26^{tdTomato}* Cre-dependent mouse line⁶¹ was obtained from Jackson Laboratories (Stock number 007908). The *R26^{GCaMP6f}* Cre-dependent mouse line was obtained from Jackson Laboratories (Stock number 024105). TCA-GFP Tg line has been described previously²⁷. The *R26^{Kir2.1-mCherry}* mouse line was generated by inserting a *CAG-lox-STOP-lox-Kir2.1-mCherry-WPRE-pA* cassette into the *Rosa26* gene locus as described below. Each of the *R26* reporter mice carry a *Rosa26* locus with a floxed STOP cassette that prevents the expression of the gene indicated. The reporter mice were crossed with an inducible thalamic-specific *Gbx2^{CreER}* line⁶² in order to generate *Gbx2^{CreER/+};R26^{X/+}* double mutant embryos. The *Gbx2^{CreER}* line expresses *CreER(T2)-ires-eGfp* under the control of the *Gbx2* promoter. Tamoxifen induction of Cre recombination in the double mutant embryos was performed by gavage administration of tamoxifen (5-7 mg dissolved in corn oil, Sigma) at E14.5 to specifically target the MGv thalamic nucleus or at E10.5 to label all principal thalamic nuclei. The *R26^{tdTomato}* were crossed with the retinal ganglion cell specific *Brn3b^{Cre}* line (courtesy of Dr. Vann Bennett) in order to generate *Brn3b^{Cre/+};R26^{tdTomato/+}* double mutant embryos. The *Rorb^{β^{-/-}}* mouse has been described previously⁶³. The *Rorb^{β^{fl}}* mice were crossed to a *Nestin^{Cre}* line previously described⁶⁴ (courtesy of Angel Barco; Jackson 003771) to conditional delete *Rorb* from all neurons. All the transgenic animals used in this study were maintained on an ICR/CD-1 or C57BL/6 genetic background and all the animals were genotyped by PCR. The Committee on Animal Research at the University Miguel Hernández approved all the animal procedures, which were carried out in compliance with Spanish and European Union regulations.

Results

Generation of the $R26^{Kir2.1-mCherry}$ mouse line

The human *Kir2.1* gene was fused to *mCherry* by removing the stop codon and inserting mCherry in frame with a NotI linker using TOPO (Invitrogen) and conventional cloning. The resulting *Kir2.1-mCherry* fusion gene was then introduced into a *Rosa26-CAG-lox-STOP-lox* targeting construct (Ai27, a gift from Hongkui Zeng, Addgene plasmid # 34630: ^{61,65}), replacing the existing insert by conventional cloning. The resulting targeting construct was electroporated into E14 ES (129 Sv Ola) cells and colonies with successful insertion were aggregated with morula-stage embryos obtained from inbred (C57BL/6 x DBA/2) F1 mice to generate chimeric mice by standard procedures. Chimeric mice were bred with C57BL/6J mice to obtain germline transmission to F1 mice. These mice were then screened for reporter expression by crossing with a Cre mouse. Two animals were selected from the same ES clone that successfully passed the construct through the germline and that displayed the expected Cre-activated expression. In the studies presented here, this line was outbred onto an ICR background to strengthen its resistance to tamoxifen treatments, as described above.

Histology

For *in situ* hybridization and immunohistochemistry at postnatal stages, mice were perfused with 4% paraformaldehyde (PFA) in PBS (0.01M), and their brains were removed and post-fixed in the same fixative overnight. For immunohistochemistry of the embryonic tissue, the brains were dissected out and fixed immediately in 4% PFA overnight. Cytochrome Oxidase (CyOx) staining was performed to label the somatosensory pathway. Cortical hemispheres were cryoprotected with sucrose and cut tangentially at 80-100 μ m with a cryotome (MICRON). Sections were incubated overnight at 37 °C in a CyOx solution (0.03% cytochrome c (Sigma), 0.05% 3,3'-diaminobenzidine (DAB; Sigma) and 4% sucrose in 0.01M PBS). Immunohistochemistry was performed on vibratome or cryotome brain sections that were first incubated for 1h at room temperature in a blocking solution containing 1% BSA (Sigma) and 0.3% Triton X-100 (Sigma) in PBS 0.01M. Subsequently, the sections were incubated overnight at 4°C with the primary antibodies: rabbit anti-vGlut2 (1:500, Synaptic Systems, #135402), chicken anti-GFP (1:3000; Aves Labs, #GFP-1020) and rat anti-RFP (1:1000 Chromotek, #5F8). The sections were then rinsed three times in PBS 0.01M and incubated for 2h at room temperature with secondary antibodies: Alexa546 donkey anti-rabbit (1:500,

ThermoFisher, #A10040), Alexa488 goat anti-chicken (1:500, ThermoFisher, #A11039), Alexa594 donkey anti-rat (1:500, ThermoFisher, #A21209), Alexa488 donkey anti-rabbit (1:500, ThermoFisher, #A21206). Finally, the sections were counterstained with the fluorescent nuclear dye Dapi (Sigma-Aldrich).

In situ hybridization was performed on 60-100 μ m vibratome sections using digoxigenin (DIG)-labeled antisense probe for *Rorb*, *Crabp2* and *Cck*. Hybridization was carried out overnight at 65°C, and after hybridization the sections were washed and incubated overnight at 4°C with an alkaline phosphatase-conjugated anti-DIG antibody (1/2500-1/4000, Roche). To visualize the RNA-probe binding, colorimetric reaction was performed for 1-2 days at room temperature in a solution containing NBT (nitro-blue tetrazolium chloride, Roche) and BCIP (5-bromo-4-chloro-3'-indoly phosphate p-toluidine salt, Roche). After development, the sections were washed and mounted in Glycerol Jelly (Merck Millipore).

Dye tracing studies

For axonal tracing at postnatal stages, animals were perfused with 4% paraformaldehyde in PBS 0.01M, and their brain was dissected out and post-fixed overnight in the same fixative. Small DiI (1,1'-dioctadecyl 3,3,3',3'-tetramethylindocarbocyanine perchlorate; Invitrogen) or DiA (4-[4-(dihexadecylamino) styryl]-N-methylpyridinium iodide) crystals were inserted into the distinct primary cortical areas, thalamus, eyes or eye cavities, the trigeminal nucleus and the inferior colliculus. The dyes were allowed to diffuse at 37°C in PFA solution for 1-4 weeks. Vibratome sections (60-100 μ m) were then counterstained with the fluorescent nuclear dye Dapi (Sigma-Aldrich).

***In utero* electroporation and *in utero* enucleation**

For *in utero* electroporation, pregnant females (E11.5) were deeply anesthetized with isoflurane to perform laparotomies. The embryos were exposed and the third ventricles of the embryonic brains were visualized through the uterus with an optic fiber light source. The full-length *Rorb* (a generous gift from Jeffrey Macklis) or a backbone construct were concentrated to 1.5 μ g μ l⁻¹ and mixed together with a plasmid encoding *Gfp* at 0.9 μ g μ l⁻¹ and 1% Fast Green (Sigma). The plasmids were injected into the third cerebral ventricle of each embryo with an injector (Nanoliter 2010, WPI). For electroporation, the negative and positive palettes were placed near the head of the

Results

embryo, and 5 square electric pulses of 45 V and 50ms were delivered through the uterus at 950ms intervals using a square pulse electroporator (CUY21 Edit: NepaGene Co., Japan). The surgical incision was then closed and embryos were allowed to develop until either E18.5 or P6. To analyze the brain at E18.5 it was removed and fixed directly in 4% PFA, whereas P6 mice were first perfused with 4% PFA and then processed for further analysis.

For *in utero* enucleation, the same surgical procedure was carried out on pregnant females at E14.5 but once the uterus was exposed, both eyes were cauterized in half of the embryos of each litter. The surgical incision was closed and embryos were allowed to develop until postnatal stages.

Postnatal whisker trimming

To perform postnatal whisker trimming in enucleated and control mice, all the whiskers were cut to the level of the guard hairs on both sides of the face daily from P0 to P4. Pups were perfused with 4% PFA, and their brain was dissected out and post-fixed overnight in the same fixative.

Measurement of brain areas and data analysis

ImageJ software was used to measure the size of the thalamic nuclei, the individual barrels and the PMBSF areas. For PMBSF and individual barrel areas data was normalized. In the case of the individual barrels, each barrel area from a given experimental condition was normalized to the corresponding barrel mean area in the control, which was considered as 1. To ensure consistent analysis, we choose rows B1-3, C1-3, D1-4 and E1-4 for mice analyzed at P4, while B1-4, C1-5, D1-5 and E1-5 were chosen to analyze older mice. These barrels were constantly present in the slices obtained after processing the brains. For the quantification of the individual barrel area in the *in utero Rorb* electroporations, brains with target electroporation in the VPM nucleus were selected. The electroporated side was coronally cut for the thalamus and tangentially cut for analyzing the cortex. A TCA-GFP mouse was used to measure the size of the primary cortical areas and the area and volume of the distinct thalamic nuclei. In order to quantify the size of cortical areas, TCA-GFP (control, embBE and MGV^{Kir}) mice were perfused and directly process to obtain images under the stereo fluorescent microscope (Leica MZ10 F). Coronal serial slices of 80-100 μ m were obtained from TCA-GFP brains and distinct thalamic nuclei were immunolabel with Gfp and Vglut2 in order to better detect

the structures. NeuroLucida explorer® from MBF Bioscience was used to quantify the volume of dLGN, VPM and MGv thalamic nuclei.

Organotypic thalamic cultures

To analyse *Rorb* expression after KCl treatment *ex vivo*, pregnant mice were sacrificed and their embryos were recovered at E16.5. Organotypic slice cultures of embryonic thalamus were prepared as previously described⁶⁶. Thalamic coronal slices were placed for 5hr at 37°C with 5% CO₂ in maintenance medium (Glutamax 1×, 45% glucose solution 50mM, penicillin/streptomycin 100U per microliter, 2% B27 and 95% Neurobasal). For the experimental condition 20mM of KCl was added. After incubation, and in order to perform RNA extraction and qPCR, VPM nuclei were dissected out and collected in pulls of 3 embryos.

Microdissection of thalamic nuclei

To collect tissue from the VPM nucleus at neonatal stages, animals were sacrificed and their brain was dissected out in RNase-free conditions to prevent RNA degradation. Vibratome sections (200µm) were obtained and collected in ice-cold oxygenated aCSF (117mM NaCl, 4.7mM KCl, 1.2mM MgCl₂, 2.5mM CaCl₂, 1.2mM NaH₂PO₄, 25mM NaHCO₃ and 0.45% D-glucose), and the thalamic nucleus was rapidly microdissected under a microscope. The tissue was maintained overnight at 4 °C in RNA-Later (Sigma) and stored at -80°C for subsequent RNA extraction.

Affymetrix Microarray

For microarray hybridization, RNA was extracted from the tissue collected using the RNeasy Mini Kit (Qiagen), including a DNaseI step. Complimentary RNAs (two rounds of amplification) were hybridized to Affymetrix GeneChip Mouse Genome arrays 430 v2, and the signal intensities were analyzed using Partek Genomics suites (Partek, St. Louis, MI, USA) and Matlab (The MathWorks Inc, Natick, MA, USA). The data were normalized using RMA and changes in gene expression > 1.5-fold with a p-value < 0.05 were considered to reflect a significant difference in expression.

Purification of total RNA and quantitative real-time PCR

VPM thalamic nucleus was dissected from coronal slices of 300µm at E16.5. The total RNA was isolated using the kit NucleoSpin® RNA (Macherey-Nagel, Düren, Germany),

Results

washed with the recommended buffers and eluted with RNase-free water by centrifugation. Quantification was done by optical density (OD) using a Nanodrop 2000 Spectrophotometer (Thermo Scientific, Wilmington, DE, USA) and the purity was evaluated by measuring the ratio of OD at 260 and 280nm. cDNA was obtained from 1µg of total RNA using the specific protocol for First-Strand cDNA synthesis in two-step RT-PCR (Thermo Scientific Random hexamer #SO142, RevertAid Reverse Transcriptase #EP0441, RiboLock RNase Inhibitor #EO0381, dNTP Mix #R0191) and stored at -20°C. Quantitative PCR was performed in a StepOnePlus™ Real-Time PCR System (Applied Biosystems, Foster City, CA, USA) using the MicroAmp® fast 96-well reaction plate (Applied Biosystems) and the Power SYBR® Green PCR Master Mix (Applied Biosystems). The target *Rorb* gene expression (Gene ID: 225998) was determined by the primers 5'-TTGTGGCGATAAATCCTCCG-3' and 5'-TGCTGGCTCCTCCTGAAGAAT-3'. As a control we have used a housekeeping gene *Gapdh*, (Gene ID: 14433) determined by the primers 5'-CGGTGCTGAGTATGTCGTGGAGT-3' and 5'-CGTGGTTCACACCCATCACAAA-3'. A master mix was prepared for each primer set containing the appropriate volume of SYBR® Green, primers and template cDNA. All reactions were performed in duplicate as follows: 95°C for 30s and 45 cycles at 95°C for 5s and 60°C for 35s. The amplification efficiency for each primer pair and the cycle threshold (Ct) were determined automatically by the StepOne™ Software, v2.2.2 (Applied Biosystems). *Rorb* transcript level was represented relative to the *Gapdh* signal adjusting for the variability in cDNA library preparation.

Primary thalamic cell culture and transfection

To establish primary thalamic neuron cultures, pregnant mice were sacrificed and their embryos were recovered at E14.5. The thalamus was dissected, collected in Krebs solution, trypsinized, and then dissociated with a fire-polished Pasteur pipette. 200000-300000 cells/well were finally plated with plating medium (sodium pyruvate 1mM, Glutamax 1×, 45% glucose solution 50mM, penicillin/streptomycin 100U per microliter, 10% FBS, and 86% MEM). Thalamic neurons were transfected using Amaxa™ Basic Nucleofector™ Kit (VPI-1003) with 1µg of the full-length *Rorb* construct together with 1µg of a plasmid encoding *Gfp*. Controls were transfected with 1µg of a backbone construct together with 1µg of *Gfp*. After transfection, cultures were placed for ten days

in maintenance medium (Glutamax 1×, 45% glucose solution 50mM, penicillin/streptomycin 100U per microliter, 2% B27 and 95% neurobasal) at 37°C with 5% CO₂. Maintenance medium was carefully replaced every 2 days.

Quantification of axonal branches and axonal length

ImageJ software (NeuronJ plugin) was used to analyze axon branching *in vitro*. Random fields were selected from three independent experiments. Axonal branches from neurons transfected with *i-Gfp* or *Rorβ-i-Gfp* were measured. Branches order criteria was determined by following the number of neurite bifurcations from the cell body. Total neurite length was determined by summing the lengths of all neurites for each neuron. For single axon reconstructions of VPM electroporated neurons *in vivo*, coronal sections of 60μm were cut in a vibratome and single terminals of somatosensory TCAs were reconstructed in an individual barrel from the PMBSF using NeuroLucida explorer® from MBF Bioscience. The area occupied by the TCA terminals was measured by outlining the tips of each afferent with the ImageJ software.

Calcium imaging in thalamocortical slices

Pregnant adult mice were sacrificed by decapitation after administering isoflurane, and their embryos were rapidly extracted and decapitated. Postnatal (P0-P3) and embryonic (E13.5-E18.5) mouse brains were immediately dissected out and kept in an ice-cold gassed slicing solution (95% O₂ and 5% CO₂) containing (in mM): 2.5 KCl, 7 Mg SO₄, 0.5 CaCl₂, 1 NaH₂PO₄, 26 Na₂HCO₃, 11 glucose and 228 sucrose. Oblique vibratome slices (300-350μm thick: VT1200 Leica Microsystems Germany) were obtained along two axes: 1) 45 ± 2° to preserve the somatosensory (VB) and visual (dLGN) thalamocortical nuclei and their connectivity; and 2) – 45 ± 2° to preserve the auditory (MGv) and somatosensory (VB) thalamic nuclei. During the recovery period, the slices were placed at room temperature (RT) in standard aCSF (119 NaCl, 5 KCl, 1.3 Mg SO₄, 2.4 CaCl₂, 1 NaH₂PO₄, 26 Na₂HCO₃, 11 glucose) saturated by gassing with 95% O₂ and 5% CO₂.

For dye loading, the slices were incubated for 30-45min in 2ml of gassed aCSF (35–37°C) with 10μl Cal520TM AM (AAT Bioquest) calcium dye (1mM in DMSO + 20% pluronic acid). The loaded slices were left for 1 hour at RT in gassed aCSF. The slices from *Gbx2*^{CreER/+}; *R26*^{GCaMP6-EGFP/+} mice did not require incubation. Then, the slices were

Results

placed in a recording chamber of an upright Leica DM LFSA stage perfused (3.7ml per minute) with warmed (32°C) and gassed aCSF. Time lapse recording of Ca²⁺ dynamics was obtained through water immersion objectives (L 10x/0.30 N.A. Leica, L 20x/0.50 Leica) or dry objectives (HCX PL FLUOTAR 5x/0.15 Leica, PL FLUOTAR 2.5x/0.07) after exciting the slices at 492nm with a mercury arc lamp. We acquired images with a digital CCD camera (Hamamatsu ORCA R2 C10600 10B), using an interframe interval of 250ms and an exposure time of 200ms. The length of each time lapse recording was 3,000 frames.

Pharmacological experiments were performed adding drugs in the warmed (32°C), bubbled (95% O₂ and 5% CO₂) and perfused (3.7ml per minute) aCSF in the recording chamber. Carbenoxolone (Carbenoxolone disodium salt, Sigma) was applied at a concentration of 50µM. Tetrodotoxin (Abcam) was prepared at a concentration of 1 µM and mefloquine (Mefloquine Hydrochloride, Sigma-Aldrich) at 25µM. High potassium concentration was applied by adding KCl to the aCSF (containing 5mM of KCl) to reach 9, 10 and 12mM concentrations. Recordings were performed 5 minutes after the start of drug application.

Data analysis of calcium imaging

Data were exported from Leica MM Fluor 1.6.0TM acquisition software as 3,000 frame-long time-lapse sequences of TIFF format images and analyzed in ImageJ and MatlabTM. Fluorescence traces of individual cells (recorded with L 20x/0.50 objective) were analyzed with custom developed routines in MatlabTM 67 and the calcium events were identified using asymmetric least square baselines and Schmitt trigger thresholds. We used 5% of the baseline noise as the upper threshold and 2% as the lower threshold. Onset and offset identification allowed raster plots to be generated and the extent of network correlation to be estimated. We define “co-active” as meaning those onset transients occurring simultaneously within ± 1 frame time window (500ms). The *correlation test* identified incidences where a significant fraction of the network’s cells were active synchronously. The minimal size of these groups for each recording session was defined by the corresponding simulated random sets. For each of the 1,000 random datasets, we counted the number of co-active cells within each time-window and this defined a distribution of the expected counts of co-active cells due to random activity. The threshold for significant group co-activation was set as the 95th percentile of this distribution.

Temporal color-coding was performed using freely available Temporal-Color Coder ImageJ plugin.

Statistics

Statistical analysis was carried out in GraphPad Prism6TM and MatlabTM. Data are presented as mean and SEM. Statistical comparison between groups was performed using unpaired two-tailed Student's *t* test or Mann-Whitney U-Test non-parametric two-tailed test when data failed a Kolmogorov-Smirnov or a Shapiro Wilk normality tests. For the whisker trimming experiments, a Two-way ANOVA test with Tukey post hoc analysis was used when interaction was not significant. For the drug application experiments Wilcoxon matched-pairs signed rank test was used. Simple effect analysis was performed when interaction was significant. P values < 0.05 were considered statistically significant and set as follows **P* < 0.05; ***P* < 0.01 and ****P* < 0.001. No statistical methods were used to predetermine the sample size, but our sample sizes are considered adequate for the experiments and consistent with the literature. The mice were not randomized. The investigators were blinded to sample identity except in the calcium activity experiments.

Data Availability

Microarray data has been deposited in the NCBI GEO database as GEO GSE76767.

References

1. Miyashita-Lin, E., Hevner, R., Wassarman, K., Martinez, S. & Rubenstein, J. Early neocortical regionalization in the absence of thalamic innervation. *Science* **285**, 906-909 (1999).
2. O'Leary, D.D., Chou, S.J. & Sahara, S. Area patterning of the mammalian cortex. *Neuron* **56**, 252-269 (2007).
3. Grove, E.A. & Fukuchi-Shimogori, T. Generating the cerebral cortical area map. *Annu Rev Neurosci* **26**, 355-380 (2003).
4. Garel, S., Huffman, K.J. & Rubenstein, J.L. Molecular regionalization of the neocortex is disrupted in Fgf8 hypomorphic mutants. *Development* **130**, 1903-1914 (2003).
5. Rakic, P. Specification of cerebral cortical areas. *Science* **241**, 170-176 (1988).
6. Erzurumlu, R.S., Murakami, Y. & Rijli, F.M. Mapping the face in the somatosensory brainstem. *Nat Rev Neurosci* **11**, 252-263 (2010).
7. Erzurumlu, R.S. & Gaspar, P. Development and critical period plasticity of the barrel cortex. *Eur J Neurosci* **35**, 1540-1553 (2012).
8. Karlen, S. & Krubitzer, L. Effects of Bilateral Enucleation on the Size of Visual and Nonvisual Areas of the Brain. *Cerebral Cortex* **19**, 1360-1371 (2009).
9. Larsen. What are the effects of severe visual impairment on the cortical organization and connectivity of primary visual cortex? *Frontiers in Neuroanatomy* (2009).
10. Espinosa, J.S. & Stryker, M.P. Development and plasticity of the primary visual cortex. *Neuron* **75**, 230-249 (2012).
11. Huberman, A.D., Speer, C.M. & Chapman, B. Spontaneous retinal activity mediates development of ocular dominance columns and binocular receptive fields in v1. *Neuron* **52**, 247-254 (2006).
12. Ackman, J.B. & Crair, M.C. Role of emergent neural activity in visual map development. *Curr Opin Neurobiol* **24**, 166-175 (2014).
13. Meister, M., Wong, R.O., Baylor, D.A. & Shatz, C.J. Synchronous bursts of action potentials in ganglion cells of the developing mammalian retina. *Science* **252**, 939-943 (1991).
14. Feller, M.B., Wellis, D.P., Stellwagen, D., Werblin, F.S. & Shatz, C.J. Requirement for cholinergic synaptic transmission in the propagation of spontaneous retinal waves. *Science* **272**, 1182-1187 (1996).

15. Chou, S.J., *et al.* Geniculocortical input drives genetic distinctions between primary and higher-order visual areas. *Science* **340**, 1239-1242 (2013).
16. Lokmane, L., *et al.* Sensory map transfer to the neocortex relies on pretarget ordering of thalamic axons. *Curr Biol* **23**, 810-816 (2013).
17. Karlen, S.J., Kahn, D.M. & Krubitzer, L. Early blindness results in abnormal corticocortical and thalamocortical connections. *Neuroscience* **142**, 843-858 (2006).
18. Bronchti, G., *et al.* Auditory activation of "visual" cortical areas in the blind mole rat (*Spalax ehrenbergi*). *Eur J Neurosci* **16**, 311-329 (2002).
19. Chabot, N., *et al.* Subcortical auditory input to the primary visual cortex in anophthalmic mice. *Neurosci Lett* **433**, 129-134 (2008).
20. Zembrzycki, A., Chou, S.J., Ashery-Padan, R., Stoykova, A. & O'Leary, D.D. Sensory cortex limits cortical maps and drives top-down plasticity in thalamocortical circuits. *Nat Neurosci* **16**, 1060-1067 (2013).
21. Rauschecker, J.P., Tian, B., Korte, M. & Egert, U. Crossmodal changes in the somatosensory vibrissa/barrel system of visually deprived animals. *Proc Natl Acad Sci U S A* **89**, 5063-5067 (1992).
22. Zheng, D. & Purves, D. Effects of increased neural activity on brain growth. *Proc Natl Acad Sci U S A* **92**, 1802-1806 (1995).
23. Fetter-Pruneda, I., *et al.* Shifts in developmental timing, and not increased levels of experience-dependent neuronal activity, promote barrel expansion in the primary somatosensory cortex of rats enucleated at birth. *PLoS One* **8**, e54940 (2013).
24. Dehay, C., Horsburgh, G., Berland, M., Killackey, H. & Kennedy, H. Maturation and connectivity of the visual cortex in monkey is altered by prenatal removal of retinal input. *Nature* **337**, 265-267 (1989).
25. Bronchti, G., Schonenberger, N., Welker, E. & Van der Loos, H. Barreffield expansion after neonatal eye removal in mice. *Neuroreport* **3**, 489-492 (1992).
26. Kozanian, O.O., Abbott, C.W. & Huffman, K.J. Rapid Changes in Cortical and Subcortical Brain Regions after Early Bilateral Enucleation in the Mouse. *PLoS One* **10**, e0140391 (2015).
27. Mizuno, H., *et al.* NMDAR-regulated dynamics of layer 4 neuronal dendrites during thalamocortical reorganization in neonates. *Neuron* **82**, 365-379 (2014).
28. Bechara, A., *et al.* Hoxa2 Selects Barrelette Neuron Identity and Connectivity in the Mouse Somatosensory Brainstem. *Cell reports* **13**, 783-797 (2015).

Results

29. Woolsey, T.A. & Van der Loos, H. The structural organization of layer IV in the somatosensory region (SI) of mouse cerebral cortex. The description of a cortical field composed of discrete cytoarchitectonic units. *Brain Res* **17**, 205-242 (1970).
30. Landers, M., Haidarliu, S. & Philip Zeigler, H. Development of rodent macrovibrissae: effects of neonatal whisker denervation and bilateral neonatal enucleation. *Somatosensory & motor research* **23**, 11-17 (2006).
31. Tritsch, N.X., *et al.* Calcium action potentials in hair cells pattern auditory neuron activity before hearing onset. *Nat Neurosci* **13**, 1050-1052 (2010).
32. Blankenship, A. & Feller, M. Mechanisms underlying spontaneous patterned activity in developing neural circuits. *Nat Rev Neurosci* **11**, 18-29 (2010).
33. Yuste, R., Nelson, D.A., Rubin, W.W. & Katz, L.C. Neuronal domains in developing neocortex: mechanisms of coactivation. *Neuron* **14**, 7-17 (1995).
34. Barnett, H.M., *et al.* Relationship between individual neuron and network spontaneous activity in developing mouse cortex. *J Neurophysiol* **112**, 3033-3045 (2014).
35. Lacar, B., Young, S.Z., Platel, J.C. & Bordey, A. Gap junction-mediated calcium waves define communication networks among murine postnatal neural progenitor cells. *Eur J Neurosci* **34**, 1895-1905 (2011).
36. Elias, L.A. & Kriegstein, A.R. Gap junctions: multifaceted regulators of embryonic cortical development. *Trends Neurosci* **31**, 243-250 (2008).
37. Becker-Andre, M., Andre, E. & DeLamarter, J.F. Identification of nuclear receptor mRNAs by RT-PCR amplification of conserved zinc-finger motif sequences. *Biochem Biophys Res Commun* **194**, 1371-1379 (1993).
38. Jabaudon, D., J Shnider, S., J Tischfield, D., J Galazo, M. & Macklis, J.D. ROR Induces Barrel-like Neuronal Clusters in the Developing Neocortex. *Cerebral Cortex* **22**, 996-1006 (2012).
39. Nakagawa, Y. & O rsquo Leary, D.D.M. Dynamic Patterned Expression of Orphan Nuclear Receptor Genes RORalpha and RORbeta in Developing Mouse Forebrain. *Developmental neuroscience* **25**, 234-244 (2003).
40. Gezelius, H. & Lopez-Bendito, G. Thalamic neuronal specification and early circuit formation. *Dev Neurobiol* (2016).
41. Mire, E., *et al.* Spontaneous activity regulates Robo1 transcription to mediate a switch in thalamocortical axon growth. *Nature neuroscience*, 1-12 (2012).
42. Lopez-Benditó, G. & Molnár, Z. Thalamocortical development: how are we going to get there? *Nature Reviews Neuroscience* **4**, 276-289 (2003).

43. Hensch, T.K. Critical period plasticity in local cortical circuits. *Nat Rev Neurosci* **6**, 877-888 (2005).
44. Dye, C.A., Abbott, C.W. & Huffman, K.J. Bilateral enucleation alters gene expression and intraneocortical connections in the mouse. *Neural Dev* **7**, 5 (2012).
45. Zembrzycki, A., Perez-Garcia, C.G., Wang, C.F., Chou, S.J. & O'Leary, D.D. Postmitotic regulation of sensory area patterning in the mammalian neocortex by Lhx2. *Proc Natl Acad Sci U S A* **112**, 6736-6741 (2015).
46. Pouchelon, G., Frangeul, L., Rijli, F.M. & Jabaudon, D. Patterning of pre-thalamic somatosensory pathways. *Eur J Neurosci* **35**, 1533-1539 (2012).
47. Ackman, J.B., Burbridge, T.J. & Crair, M.C. Retinal waves coordinate patterned activity throughout the developing visual system. *Nature* **490**, 219-225 (2012).
48. Mooney, R., Penn, A.A., Gallego, R. & Shatz, C.J. Thalamic relay of spontaneous retinal activity prior to vision. *Neuron* **17**, 863-874 (1996).
49. Weliky, M. Correlational Structure of Spontaneous Neuronal Activity in the Developing Lateral Geniculate Nucleus in Vivo. *Science (New York, NY)* **285**, 599-604 (1999).
50. Linden, M.L., Heynen, A.J., Haslinger, R.H. & Bear, M.F. Thalamic activity that drives visual cortical plasticity. *Nat Neurosci* **12**, 390-392 (2009).
51. Stellwagen, D. & Shatz, C.J. An instructive role for retinal waves in the development of retinogeniculate connectivity. *Neuron* **33**, 357-367 (2002).
52. Xu, H.P., *et al.* An instructive role for patterned spontaneous retinal activity in mouse visual map development. *Neuron* **70**, 1115-1127 (2011).
53. Parri, H.R., Gould, T.M. & Crunelli, V. Spontaneous astrocytic Ca²⁺ oscillations in situ drive NMDAR-mediated neuronal excitation. *Nat Neurosci* **4**, 803-812 (2001).
54. Schitine, C., Nogaroli, L., Costa, M.R. & Hedin-Pereira, C. Astrocyte heterogeneity in the brain: from development to disease. *Frontiers in cellular neuroscience* **9**, 76 (2015).
55. Benito, E. & Barco, A. The neuronal activity-driven transcriptome. *Mol Neurobiol* **51**, 1071-1088 (2015).
56. Castillo-Paterna, M., *et al.* DCC functions as an accelerator of thalamocortical axonal growth downstream of spontaneous thalamic activity. *EMBO Rep* **16**, 851-862 (2015).
57. Spitzer, N. Electrical activity in early neuronal development. *Nature* **444**, 707-712 (2006).

Results

58. Cohen, L.G.L., *et al.* Functional relevance of cross-modal plasticity in blind humans. *Nature* **389**, 180-183 (1997).
59. Finney, E.M., Fine, I. & Dobkins, K.R. Visual stimuli activate auditory cortex in the deaf. *Nat Neurosci* **4**, 1171-1173 (2001).
60. Sadato, N., *et al.* Activation of the primary visual cortex by Braille reading in blind subjects. *Nature* **380**, 526-528 (1996).
61. Madisen, L., *et al.* A robust and high-throughput Cre reporting and characterization system for the whole mouse brain. *Nat Neurosci* **13**, 133-140 (2010).
62. Chen, L., Guo, Q. & Li, J. Transcription factor Gbx2 acts cell-nonautonomously to regulate the formation of lineage-restriction boundaries of the thalamus. *Development* **136**, 1317-1326 (2009).
63. Liu, H., *et al.* An isoform of retinoid-related orphan receptor beta directs differentiation of retinal amacrine and horizontal interneurons. *Nat Commun* **4**, 1813 (2013).
64. Tronche, F., *et al.* Disruption of the glucocorticoid receptor gene in the nervous system results in reduced anxiety. *Nat Genet* **23**, 99-103 (1999).
65. Madisen, L., *et al.* A toolbox of Cre-dependent optogenetic transgenic mice for light-induced activation and silencing. *Nature neuroscience* **15**, 793-802 (2012).
66. López-Bendito, G., *et al.* Tangential neuronal migration controls axon guidance: a role for neuregulin-1 in thalamocortical axon navigation. *Cell* **125**, 127-142 (2006).
67. Carron, R., *et al.* Early hypersynchrony in juvenile PINK1(-)/(-) motor cortex is rescued by antidromic stimulation. *Frontiers in systems neuroscience* **8**, 95 (2014).

Acknowledgements

We are grateful M. Docquier and members of the NCCR genomics platform for their help with the expression arrays, to Denis Jabaudon for advice and help with the RNA extraction from thalamic structures, and to James Li for sharing the *Gbx2^{CreER}* mice. We are thankful to Oscar Marin, Angela Nieto, Paola Arlotta and members of G. López-Bendito's laboratory for stimulating discussions and comments. V. M-J holds a "Severo Ochoa" PhD fellowship and N. A-B a FPI fellowship, both from the MINECO. C.M. held a JAE-Predoc fellowship from the CSIC, and H.G. held postdoctoral fellowships from the Swedish Research council and Brain Foundation. Supported by the Swiss National Science Foundation (31003A_149573) and the Novartis Research Foundation to F.M.R., the JSPS KAKENHI (JP16H06459) to T.I and by the Spanish MINECO BFU2012-34298 and BFU2015-64432-R, and two European Commission Grants ERC-2009-StG-20081210 and ERC-2014-CoG-647012 to G.L-B. G. L-B is an EMBO YIP Investigator and a FENS-Kavli scholar.

Authors Contributions

G.L-B conceived the idea. V.M-J performed the experiments related to the embryonic enucleation mouse model, analysis of analysis of *Brn3b^{Cre};R26^{tdTomato}*, *Rorβ* knockout and and *Nestin^{Cre};Rorβ^{fl}* mice, and performed the dissociated thalamic cultures. N.A-B, performed the experiments related to the spontaneous activity in the MGv silenced mouse model. A.F performed the Ca²⁺ imaging experiments. C.M and V.M-J performed the microarray assay. H.G., S.D. and F.M.R generated the *R26^{Kir2.1-mCherry}* mouse line. B.A and V.M-J performed the *in utero* electroporations. L.R-M performed mice perfusions and the *in situ* hybridization experiments. R.S genotyped the mouse colonies, generated the *in situ* probes and plasmids for electroporation and performed the quantitative PCRs. O.S analyzed the microarray data. T.I provided the TCA-GFP Tg mouse line. R.Sc provided the *Rorβ* conditional mouse. M.R and S.N provided the *Rorβ* full knockout brains. V.M-J, A.F and N.A-B conducted the data analysis and M.V, F.M.R and G.L-B wrote the paper.

Conflict of Interest

The authors have no conflict of interest to declare.

Prenatal thalamic waves regulate cortical area size prior to sensory processing

Verónica Moreno-Juan^{1,9}, Anton Filipchuk^{1,9}, Noelia Antón-Bolaños^{1,9}, Cecilia Mezzera^{1,2}, Henrik Gezelius¹, Belen Andrés¹, Luis Rodríguez-Malmierca¹, Rafael Susín¹, Olivier Schaad^{3,4}, Michael Rutlin^{5,6}, Sacha Nelson⁵, Sebastien Ducret⁷, Miguel Valdeolmillos^{1,8}, Filippo M. Rijli^{7,8} and Guillermina López-Bendito^{1,*}

¹Instituto de Neurociencias de Alicante, Universidad Miguel Hernández-Consejo Superior de Investigaciones Científicas (UMH-CSIC), Sant Joan d'Alacant, Spain

²Champalimaud Neuroscience Programme, Champalimaud Centre for the Unknown, 1400-038 Lisbon, Portugal

³NCCR frontiers in Genetics, University of Geneva, Geneva, Switzerland

⁴Department of Biochemistry, Sciences II, University of Geneva, Geneva, Switzerland

⁵Department of Biology and National Center for Behavioral Genomics, Brandeis University, Waltham, MA 02454, USA

⁶Department of Biochemistry and Molecular Biophysics, HHMI, Columbia University Medical Center, New York, NY 10032, USA

⁷Friedrich Miescher Institute for Biomedical Research, Maulbeerstrasse 66, 4058 Basel, Switzerland

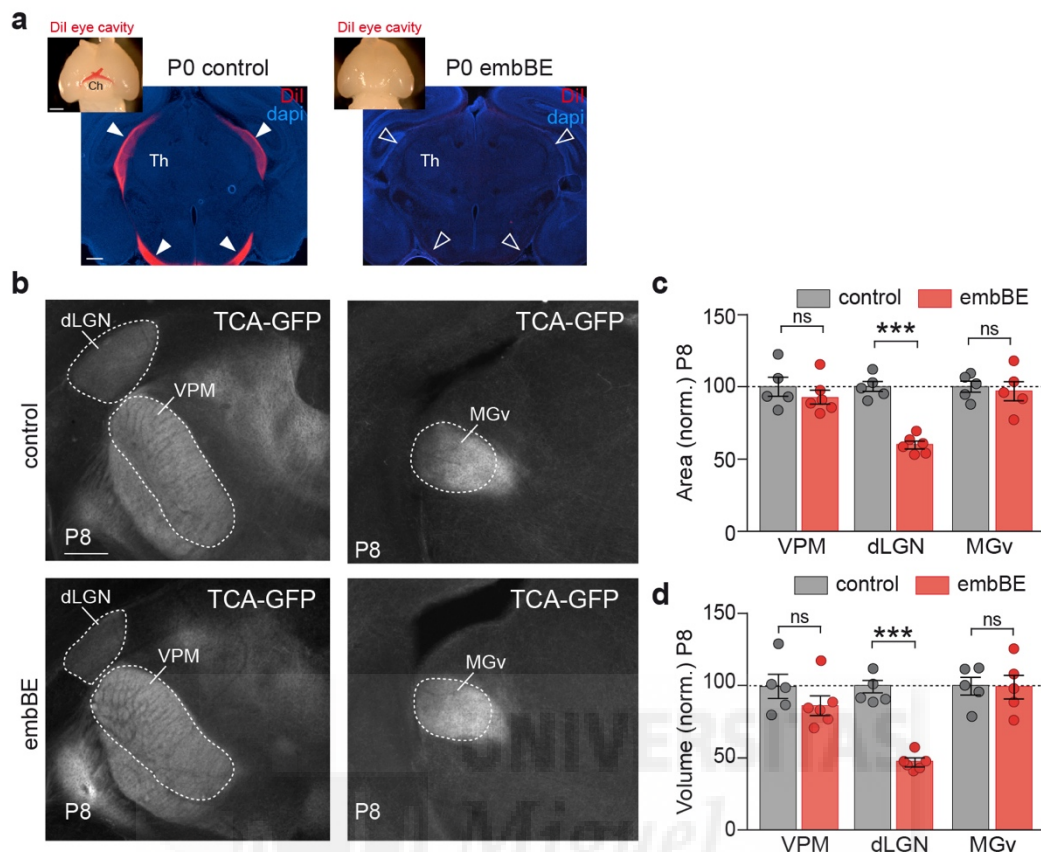
⁸These authors contributed equally to this work

⁹Co-first author

*Correspondence to: g.lbendito@umh.es

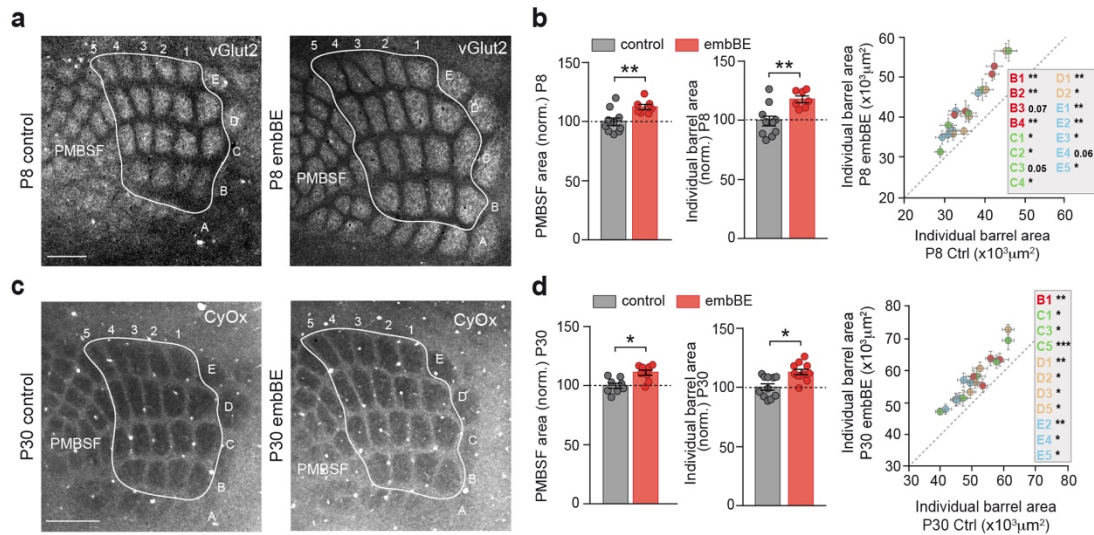
Nature Communications 2017 Feb 3;8:14172. Doi: 10.1038/ncomms14172

SUPPLEMENTARY INFORMATION

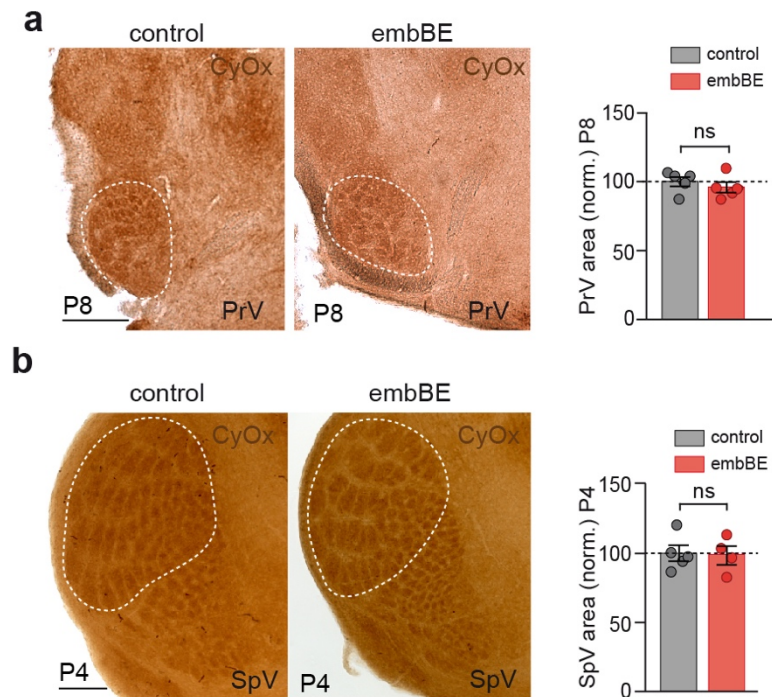


Supplementary Figure 1 Embryonic complete ablation of the retinal input (embBE) triggers a reduction in the dLGN size at P8. **(a)** Bilateral DiI injections into the eye cavity of control and embBE mice at P0 revealing the efficiency of the *in utero* enucleation. **(b)** Coronal sections from the TCA-GFP transgenic mice showing the area of the dLGN, VPM and MGv nuclei in control and embBE conditions. **(c)** Quantification of the area size for each principal thalamic nucleus shown in **b** (dLGN: control: $100 \pm 3.61\%$, $n = 5$; embBE: $60.18 \pm 2.46\%$, $n = 6$ *** $P < 0.001$. VPM: control: $100 \pm 6.54\%$, $n = 5$; embBE: 92.84 ± 4.89 , $n = 6$; $P = 0.39$. MGv: control: $100 \pm 3.76\%$, $n = 6$; embBE: $97.29 \pm 6.63\%$, $n = 5$; $P = 0.73$.; Two-tailed Student's t-test). **(d)** Quantification of the dLGN, VPM and MGv volume at P8 (dLGN: control: $100 \pm 4.48\%$, $n = 5$; embBE: $46.96 \pm 2.35\%$ $n = 6$; *** $P < 0.001$. VPM: control: $100 \pm 8.49\%$, $n = 5$; embBE: 86.46 ± 6.85 , $n = 6$; $P = 0.24$. MGv: control: $100 \pm 6.32\%$; embBE: $99.8 \pm 8.55\%$; $P = 0.98$; Two-tailed Student's t-test). Graphs represent mean \pm SEM. Scale bars, $300\mu\text{m}$ (1mm, insets in **a**).

Results

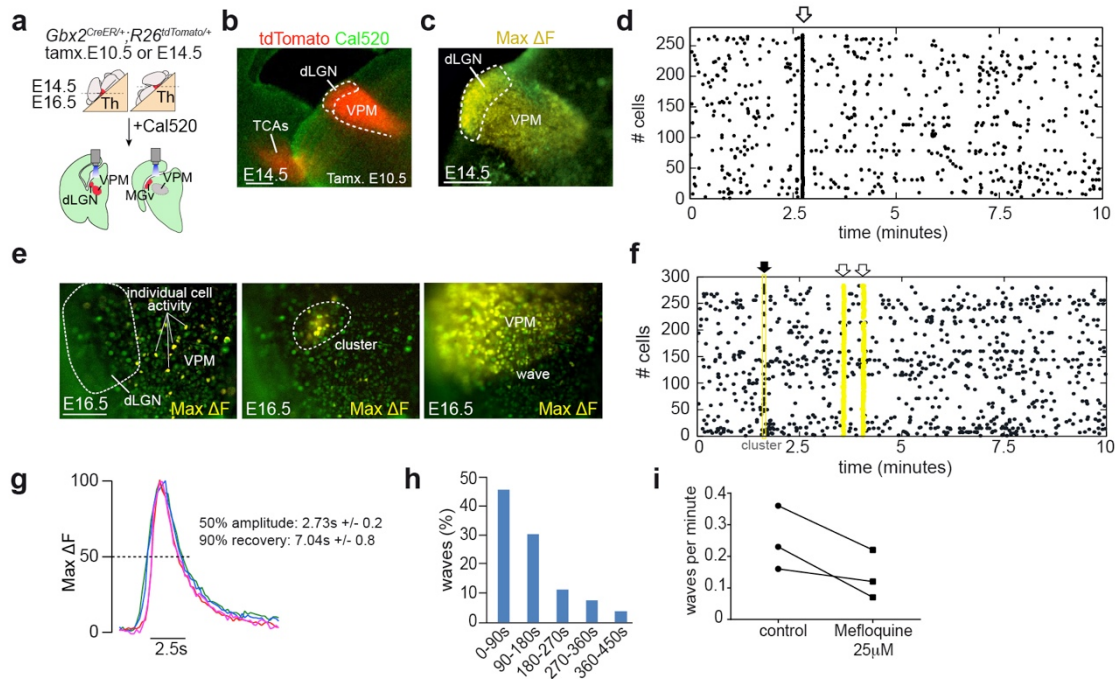


Supplementary Figure 2 EmbBE triggers experience-independent adaptations in S1 at P8 that are maintained in the adult. **(a)** vGlut2-immunostaining of the PMBSF in the S1 of control ($n = 10$) and embBE ($n = 7$) mice at P8. **(b)** Quantification of the total PMBSF area and the individual barrel area in the control and embBE brains at P8 (control: $100 \pm 3.11\%$, $n = 10$; embBE: $112.4 \pm 2.27\%$, $n = 7$; $**P = 0.01$; control: $100 \pm 4.27\%$, $n = 10$; embBE: $118.7 \pm 2.74\%$, $n = 7$; $**P = 0.016$, respectively; Two-tailed Student's t-test). Right panel: plot of each individual barrel area at P8. **(c)** CyOx (Cytochrome Oxidase) staining of the PMBSF in the S1 of control and embBE mice at P30. **(d)** Quantification of the total PMBSF area (control: $100 \pm 2.2\%$, $n = 8$; embBE: $111.2 \pm 2.1\%$, $n = 9$, $**P = 0.0026$; Two-tailed Student's t-test) and individual barrel area (control $n = 11$; embBE $n = 11$ $**P = 0.0018$; Two-tailed Student's t-test). Right panel: plot of each individual barrel area at P30. Graphs represent mean \pm SEM. Scale bars, $300\mu\text{m}$ in **a**, and $500\mu\text{m}$ in **c**.

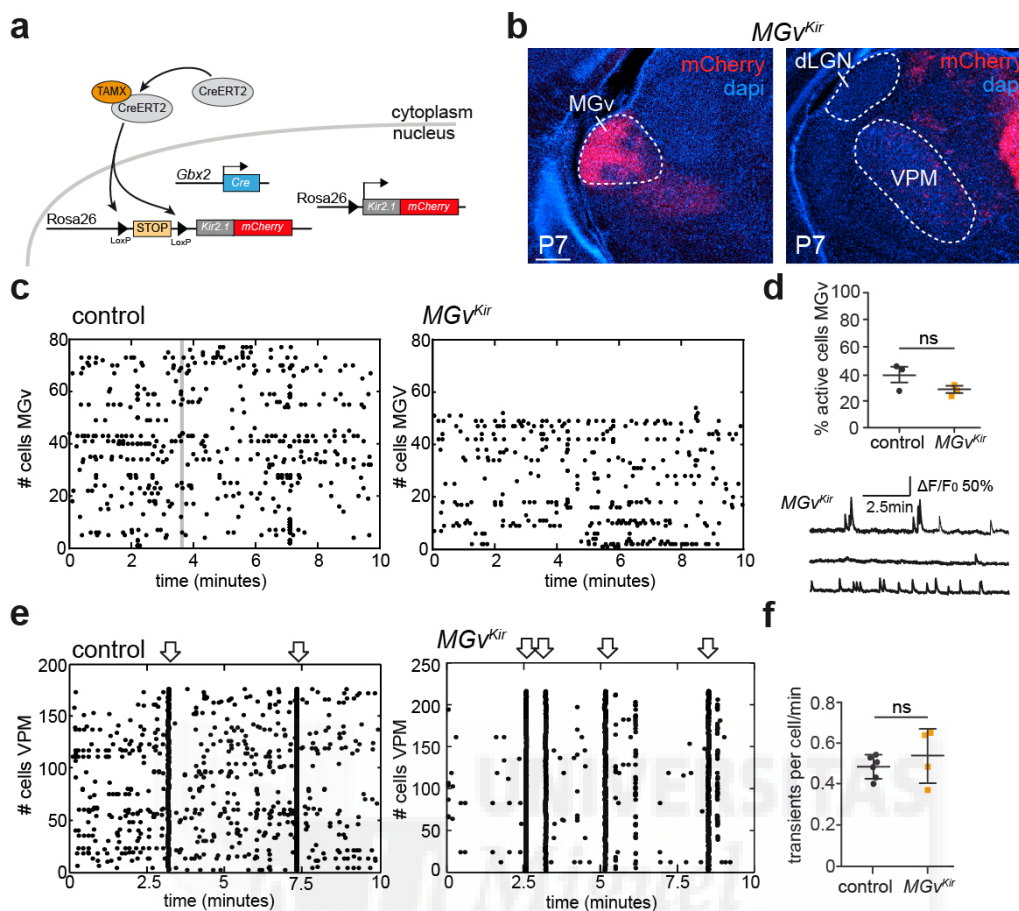


Supplementary Figure 3 Subcortical somatosensory structures are not affected in embBE mice. **(a)** CyOx staining showing the barrelettes in the PrV nucleus of the hindbrain in control and embBE animals at P8, quantification of the total PrV area (control $100 \pm 3.36\%$, $n = 5$; embBE: $95.8 \pm 3.76\%$, $n = 5$; $P = 0.42$; Mann-Whitney U-Test). **(b)** CyOx staining showing the barrelettes in the SpV nucleus of the hindbrain in control and embBE animals at P8, quantification of the total SpV area (control $100 \pm 5.76\%$, $n = 5$; embBE: $98.6 \pm 6.5\%$, $n = 4$; $P > 0.99$; Mann-Whitney U-Test). Graphs represent mean \pm SEM. Scale bars, $300\mu\text{m}$.

Results



Supplementary Figure 4 Spontaneous Ca^{2+} activity in the developing thalamus. **(a)** Schematic representation of the different orientations used to obtain the thalamocortical acute slices. Embryonic acute thalamocortical slices from *Gbx2^{CreER/+};R26^{tdTomato/+}* mice with tamoxifen administrated at E10.5 (to label dLGN and VPM) or at E14.5 (to specifically label MGv). **(b)** Acute slice showing tdTomato in the dLGN and VPM nuclei and loaded with Cal 520TM calcium dye at E14.5. Thalamocortical projections (TCAs) are also labeled. **(c)** Maximum projection of a Ca^{2+} wave (yellow) at E14.5 covering the dLGN-VPM nuclei. **(d)** Raster plot showing the onsets of individual cells Ca^{2+} transients between dLGN-VPM nuclei at E14.5. Open arrow indicates a wave. **(e)** Asynchronous Ca^{2+} transients in individual thalamic cells (left), clusters of synchronously co-active thalamic cells (middle) and a Ca^{2+} wave (right) at E16.5. **(f)** Raster plot showing the onsets of individual cells Ca^{2+} transients. Clusters are represented by small groups of cells with simultaneous Ca^{2+} transients onsets (black arrow), while the waves involve almost all the cells within the nucleus (open arrows), including those that remain predominantly inactive during the inter-wave intervals. **(g)** Kinetics of the Ca^{2+} transients during a wave in four different ROIs. The amplitude of the transients has been normalized and the time aligned in the maximum. Wave width at 50% of the maximum amplitude: 2.73 \pm 0.2s and 90% recovery: 7.04 \pm 0.8s after wave onset. **(h)** Relative frequency distribution of inter-wave intervals measured at 90s periods. **(i)** Quantification of the effect on the frequency of dLGN-VPM waves after treatment with the connexin36 gap junction blocker, Mefloquine (25 μ M). Scale bars, 200 μ m in **b** and **c**, and 100 μ m in **e**.

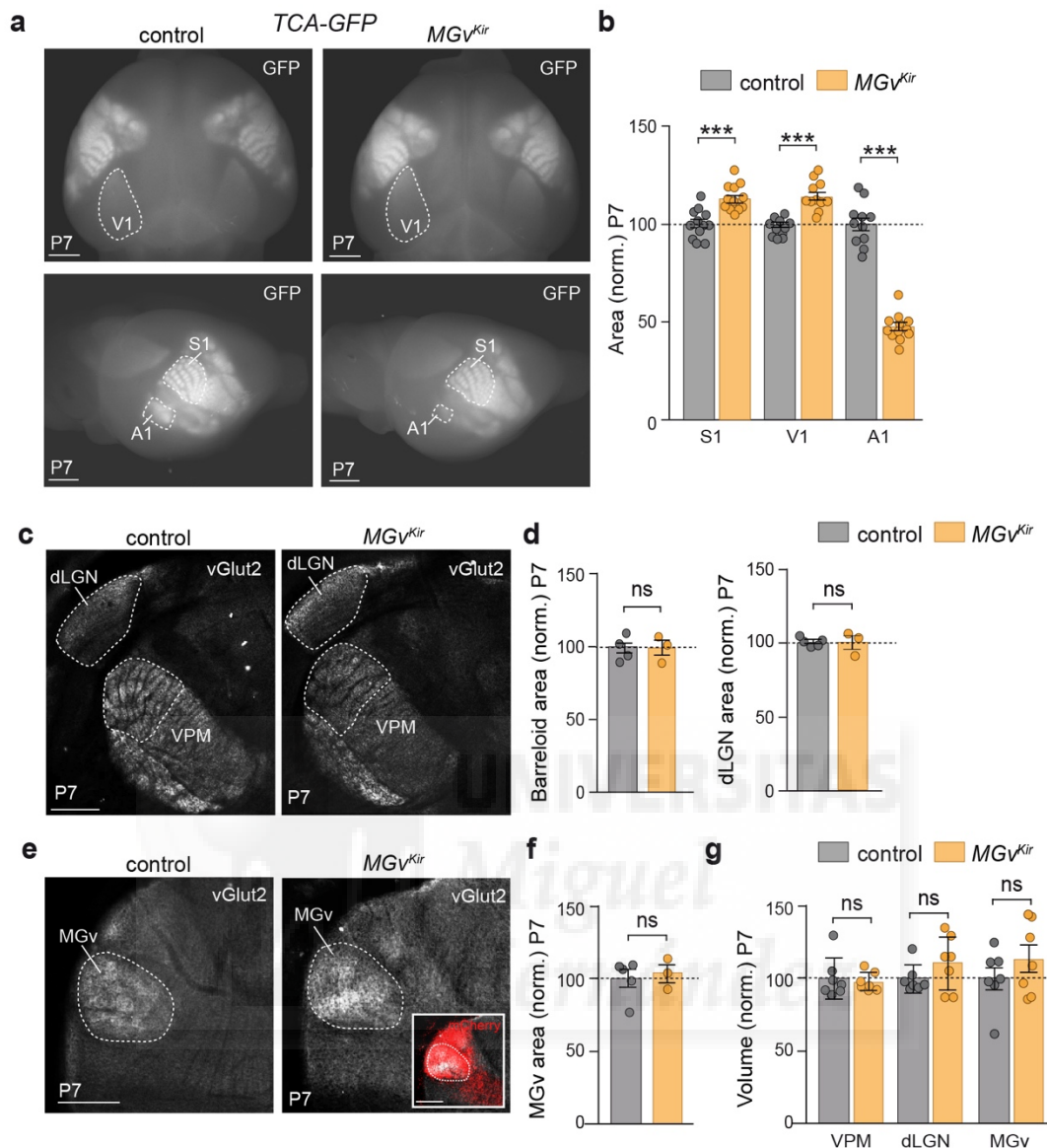


Supplementary Figure 5 Selective targeting of Kir2.1 to the MGv thalamic nucleus in the MGv^{Kir} mouse. **(a)** Schema showing the genetic strategy used to selectively overexpress Kir2.1 in MGv neurons. **(b)** Tamoxifen administration at E14.5 specifically targets MGv thalamic neurons in $Gbx2^{CreER/+};R26^{Kir/+}$ animals. Note the lack of recombination in the somatosensory and visual thalamic nuclei. **(c)** Raster plots of Ca^{2+} activity recorded during 10 minutes in the MGv of control (left panel) and MGv^{Kir} expressing (right panel) mice. To quantify the effect of Kir2.1 overexpression, neurons contributing only to the wave (grey line) were removed in the control raster plot for comparison to the MGv^{Kir} mouse. In the present example, 77 out of 273 cells were active in the MGv control and 54 out of 227 in the MGv of the MGv^{Kir} . **(d)** Quantification of the percentage of active cells in the MGv nucleus of control ($39 \pm 6\%$, excluding the waves; $n = 3$) and MGv^{Kir} ($28 \pm 2\%$; $n = 3$) mice (upper panel, right); ns, not significant, $P = 0.3$, Mann-Whitney U-test. **(e)** Raster plots showing the onsets of individual cells Ca^{2+} transients at E16.5 in the VPM from control (left panel) and MGv^{Kir} (right panel) mice. The higher frequency of waves in the VPM of MGv^{Kir} is accompanied by lower inter-wave asynchronous activity. **(f)** Quantification of the average number of Ca^{2+} transients per cell per minute (including

Results

asynchronous scatter and wave evoked transients) shows no significant difference between VPM control and VPM MGv^{Kir} (control: 0.48 ± 0.02 , $n = 6$; MGv^{Kir} : 0.54 ± 0.07 , $n = 4$; ns, not significant, $P = 0.61$, Mann-Whitney U-test). Graphs represent mean \pm SEM.



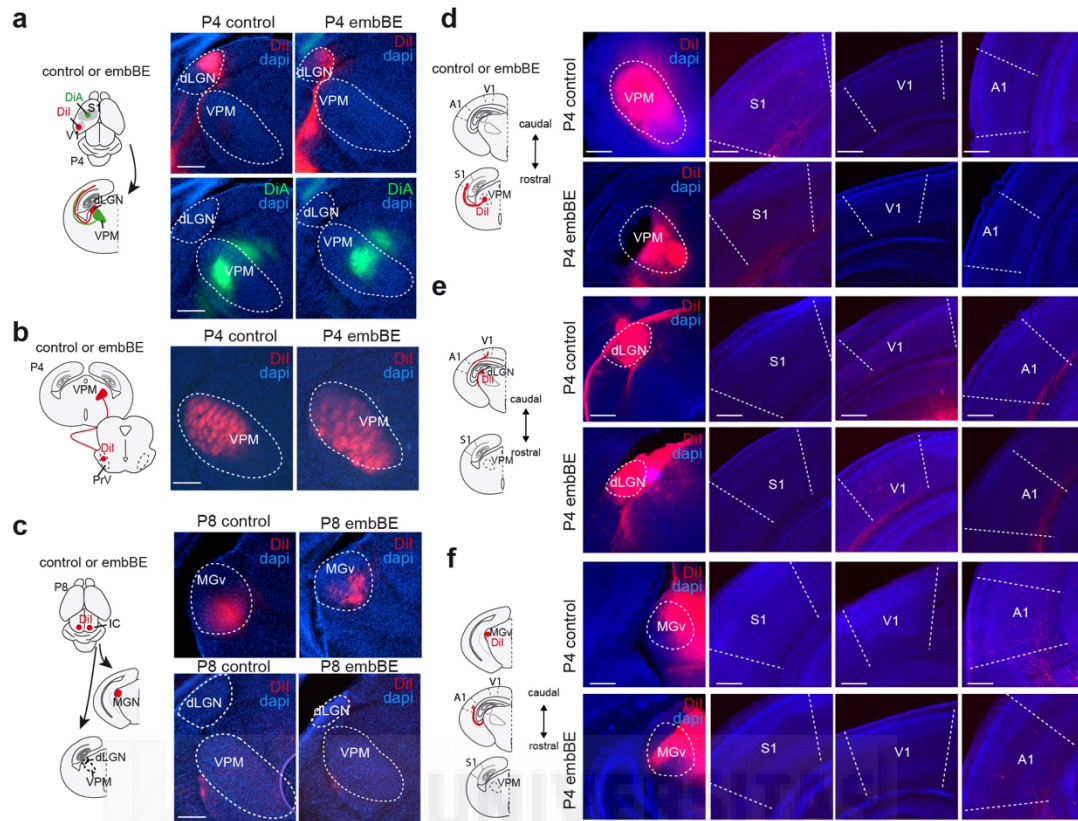


Supplementary Figure 6 Primary cortical areas size modifications in the MGv^{Kir} mouse. **(a)** Labeling of principal sensory cortical areas in control mice (TCA-GFP+) or MGv^{Kir} mice (TCA-GFP+) at P7. **(b)** Quantification of the S1, V1 and A1 areas shown in **a** (S1 area: control: $100 \pm 2.19\%$, $n = 11$; MGv^{Kir} : $112.3 \pm 1.96\%$, $n = 12$; $***P < 0.001$, Two-tailed Student's t-test. V1 area: control: $100 \pm 1.36\%$, $n = 11$; MGv^{Kir} : $114.6 \pm 2.07\%$, $n = 12$; $***P < 0.001$, Mann-Whitney U-Test. A1 area: control: $100 \pm 3.03\%$, $n = 11$; MGv^{Kir} : $48.06 \pm 1.99\%$, $n = 12$; $***P < 0.001$; Two-tailed Student's t-test). **(c)** vGlut2-immunostaining of the VPM and dLGN nuclei of the thalamus in control and MGv^{Kir} mice at P7. **(d)** Quantification of the total barreloid area and dLGN area (barreloid area: control $100 \pm 3.43\%$, $n = 5$, MGv^{Kir} : $99.93 \pm 5.37\%$, $n = 3$, $P > 0.99$, Mann-Whitney U-Test. dLGN area: control $100 \pm 1.38\%$, $n = 5$, MGv^{Kir} : $99.44 \pm 4.59\%$, $n = 3$, $P = 0.79$, Mann-Whitney U-Test). **(e)** vGlut2-immunostaining of the MGv thalamic nucleus in

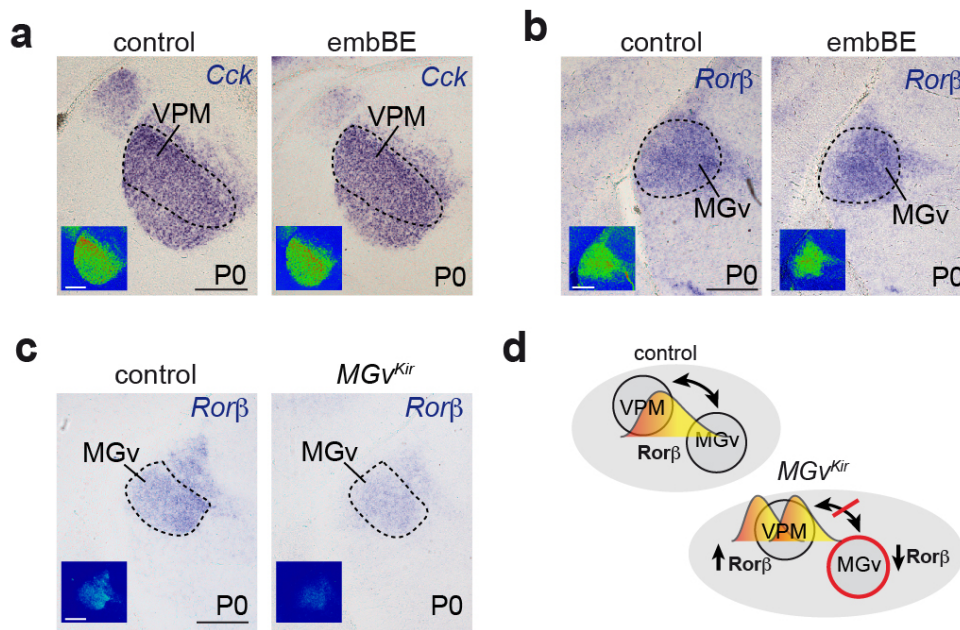
Results

control and MGv^{Kir} mice at P7. Inset in lower panel shows the recombination in the MGv in MGv^{Kir} mice. **(f)** Quantification of the total MGv area (control $100 \pm 6.11\%$, $n = 5$; MGv^{Kir} : $103.8 \pm 6.07\%$, $n = 3$; $P > 0.99$; Mann-Whitney U-Test). **(g)** Quantification of the volumes of VPM, dLGN and MGv (VPM: control $100 \pm 5.35\%$, $n = 7$; MGv^{Kir} : $97.76 \pm 2.44\%$, $n = 7$; $P = 0.71$; Two-tailed Student's t-test. dLGN: control $100 \pm 3.67\%$, $n = 7$; MGv^{Kir} : $111.1 \pm 7.1\%$, $n = 7$; $P = 0.19$; Two-tailed Student's t-test. MGv: control $100 \pm 7.51\%$, $n = 7$; MGv^{Kir} : $113.9 \pm 9.51\%$, $n = 7$; $P = 0.274$; Two-tailed Student's t-test). Graph represent mean \pm SEM. Scale bars, 1mm in **a** and $300\mu\text{m}$ in **c** and **e**.

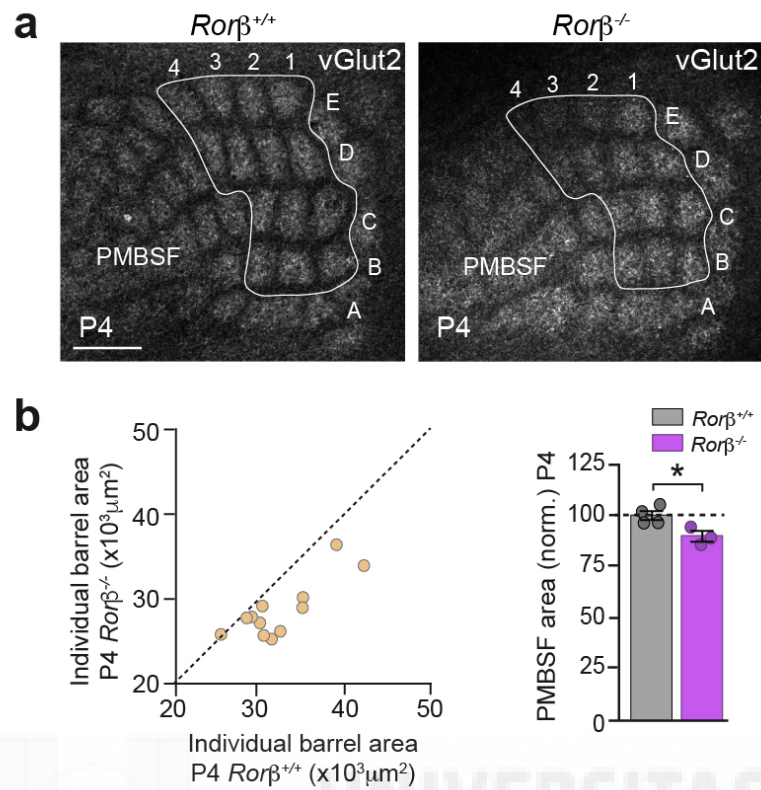




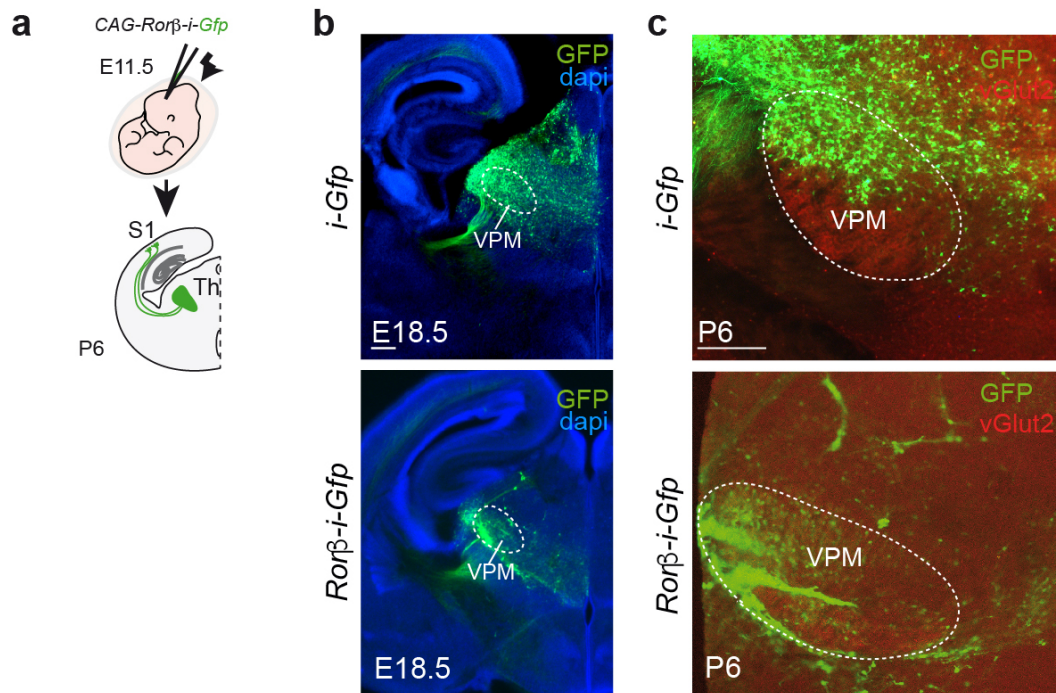
Supplementary Figure 7 Thalamocortical projections and sub-thalamic afferents are not rewired in embBE mice. **(a)** Experimental design to study the effect of embryonic retinal ablation on the topography of TCAs after injection of DiI and DiA crystals into the primary visual (V1) and primary somatosensory (S1) cortices, respectively. Coronal sections show the topography of visual and somatosensory TCAs in control ($n = 6$) and embBE ($n = 6$) mice at P4. **(b)** Experimental design to study the effect of embryonic retinal ablation on the targeting of somatosensory thalamic afferents after injection of DiI into the PrV nucleus of the hindbrain. Coronal sections show PrV axons targeting the VPM thalamic nucleus in both control ($n = 2$) and embBE ($n = 2$) mice at P4. **(c)** Experimental design used to study the effect of removing retinal input embryonically on the targeting of auditory thalamic afferents from the inferior colliculus (IC). Coronal sections show the topographical connectivity of IC axons into the auditory thalamic nucleus (MGN) in control ($n = 8$) and embBE animals ($n = 8$). **(d-f)** Experimental design to study the effect of embryonic retinal ablation on TCAs after injection of DiI crystals into specific thalamic nuclei at P4 (VPM, **d**; dLGN, **e** and MGv, **f**). Coronal sections show normal targeting of TCAs to S1, V1 or A1 cortices, respectively. Control ($n = 3$) and embBE ($n = 3$) mice. Scale bars, 300 μ m.



Supplementary Figure 8 Downregulation of *Rorb* expression in the MGv in the absence of thalamic waves in this nucleus. **(a)** *In situ* hybridization for *Cck* in coronal sections from control and embBE animals at P0. Note that the expression of *Cck* is not altered in the VPM. **(b)** *In situ* hybridization for *Rorb* in coronal sections from control and embBE animals at P0. Note that the expression of *Rorb* is not altered in the MGv. **(c)** *Rorb* mRNA expression in coronal sections from control ($n = 5$) and *MGv^{Kir}* ($n = 5$) animals at P0. Note that *Rorb* is downregulated in the MGv. **(d)** Schema representing the results found on the changes in *Rorb* expression in the *MGv^{Kir}* mouse. Scale bars, 300 μ m.



Supplementary Figure 9 Reduced PMBSF in the absence of *Rorβ*. **(a)** vGlut2-immunostaining in tangential sections of the PMBSF at P4 from $Ror\beta^{+/+}$ ($n = 4$) and $Ror\beta^{-/-}$ mice ($n = 3$). **(b)** Quantification of the PMBSF area at P4 in $Ror\beta^{+/+}$ and $Ror\beta^{-/-}$ mice ($*P = 0.02$; Two-tailed Student's t-test). Graphs represent mean \pm SEM. Scale bars, 300 μm



Supplementary Figure 10 Overexpression of *Rorb* in VPM neurons. **(a)** Scheme of the experimental paradigm used to test the effect of thalamic *Rorb* gain-of-function on the development of the somatosensory cortex. **(b)** E18.5 coronal sections showing GFP immunostaining (green) and dapi staining (blue) in brains electroporated with a *i-Gfp* or *Rorb-i-Gfp* constructs at E11.5. **(c)** Coronal sections of P6 brains electroporated with a *i-Gfp* or *Rorb-i-Gfp* constructs at E11.5 showing vGlut2 and GFP immunostaining in the VPM nucleus. Scale bars, 300 μ m.

Legends to Supplementary Movies

Supplementary Movie 1. Pseudo color movie showing the dynamics of Cal520TM dye fluorescence change during Ca²⁺ wave propagation from dLGN to VPM nucleus in an acute slice from an E16.5 control embryo (7s real time time-lapse, 250ms interframe interval).

Supplementary Movie 2. Pseudo color movie showing the dynamics of Cal520TM dye fluorescence change during Ca²⁺ wave propagation from VPM to dLGN nucleus in an acute slice from an E16.5 control embryo (7s real time time-lapse, 250ms interframe interval).

Supplementary Movie 3. Pseudo color movie showing the dynamics of Cal520TM dye fluorescence change during Ca²⁺ wave propagation from VPM to MGv nucleus in an acute slice from an E16.5 control embryo (7s real time time-lapse, 250ms interframe interval).

Supplementary Movie 4. Gray scale movie showing the dynamics of GCaMP6f indicator change during Ca²⁺ wave propagation from VPM /dLGN nuclei to the cortex in an acute slice from an E16.5 *Gbx2*^{CreER/+}; *R26*^{GCaMP6-EGFP/+} embryo (11s real time time-lapse, 250ms interframe interval).

Supplementary Movie 5. Pseudo color movie showing the dynamics of Cal520TM dye fluorescence change during Ca²⁺ waves propagation from VPM to dLGN nucleus, as well as those restricted in the VPM only, in an acute slice from a *MGv*^{Kir} E16.5 embryo (accelerated time-lapse representing 2min real time recording, 250ms interframe interval).

Supplementary Movie 6. Pseudo color movie showing the dynamics of Cal520TM dye fluorescence change during Ca²⁺ waves propagation from VPM to dLGN nucleus in an acute slice from an embBE E17 embryo (accelerated time-lapse representing 2min real time recording, 250ms interframe interval).

Chapter II: Common mechanisms involved in cross-modal plasticity of sensory systems.

In the second and third chapters of Results, I present unpublished data produced during the last period of my stay in the laboratory.

As aforementioned, a classical paradigm extensively used to unravel the role of the afferent input during the development of the cortex is the deprivation of one sensory modality. The sensory deprivation leads to an adaptive reorganization of the deprived and non-deprived sensory circuits. As was presented in the previous part of the results, our laboratory has shown that when visual input is removed embryonically, the thalamus triggers a profound reorganization of the somatosensory cortex through changes in thalamic gene expression and thalamocortical axonal branching (Moreno-Juan et al., 2017). This cross-modal adaptation takes place in the thalamus through spontaneous activity patterns that communicate distinct sensory thalamic nuclei its modification can lead to changes in thalamic gene expression that are crucial for the correct development of cortical maps. Although the discovery of this mechanism has been important, we still do not know how general is and whether other sensory systems follow the same rules. By performing embryonic peripheral auditory deprivation (embryonic cochleations), in this second part of the results we have gained evidence that the mechanism described for experience-independent cross-modal plasticity is preserved among sensory systems.

Results

Embryonic deprivation of the auditory input

We developed a new strategy in which we cauterize bilaterally both cochleas in mouse embryos, namely embryonic bilateral cochleation (embBC). The surgeries were done at E14.5, well before the auditory axons from the IC arrive to the auditory thalamus (MGv) (**Figure 1a**). We have chosen this early stage of development to mimic the congenital deafness. First, we demonstrate that the external ear is completely lost (**Figure 1c**) by placing DiI crystals in the cochlear nucleus, which is the first station where the peripheral auditory axons arrive. Thus, the cochlea is retrogradely label. Our results show that in the embBC the cochlea is highly impaired compared to the control condition (**Figure 1d**).

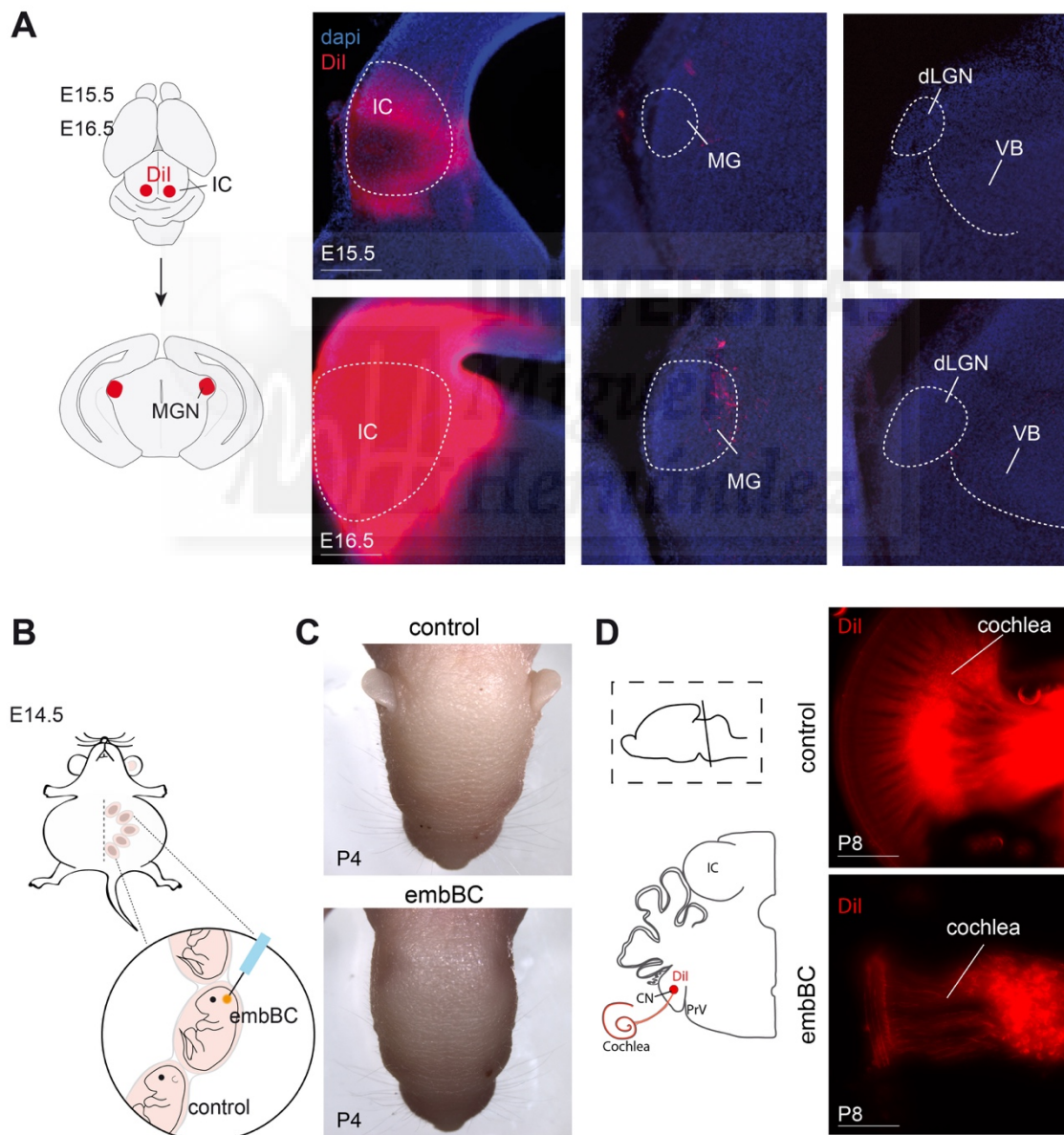


Figure 1 | Embryonic bilateral deprivation of the auditory input. **(A)** Experimental design to study the development of the projections from the Inferior Colliculus (IC) towards the MGv. Injections in the IC with DiI were done in E15.5 and E16.5 mice. Coronal sections show the topography of the axons from the IC towards the MGv in E15.5 (n=3) and in E16.5 (n=3) control mice. **(B)** Experimental design to ablate the auditory input embryonically. **(C)** Images showing a control and embBC animal at P4. **(D)** Experimental design to study the efficacy of the auditory ablation. DiI crystals were placed in the Cochlear Nucleus (CN) of control (n=5) and embBC (n=5) animals at P8. Scale bars 300 μ m.

Auditory embryonic deprivation leads to an experience-independent expansion of the barrel-field

We next determine whether the embBC leads to cross-modal changes in cortical areas, similarly to the embBE, and whether those changes could be triggered by experience-independent mechanisms. As in our previous study, we used for these experiments a transgenic mouse line expressing the green fluorescent protein (GFP) in the thalamocortical axons (TCA-GFP mouse; provided by Takuji Iwasato).

The measurements of the primary cortical areas size showed a 9.9% of expansion of S1 (control: $100 \pm 2.63\%$ n=7; embBC: $109.9 \pm 3.43\%$ n=5) and no changes in the size of V1 (control: $100 \pm 4.07\%$ n=7; embBC: $97.71 \pm 5.9\%$ n=5) neither in A1 (control: $100 \pm 3.7\%$ n=7; embBC: $93.18 \pm 4.4\%$ n=5) (**Figure 2**). Interestingly, despite of the increase in S1 size, the size of the VPM did not change after embBC (**Figure 3**), suggesting that the expansion of S1 might be triggered by axonal reorganization of the VPM thalamocortical neurons similarly to the ones shown in (Moreno-Juan et al., 2017).

Results

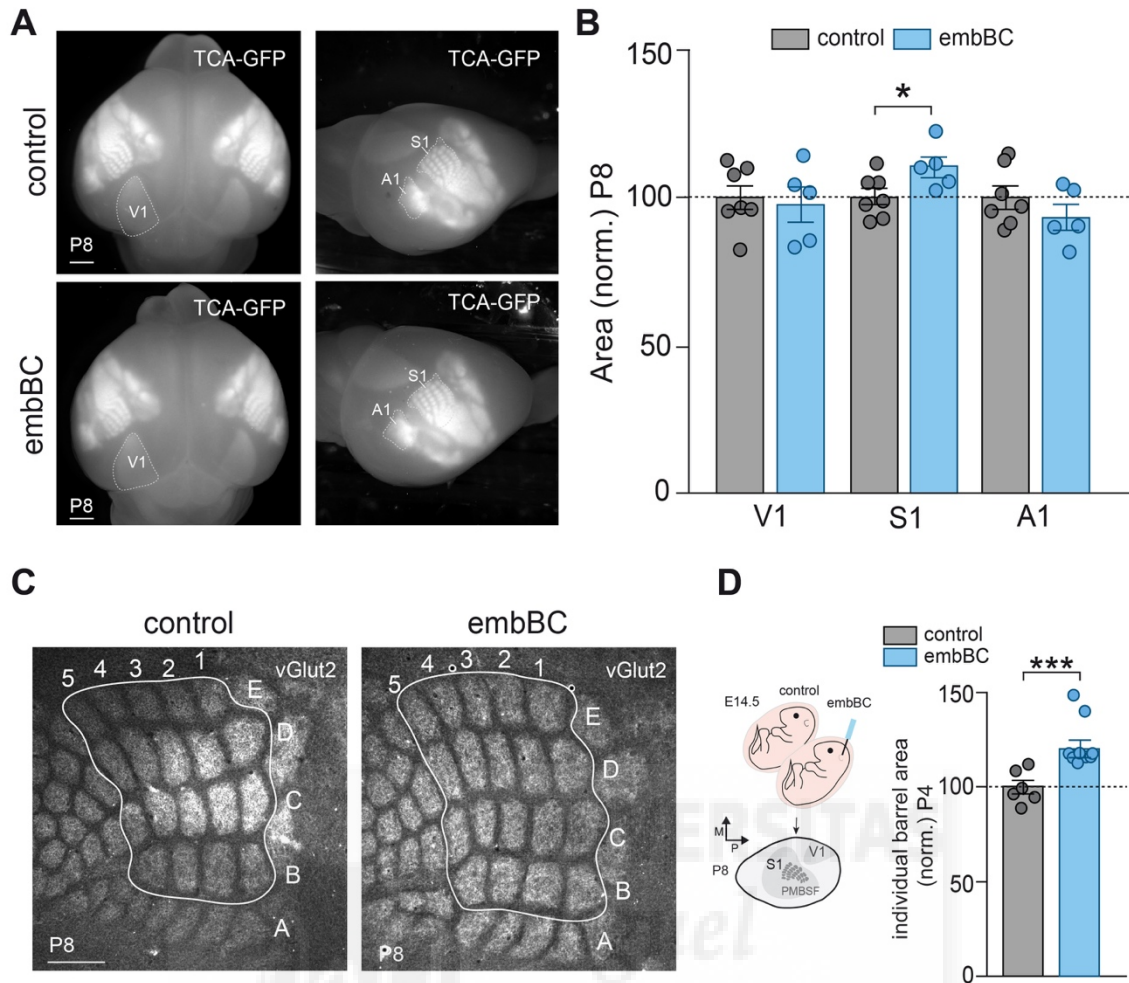


Figure 2 | Embryonic ear removal triggers experience-independent cross-modal changes in S1 somatosensory cortex. **(A)** Labelling of principal sensory cortical areas at P8 in a control TCA-GFP transgenic mouse or in a TCA-GFP mouse in which bilateral cochleation has been performed embryonically. **(B)** Quantification of the areas of S1, V1 and A1 shown in A (* $P = 0.042$ for S1; not significant for V1 $P = 0.74$ and for A1 $P = 0.26$; Two-tailed Student's t -test). **(C)** vGlut2-immunostaining in the posteromedial barrel subfield (PMBSF) of S1 in control ($n = 6$) and embBC ($n = 10$) mice at P8. **(D)** Experimental design and quantification of the individual barrel area shown in C of control ($n = 6$) and embBC ($n = 10$) mice at P8 (*** $P < 0.001$; Mann-Whitney U -test). Graphs represent mean \pm SEM. Scale bars 1mm in A, 300 μ m in C.

Next, we used immunostaining for vesicular glutamate transporter 2 (vGlut2), which labels the terminals of the TCAs in the layer 4 of the cortex, to measure the size of the individual barrel area in control and embBC mice at P8. We found an increase of 20.3% of the individual barrel area in the embBC mice (control: $100 \pm 3.64\%$ $n=6$; embBC: $120.3 \pm 4.45\%$ $n=10$). As these changes occur before active whisking (Landers et al., 2006),

these results suggest that the cross-modal adaptations in S1 to auditory peripheral loss are triggered through experience-independent mechanisms.

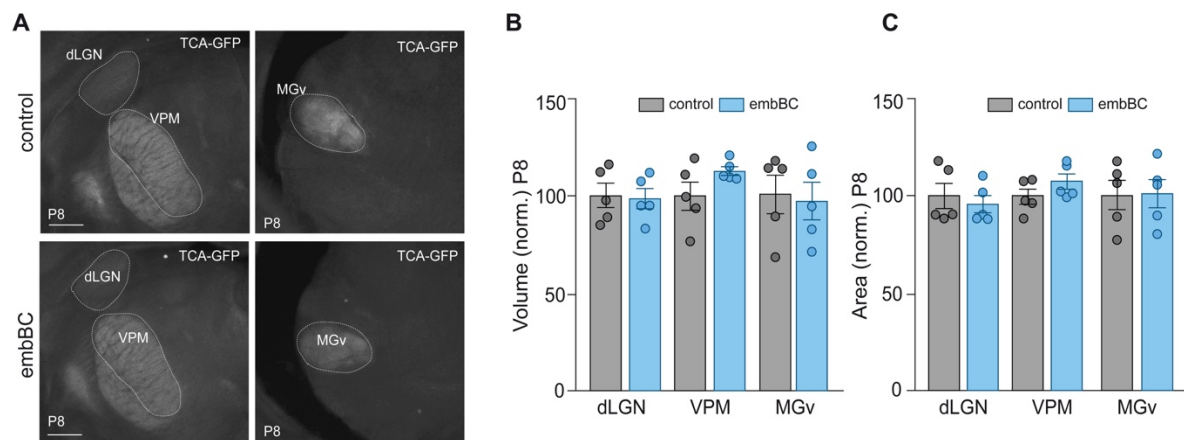


Figure 3 | Embryonic ablation of the auditory input does not trigger changes in the size of the thalamic nuclei. **(A)** Coronal sections from the TCA-GFP transgenic mice showing the area of dLGN, VPM and MGv nuclei in control and embBC conditions. **(B)** Quantification of the dLGN, VPM and MGv volume at P8 (dLGN: control $100 \pm 6.29\%$, $n = 5$; embBC 98.47 ± 5.16 , $n = 5$; $P = 0.85$; VPM: control 100 ± 7.32 , $n = 5$; embBC 112.7 ± 2.2 , $n = 5$; $P = 0.13$ MGv: control 100 ± 9.39 , $n = 5$; embBC 96.36 ± 9.53 , $n = 5$; $P = 0.79$; Two-tailed Student's t-test). **(C)** Quantification of the area size for each principal thalamic nucleus at P8 (dLGN: control $100 \pm 6.49\%$, $n = 5$; embBC 95.71 ± 4.38 , $n = 5$; $P = 0.59$; VPM: control 100 ± 3.79 , $n = 5$; embBC 107 ± 3.93 , $n = 5$; $P = 0.2$ MGv: control 100 ± 7.41 , $n = 5$; embBC 100.7 ± 7.25 , $n = 5$; $P = 0.94$; Two-tailed Student's t-test). Graphs represent mean \pm SEM. Scale bars 300 μm .

Auditory embryonic cochleation does not trigger major thalamocortical and subthalamic rewiring

The expansion of the barrel-field in S1 in the embBC mice could be explained by, at least, two possibilities: i) abnormal increase in the arborization of thalamocortical terminals; or ii) abnormal connectivity from the auditory thalamus to the somatosensory cortex. To test these possibilities, we first performed tracing studies to unravel the connectivity and topography of auditory and somatosensory thalamocortical connectivity. We performed dye injections of DiI and DiA crystals into the A1 and S1 cortices, and we analysed the retrograde labelling in the thalamus at P4. DiI crystals in S1 did label the VPM nucleus of

Results

the thalamus in control and embBC animals (control: n=3; embBC: n=3) and DiA in auditory cortex did label the MGv nucleus of the thalamus (control: n=3; embBC: n=3). Thus, we did not observe an abnormal reorganization of the thalamocortical somatosensory or auditory axons suggesting that the lack of embryonic auditory input does not cause abnormal projection from MGv to S1.

Next, we studied whether the axons from the IC were rearranged after the embryonic cochleation. To this, we injected DiI crystals in the IC of control and embBC at P4 and analysed the connectivity to the thalamus. Injections in the IC in both control and embBC mice labelled cells and axon terminals at the MGv without labelling the VPM or dLGN. These results suggest that embBC does not lead to a subthalamic rewiring of connectivity between the auditory and somatosensory systems.



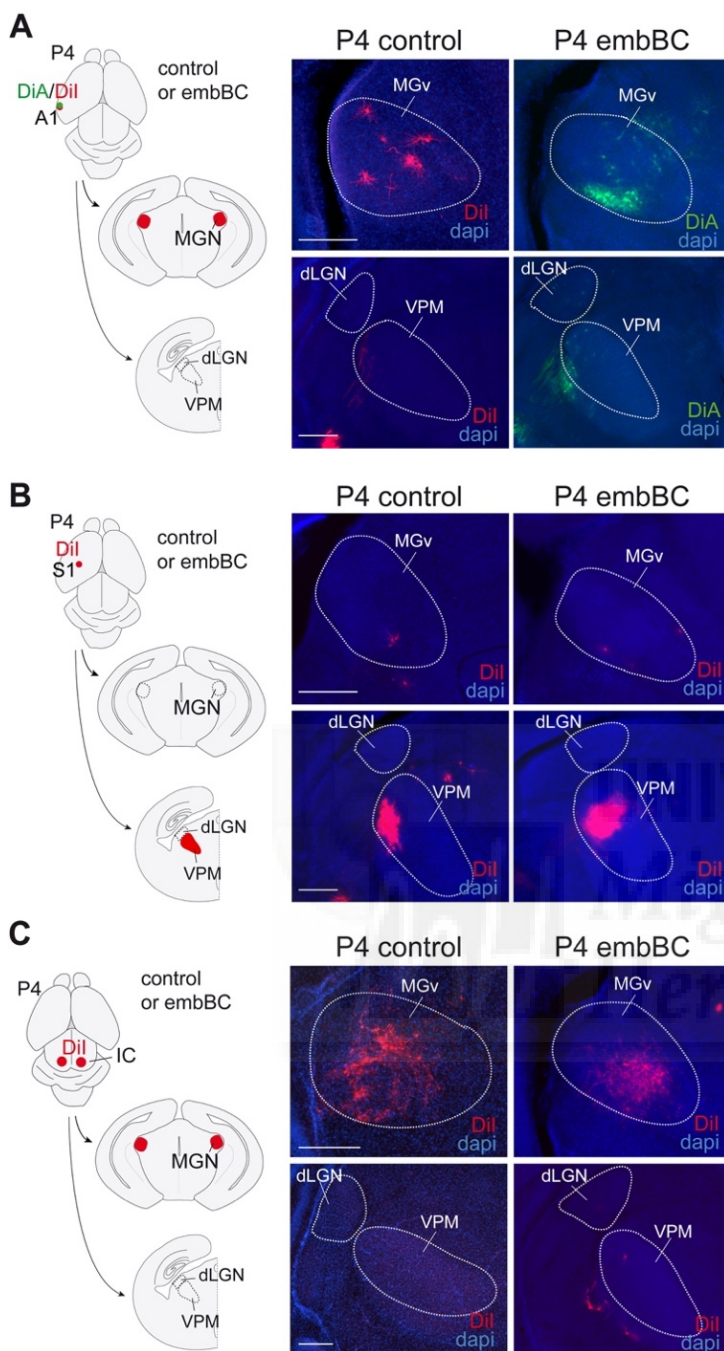


Figure 4 | Thalamocortical projections and sub-thalamic afferents are not rewired in embBC mice. (A) Experimental design to study the effect of embryonic auditory ablation on the topography of TCAs after injection of DiI or DiA crystals into the A1. Coronal sections show the topography of auditory and somatosensory TCAs in control (n=3) and in embBC (n=3) mice at P4. (B) Experimental design to study the effect of embryonic auditory ablation on the topography of TCAs after injection of DiI crystals into the S1 cortex. Coronal sections show the topography of auditory and somatosensory TCAs in control (n=3) and in embBC (n=3) mice at P4. (C) Experimental designs to study the effect of removing auditory input embryonically on the targeting of auditory thalamic afferents from the Inferior Colliculus (IC). Coronal sections show the topographical connectivity of IC axons into the auditory thalamic nucleus (MGv) in control (n=3) and in embBC (n=3) mice. Scale bars, 300 μ m.

Embryonic ablation of the auditory input triggers changes in gene expression in the somatosensory thalamus

In the first chapter of the results section, we showed that embryonic visual enucleation leads to changes in gene expression in VPM neurons at P0 and at P4 (Moreno-Juan et al., 2017). Among the genes that changed their expression in the VPM of the embBE mice,

Results

we found a significant upregulation of the RAR-related orphan receptor B (*Rorβ*). This gene was upregulated 1.9-fold in VPM neurons in the embBE at P0 and has been shown to influence somatosensory cortical development (Jabaudon et al., 2012). Moreover, we have shown that the upregulation of *Rorβ* *in vivo* in the VPM neurons by *in utero* electroporation leads to an increase in the size of the barrels in S1 by modifying the complexity of the TCAs terminals (Moreno-Juan et al., 2017). Our unpublished results also show that in the embBC, the expansion of the barrel-field also occurs during the first postnatal week, and thus we wondered whether similar changes in gene expression occur in the perinatal VPM thalamic neurons. To this, we performed *in situ* hybridization for *Rorβ* in control and embBC animals at P0 and found an upregulation of the *Rorβ* signal in the VPM in the embBC (n= 7) compared to their control littermates (n=7) (**Figure 5**). Thus, it is possible that an upregulation of *Rorβ* expression in VPM neurons induced by embBC is the responsible for the enlargement of the somatosensory cortex by increasing the axonal arborisation of thalamocortical axons terminals.

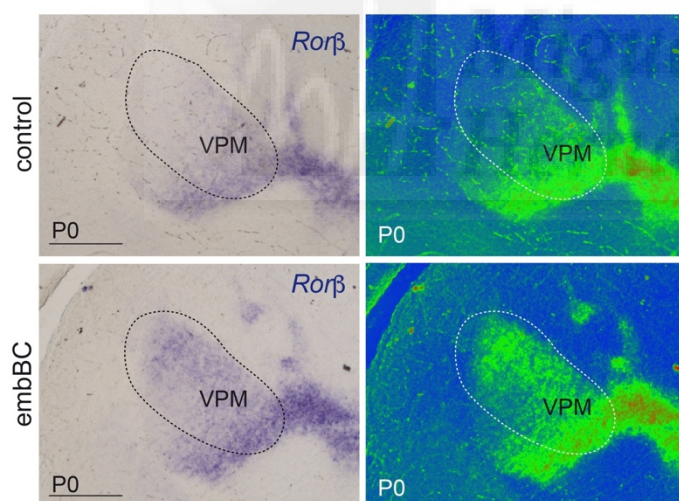


Figure 5 | Embryonic auditory deprivation leads to changes of *Rorβ* expression in VPM nucleus. *In situ* hybridization for *Rorβ* in coronal sections from control and embBC animals at P0. Note the stronger expression of *Rorβ* in VPM area of embBC animals compared to their control littermates. Scale bars, 300μm.

Chapter III: Spontaneous thalamic waves regulate cortico-thalamic innervation in the visual system

Recent publications from our laboratory have demonstrated that spontaneous thalamic activity intrinsically modulates the rate of axonal extension of TCAs (Mire et al., 2012; Castillo-Paterna et al., 2015). The modulation of the axonal growth speed by the thalamic spontaneous activity is mediated by changes the expression levels of genes such as *Robo1* and *Dcc* (Mire et al., 2012; Castillo-Paterna et al., 2015), which are axon guidance receptors already implicated in thalamocortical axon circuit formation. In the first chapter of the results of this Thesis, we showed that thalamic spontaneous calcium waves are important for the correct topographic map formation of the TCAs and are involved in the adaptations that occur in the brain after peripheral input loss (Moreno-Juan et al., 2017). As the development of the thalamo-cortical loop connectivity requires the reciprocal connectivity of corticothalamic axons to specific thalamic sensory-modality nuclei, we wonder whether the thalamic calcium waves, and thus spontaneous activity, is also required for the formation of this cortico-thalamic innervation.

Briefly, in the corticothalamic system of mice, CTAs from the visual layer 6 of the cortex arrive to the dLGN around E18.5 and start to invade this structure at P3 (Brooks et al., 2013; Seabrook et al., 2013; Grant et al., 2016). However, corticothalamic projections do not completely innervate the dLGN until later postnatal stages. Moreover, it was demonstrated that visual enucleation at P0 in mice triggers an early invasion of the dLGN by CTAs and a rewiring of layer 5b axons that switch from invading high-order thalamic nuclei to aberrantly invade the first-order nuclei, such as the dLGN. Furthermore, a recent study has shown that blocking retinal spontaneous activity by epibatidine injections in the eyes leads to a similar phenotype with CTAs invading prematurely the dLGN compared to control animals (Grant et al., 2016). Altogether, these results suggest that spontaneous retinal activity is crucial for the correct timing of invasion of the CTAs into the dLGN. However, the recent identification of the existence of the thalamic waves, which occurred in the dLGN at a similar period of time prompted us to investigate whether thalamic spontaneous activity could also play a role in this process.

Embryonic bilateral enucleation triggers changes in corticothalamic innervation

To study the role of retinal input in corticothalamic innervation of the dLGN, we performed embryonic bilateral enucleations at E14.5 in mice. To unravel the localization of CTAs, we used vGlut1 immunostaining as has been shown to label cortically derived glutamatergic terminals (Ni et al., 1995; Varoqui et al., 2002; Grant et al., 2016). As expected, a significantly higher proportion of pixels were labelled with vGlut1 immunostaining in the dLGN of embBE (n= 5) mice compared to their control littermates (n= 5) (control: $7.39 \pm 1.81\%$ n=5; embBE: $72.5 \pm 2.83\%$ n=5) (**Figure 6**) indicating an early entrance of corticothalamic axons in dLGN thalamus after embryonic visual deprivation.

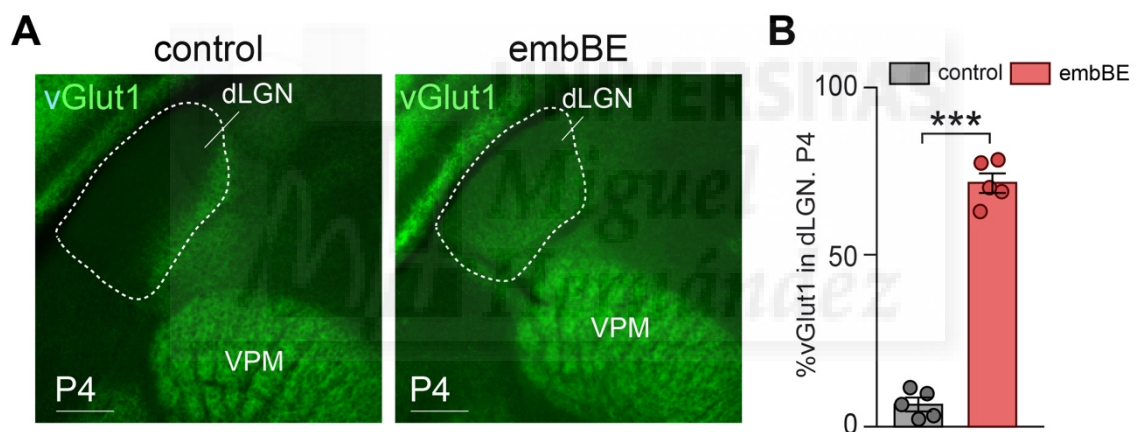


Figure 6 | Embryonic enucleation triggers changes in vGlut1 expression in the dLGN. (A) vGlut1-immunostaining in the dLGN of control and embBE mice at P4. (B) Quantification of the percentage of vGlut1-positive area occupied in the dLGN (***) $P < 0.001$; Two-tailed Student's t -test). Graphs represent mean \pm SEM. Scale bars 300 μ m in C.

Ablation of retinal input embryonically alters the pattern of wave activity in the dLGN

Our unpublished results showed that an embryonic bilateral enucleation leads to a premature invasion of the dLGN by corticothalamic axons. On the other hand, we have also shown the existence of spontaneous calcium waves in the dLGN perinatally. Thus, we next tested whether the embryonic retinal ablation may lead to changes in the thalamic spontaneous calcium activity, e.g in the dLGN, thereby influencing the invasion profile

of corticothalamic axons. Thus, we performed calcium imaging in the dLGN of control (n= 4) and embBE (n= 5) mice at E18.5 using thalamocortical slices. Interestingly, the embryonic removal of the eyes resulted in an altered wave pattern in the dLGN at this stage. The frequency of dLGN waves increased three times in embBE compared to controls (control: 0.20 ± 0.033 waves per minute; embBE 0.55 ± 0.13 waves per minute) (**Figure 7**). Therefore, these results demonstrate that the lack of retinal input at embryonic stages produces an alteration in the wave pattern of the dLGN nucleus and thus suggest that the effect on corticothalamic axon invasion may be indirect through activity-dependent mechanisms in the thalamus.

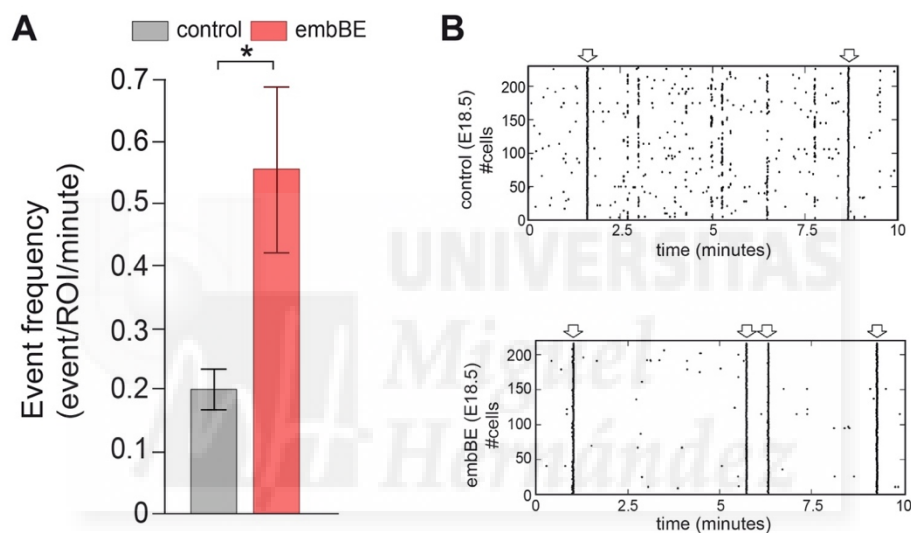


Figure 7 | Embryonic enucleation triggers alteration in wave pattern of dLGN. **(A)** Quantification of dLGN Ca²⁺ waves per minute in control (n= 4) and embBE (n= 5) animals. $P = 0.0317$; Wilcoxon Rank Sum Test. **(B)** Raster plot of the activity in more than 200 individual cells in the dLGN during 10 minutes. The arrows label synchronous Ca²⁺ transients corresponding to Ca²⁺ waves. Graphs represent mean \pm SEM.

Embryonic bilateral enucleation induces changes in gene expression in the dLGN

As we already shown in the first part of the results, changes in the frequency a pattern of thalamic waves can lead to changes in gene expression, as an increase in *Rorb* in the VPM of embBE mice. Thus, we wondered whether embryonic visual enucleation may lead to changes in gene expression in the dLGN that may play role in the regulation of the

Results

spontaneous calcium waves leading to an abnormal developmental program of corticothalamic axons. We performed an Affimetrix microarray comparing the dLGN gene expression of control and embBE mice at P0 and at P4 (**Figure 8A**). The analysis identified 176 genes whose expression changed significantly in the dLGN of embBE mice at P0. From those, 136 of the transcripts were downregulated in dLGN of embBE animals and 40 were upregulated. At P4, the microarray analysis identified 65 genes whose expression changed significantly in dLGN of embBE mice, 45 of those were downregulated and 20 were upregulated (**Figure 8B**). These results demonstrate that peripheral embryonic deprivation of the visual input triggers profound changes in the gene expression profile of the visual thalamus.

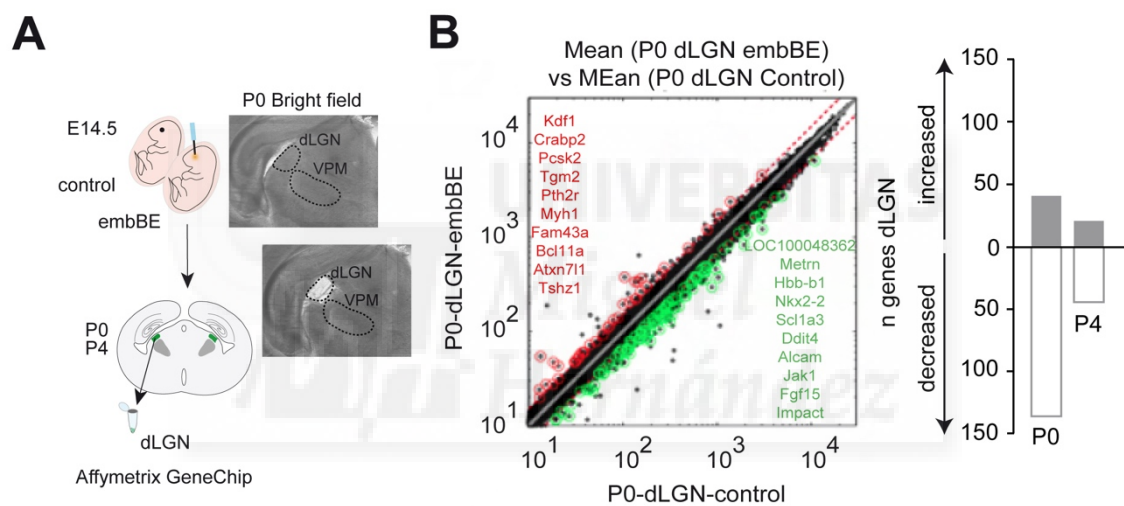


Figure 8 | Embryonic enucleation triggers changes in gene expression in dLGN neurons. (A) Scheme representing the experiment of microarray. dLGN tissue was extracted at P0 and at P4 from control and embBE animals. Bright field slices showing the procedure before and after the dissection of dLGN. (B) Scatter-plot showing the significantly upregulated (red) and downregulated (green) transcripts with a change of ≥ 1.5 or ≤ -1.5 -fold and a P value ≤ 0.05 . The top ten-transcript upregulated and downregulated are listed in red and green, respectively.

Blocking the thalamic waves alters the innervation pattern of corticothalamic axons in the dLGN

To further explore the role of the thalamic spontaneous calcium waves in the development of the corticothalamic axons and their invasion profile of the dLGN, we tested whether the lack of calcium waves in dLGN has an impact on the corticothalamic axons innervation. We hypothesised that abolishment of the dLGN waves should delay the corticothalamic axon invasion of the dLGN as opposite to the accelerated profile shown in the embBE. To test this hypothesis, we took the advantage of the $Gbx2^{CreER}; R26^{Kir}$ mice where Kir2.1 (Kir) inward rectifier potassium channel fused with mCherry protein ($R26^{Kir}$) is expressed in thalamic neurons to manipulate the thalamic spontaneous waves *in vivo* (Moreno-Juan et al., 2017). Giving tamoxifen at E10.5, Kir was broadly overexpressed in the thalamus, silencing the thalamic waves in the principal thalamic nuclei, referred as thalamic Kir mouse (Th^{Kir}) (unpublished data from N. Antón-Bolaños and G. López-Bendito). After the abolition of spontaneous calcium waves in dLGN we analysed the developmental profile of corticothalamic axons in the dLGN by immunostaining with vGlut1. We show that in the absence of dLGN waves, the percentage of vGlut1 immunostaining in dLGN was dramatically reduced in the Th^{Kir} mice at P6 suggesting that CTAs invasion phenotype is directly influenced by spontaneous thalamic activity (control: $28.30 \pm 2.57\%$ n=5; Th^{Kir} : $1.66 \pm 0.61\%$ n=4) (**Figure 9**). Interestingly, the lack thalamic waves in the dLGN leads to a decrease in size of this nucleus, as we found a 33.24% reduction of dLGN size in Th^{Kir} (n= 4) animals at P6 as compared to controls (n= 5) (control: $100 \pm 4.88\%$ n=5; Th^{Kir} : $66.76 \pm 5.67\%$ n=4).

Results

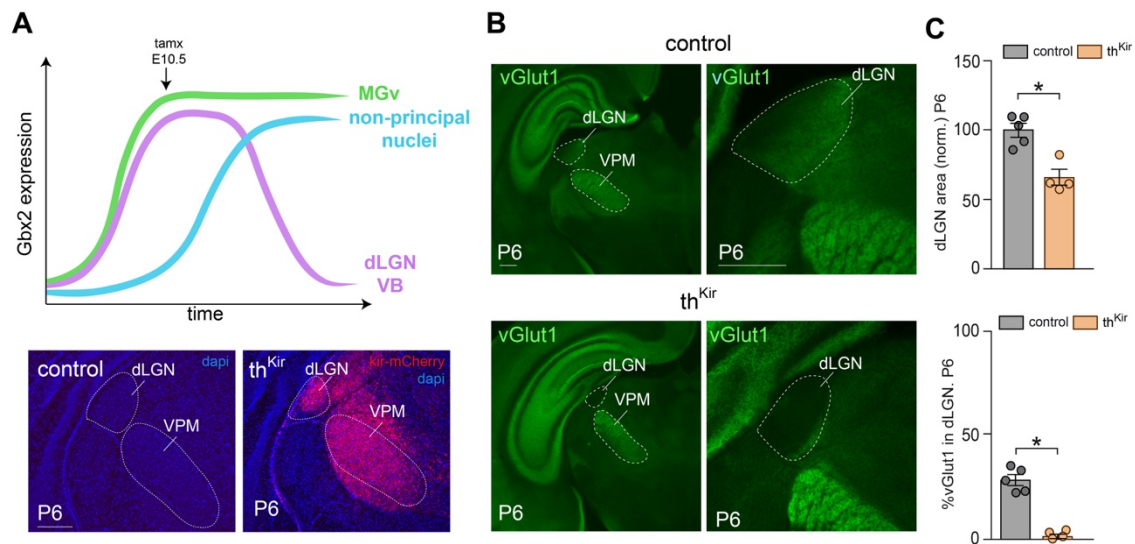


Figure 9 | Blockage of dLGN waves triggers changes in the CTAs invasion. **(A)** Scheme of labelling of the different thalamic regions by Gbx2. Giving tamoxifen at E10.5 targets the principal thalamic nuclei. **(B)** vGlut1-immunostaining in the dLGN of control (n= 5) and Th^{Kir} mice (n= 4) at P6. **(C)** Upper panel: quantification of dLGN size of control (n= 5) and Th^{Kir} animals (n=4) (* $P=0.015$; Mann-Whitney U -test). Lower panel: quantification of the percentage occupied by vGlut1 in dLGN (* $P=0.015$; Mann-Whitney U -test). Graphs represent mean \pm SEM. Scale bars 300 μ m.

The absence of thalamic calcium waves does not affect thalamocortical axonal topography

To determine whether the lack of thalamic calcium waves produces a change in the development of thalamocortical axons and their topography, we unravel the pattern of the connectivity by performing dye tracing studies in control and Th^{Kir} mice at P0. We injected DiI and DiA crystals into the visual and somatosensory areas of the cortex, respectively. As at this stage the corticothalamic axons have not entered in the thalamic nuclei, dyes only labelled cell somas at the thalamus. DiI placed in V1 backlabelled neurons in the dLGN whereas DiA in S1 and A1 backlabelled neurons in VPM and MGv, respectively, in both control and Th^{Kir} mice, suggesting that abolishment of thalamic calcium waves does not lead to major topographic rearrangements of TCAs. Surprisingly, the lack of thalamic waves does not cause any reduction of dLGN size at P0 (control: $100 \pm 4.99\%$ n=5; Th^{Kir} : $91.15 \pm 18.27\%$ n=4).

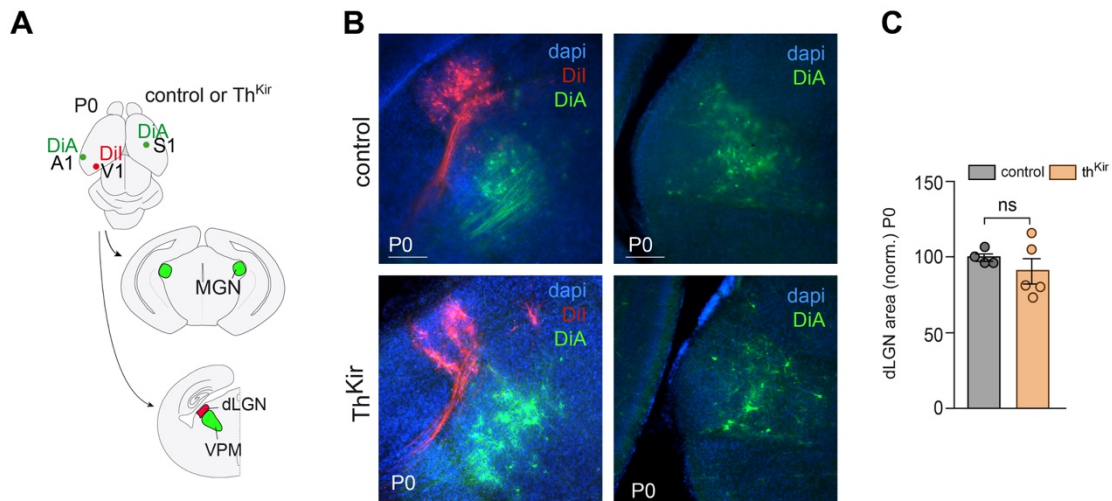


Figure 10 | Thalamocortical projections are unaffected after removal of the thalamic calcium waves (A) Experimental design to study the effect of silencing thalamic waves on the topography of TCAs after injection of DiI or DiA crystals into the primary visual (V1), primary somatosensory (S1) or primary auditory (A1) cortices. (B) Coronal sections show the topography of visual, somatosensory and auditory TCAs in control (n=4) and in embBC (n=5) mice at P0. (C) Quantification of dLGN size of control (n= 4) and Th^{Kir} animals (n=5) at P0 (ns = no significant; Mann-Whitney *U*-test). Scale bars, 300 μ m.

The absence of thalamic waves does not change retinothalamic innervation

Recent studies have shown that retinal input is necessary for the correct development of the corticothalamic innervation of dLGN (Seabrook et al., 2013; Brooks et al., 2013; Shanks et al., 2016; Grant et al., 2016). It has been also published that corticothalamic axons are essential for the correct development of the retinothalamic topographical targeting of the dLGN (Shanks et al., 2016; Diao et al., 2017). To examine the relation among thalamic spontaneous activity, and the corticothalamic and retinothalamic innervation of the dLGN, we analysed the distribution of the retinothalamic axons in the dLGN-silenced model in which TCAs fail to invade the dLGN. In order to achieve this, we injected red and green cholera toxin subunit B (CTB) in each eye to retrogradely label retinothalamic axons in the dLGN at P6 and analysed the projections at P8. Our results show that the segregation of ipsilateral and contralateral projection in the dLGN was not affected in the Th^{Kir} mouse (n= 5) as compared to the controls (n= 5) (**Figure 10**). Thus,

Results

the absence of dLGN calcium waves specifically affects the innervation profile of corticothalamic axon without affecting the retinothalamic axon targeting of the dLGN.

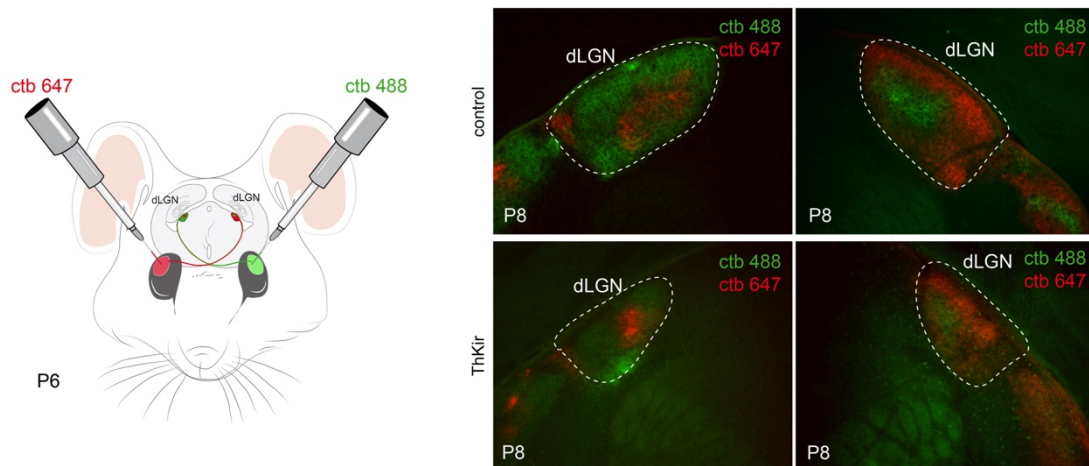
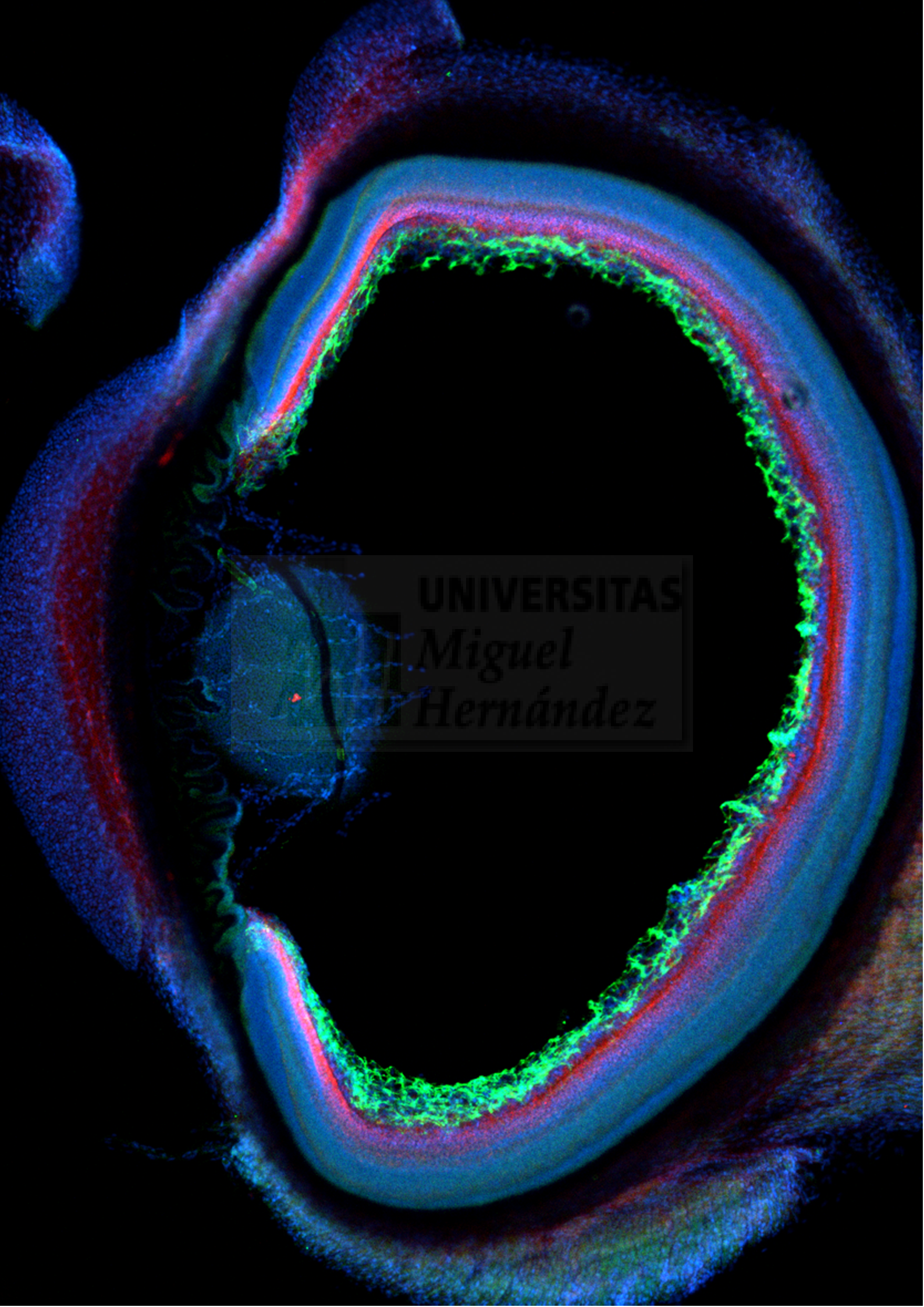


Figure 10 | Blockage the waves in the thalamus does not trigger changes in dLGN innervation of retinal axons. (A) Scheme of the experimental design. CTB red and green were injected in both eyes in order to label the contralateral and ipsilateral retinal axons in dLGN. (B) Ctb labelling in dLGN of control and Th^{Kir} mice. Graphs represent mean \pm SEM. Scale bars 300 μ m.

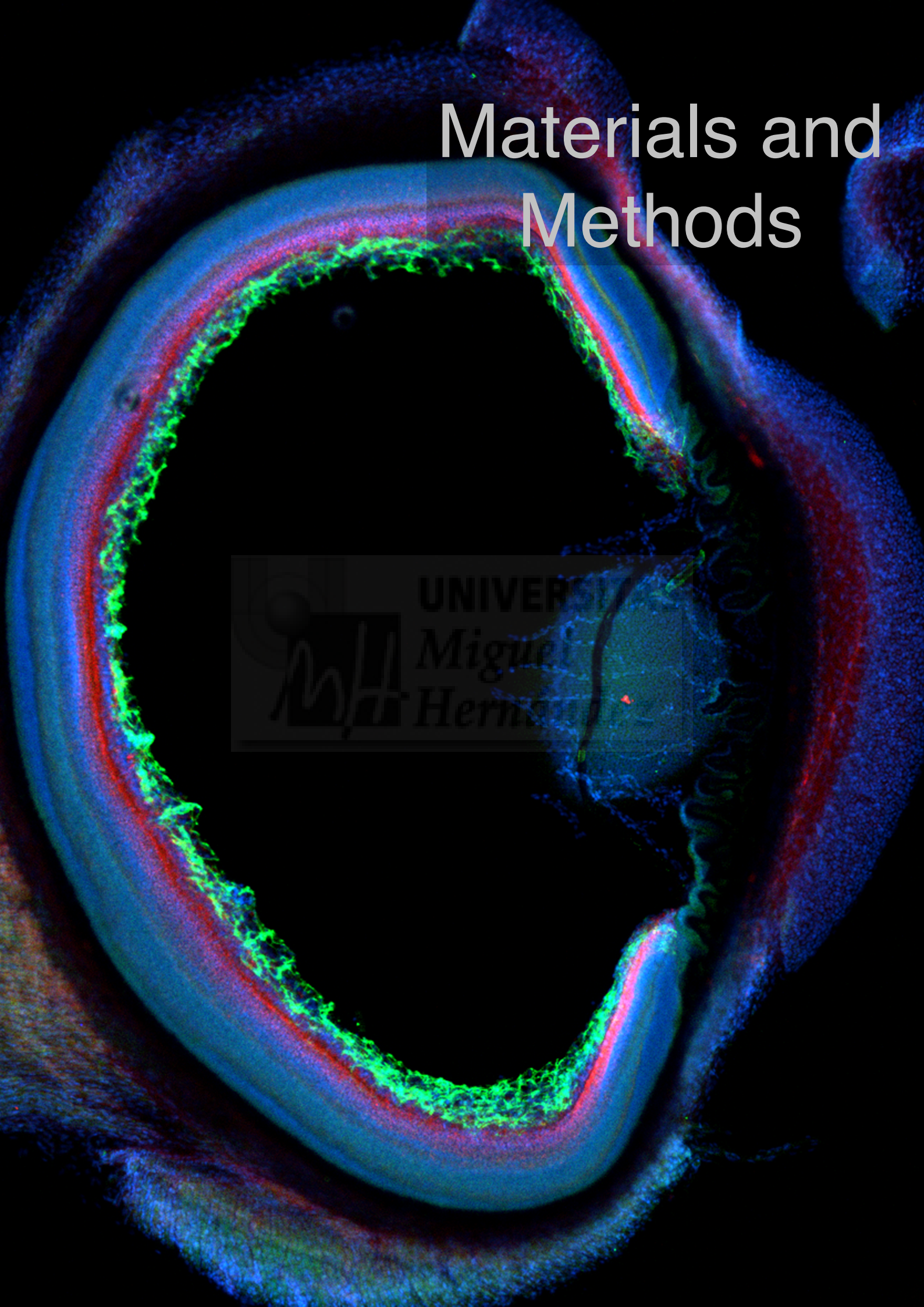




UNIVERSITAS
Miguel
Hernández

Materials and Methods

UNIVERSITY
*Miguel
Hernández*



Materials and Methods

The materials and methods used in the first section of the results are explained in detail in the copy of the article presented in this thesis. Now I will proceed to describe more in detail the methods used in the second and first sections of the results.

Mouse strains

Wild type mice maintained on a C57BL/6 background were used for the microarray expression analysis, whereas wild type mice maintained on an ICR background were used for the *in vivo* experiments, tracing studies and Ca²⁺ imaging analysis. The day on which the vaginal plug was detected was designated as E0.5. The *R26^{tdTomato}* (Chen et al., 2009) Cre-dependent mouse line was obtained from Jackson Laboratories (Stock number 007908). The *R26^{GCaMP6f}* Cre-dependent mouse line was obtained from Jackson Laboratories (Stock number 024105). *TCA-GFP Tg* line has been described previously (Liu et al., 2013). The *R26^{Kir2.1-mCherry}* mouse line was generated by inserting a *CAG-lox-STOP-lox-Kir2.1-mCherry-WPRE-pA* cassette into the *Rosa26* gene locus as described below. Each of the *R26* reporter mice carry a *Rosa26* locus with a floxed STOP cassette that prevents the expression of the gene indicated. The reporter mice were crossed with an inducible thalamic-specific *Gbx2^{CreER}* line (Tronche et al., 1999) in order to generate *Gbx2^{CreER/+};R26^{X/+}* double mutant embryos. The *Gbx2^{CreER}* line expresses *CreER(T2)-ires-eGfp* under the control of the *Gbx2* promoter. Tamoxifen induction of Cre recombination in the double mutant embryos was performed by gavage administration of tamoxifen (7 mg dissolved in corn oil, Sigma) at E14.5 to specifically target the MGv thalamic nucleus or at E10.5 to label all principal thalamic nuclei. All the transgenic animals used in this study were maintained on an ICR or C57BL/6 genetic background and all the animals were genotyped by PCR. The Committee on Animal Research at the University Miguel Hernández approved all the animal procedures, which were carried out in compliance with Spanish and European Union regulations.

In utero cochleations

Mat. & Meth.

For *in utero* cochleations, pregnant females (E14.5) were deeply anesthetized with isoflurane to perform laparotomies. The embryos were exposed both ears were cauterized in half of the embryos of each litter. The surgical incision was closed and embryos were allowed to develop until postnatal stages, when they were perfused with 4% PFA for further analysis.

Dye-tracing studies

For axonal tracing at postnatal stages, animals were perfused with 4% paraformaldehyde in PBS 0.01M, and their brain was dissected out and post-fixed overnight in the same fixative. Small DiI (1,1'-dioctadecyl 3,3,3',3'-tetramethylindocarbocyanine perchlorate; Invitrogen) or DiA (4-[4-(dihexadecylamino) styryl]-N-methylpyridinium iodide) crystals were inserted into the distinct primary cortical areas, cochlear nucleus or the inferior colliculus, and the dyes were allowed to diffuse at 37 °C in PFA solution for 1-4 weeks. Vibratome sections (60-100µm) were then counterstained with the fluorescent nuclear dye DAPI (Sigma-Aldrich).

Measurement of brain areas and data analysis

ImageJ software was used to measure the size of the thalamic nuclei, the individual barrels and the PMBSF areas. For PMBSF and individual barrel areas data was normalized. In the case of the individual barrels, each barrel area from a given experimental condition was normalized to the corresponding barrel mean area in the control, which was considered as 1. To ensure consistent analysis, we choose rows B1-3, C1-3, D1-4 and E1-4 for mice analyzed at P4, while B1-5, C1-5, D1-5 and E1-5 were chosen to analyze older mice. These barrels were constantly present in the slices obtained after processing the brains. A TCA-GFP mouse was used to measure the size of the primary cortical areas and the area and volume of the distinct thalamic nuclei. In order to quantify the size of cortical areas, TCA-GFP (control and embBC) mice were perfused and directly process to obtain images under the stereo fluorescent microscope (Leica MZ10 F). Coronal serial slices of 80 µm were obtained from TCA-GFP brains and distinct thalamic nuclei were immunolabel with GFP and Vglut2 in order to better detect the structures. NeuroLucida explorer® from MBF Bioscience was used to quantify the volume of dLGN, VPM and MGv thalamic nuclei.

Calcium imaging in thalamocortical slices

Pregnant adult mice were sacrificed by decapitation after administering isoflurane, and their embryos were rapidly extracted and decapitated. Embryonic (E18.5) from control and embBE mouse brains were immediately dissected out and kept in an ice-cold gassed slicing solution (95% O₂/5% CO₂) containing (in mM): 2.5 KCl, 7 Mg SO₄, 0.5 CaCl₂, 1 NaH₂PO₄, 26 Na₂HCO₃, 11 glucose and 228 sucrose. Oblique vibratome slices (300-350 µm thick: VT1200 Leica Microsystems Germany) were obtained along one axis at 45 ± 2° to preserve the somatosensory (VB) and visual (dLGN) thalamocortical nuclei and their connectivity. During the recovery period, the slices were placed at room temperature (RT) in standard aCSF (119 NaCl, 5 KCl, 1.3 Mg SO₄, 2.4 CaCl₂, 1 NaH₂PO₄, 26 Na₂HCO₃, 11 glucose) saturated by gassing with 95% O₂/5% CO₂.

For dye loading, the slices were incubated for 30-45 min in 2 ml of gassed aCSF (35–37 °C) with 10 µl Cal520TM AM (AAT Bioquest) calcium dye (1 mM in DMSO + 20% pluronic acid: AAT Bioquest). The loaded slices were left for 1 hour at RT in gassed aCSF. Then, the slices were placed in a recording chamber of an upright Leica DM LFSA stage perfused (3.7 ml/min) with warmed (32 °C) and gassed aCSF. Time-lapse recording of Ca²⁺ dynamics was obtained through water immersion objectives (L 10x/0.30 N.A. Leica, L 20x/0.50 Leica) or dry objectives (HCX PL FLUOTAR 5x/0.15 Leica, PL FLUOTAR 2.5x/0.07) after exciting the slices at 492 nm with a mercury arc lamp. We acquired images with a digital CCD camera (Hamamatsu ORCA-R2 C10600-10B), using an interframe interval of 250 ms and an exposure time of 200 ms. The length of each time lapse recording was 3,000 frames.

Data analysis of Calcium imaging

Data were exported from Leica MM Fluor 1.6.0TM acquisition software as 3000 frame-long time-lapse sequences of TIFF format images and motion-corrected in ImageJ. Fluorescence traces of individual cells (recorded with L 20x/0.50 objective) were analyzed with custom developed routines in MatlabTM. Peak detection of calcium transients was performed using an amplitude threshold of 5 times the standard deviation of the baseline noise.

In situ hybridization and immunohistochemistry

For *in situ* hybridization and immunohistochemistry at postnatal stages, mice were perfused with 4% paraformaldehyde (PFA) in PBS (0.01M), and their brain was removed and post-fixed overnight in the same fixative. Immunohistochemistry was performed on 60-100 μ m vibratome or cryotome brain sections that were first incubated for 1h at room temperature in a blocking solution containing 1% BSA (Sigma) and 0.25% Triton X-100 (Sigma) in PBS 0.01M. Subsequently, the sections were incubated overnight at 4 °C with the primary antibodies: rabbit anti-vGlut2 (1:500, Synaptic Systems, #135402), rabbit anti-vGlut1 (1:500, Synaptic Systems, #135303) and rat anti-RFP (1:1000 Chromotek, #5F8). The sections were then rinsed three times in PBS 0.01M and incubated for 2h at room temperature with secondary antibodies: Alexa546 donkey anti-rabbit (1:500, ThermoFisher, #A10040), Alexa594 donkey anti-rat (1:500, ThermoFisher, #A21209), Alexa488 donkey anti-rabbit (1:500, ThermoFisher, #A21206). Finally, the sections were counterstained with the fluorescent nuclear dye, DAPI (Sigma-Aldrich).

In situ hybridization was performed on 60-100 μ m vibratome sections using digoxigenin (DIG)-labeled antisense probe for *Rorb*. Hybridization was carried out overnight at 65 °C and after hybridization, the sections were washed and incubated overnight at 4 °C with an alkaline phosphatase-conjugated anti-DIG antibody (1/2500-1/4000, Roche). The sections were then washed again and the color reaction to visualize probe binding was carried out for 1-2 days at room temperature in a solution containing NBT (nitro-blue tetrazolium chloride, Roche) and BCIP (5-bromo-4-chloro-3'-indoly phosphate p-toluidine salt, Roche). After development, the sections were washed and mounted in Glycerol Jelly (Merck Millipore).

Data analysis of vGlut1 immunostaining

All the measurements were done using ImageJ software. First, the area of dLGN was measure in the DAPI pictures. The proportion of the area occupy by vGlut1 immunostaining was measured by analyzing the amount of fluorescence in the dLGN limited area. Three images of each brain were used to perform the measurements. Images were converted to grey scale and adjusted the brightness/contrast with the fluorescence intensity to standard the fluorescence intensity across the images. The images were

converted to threshold and the proportion of the particles occupying the dLGN area was measured.

Microdissection of the thalamic nuclei

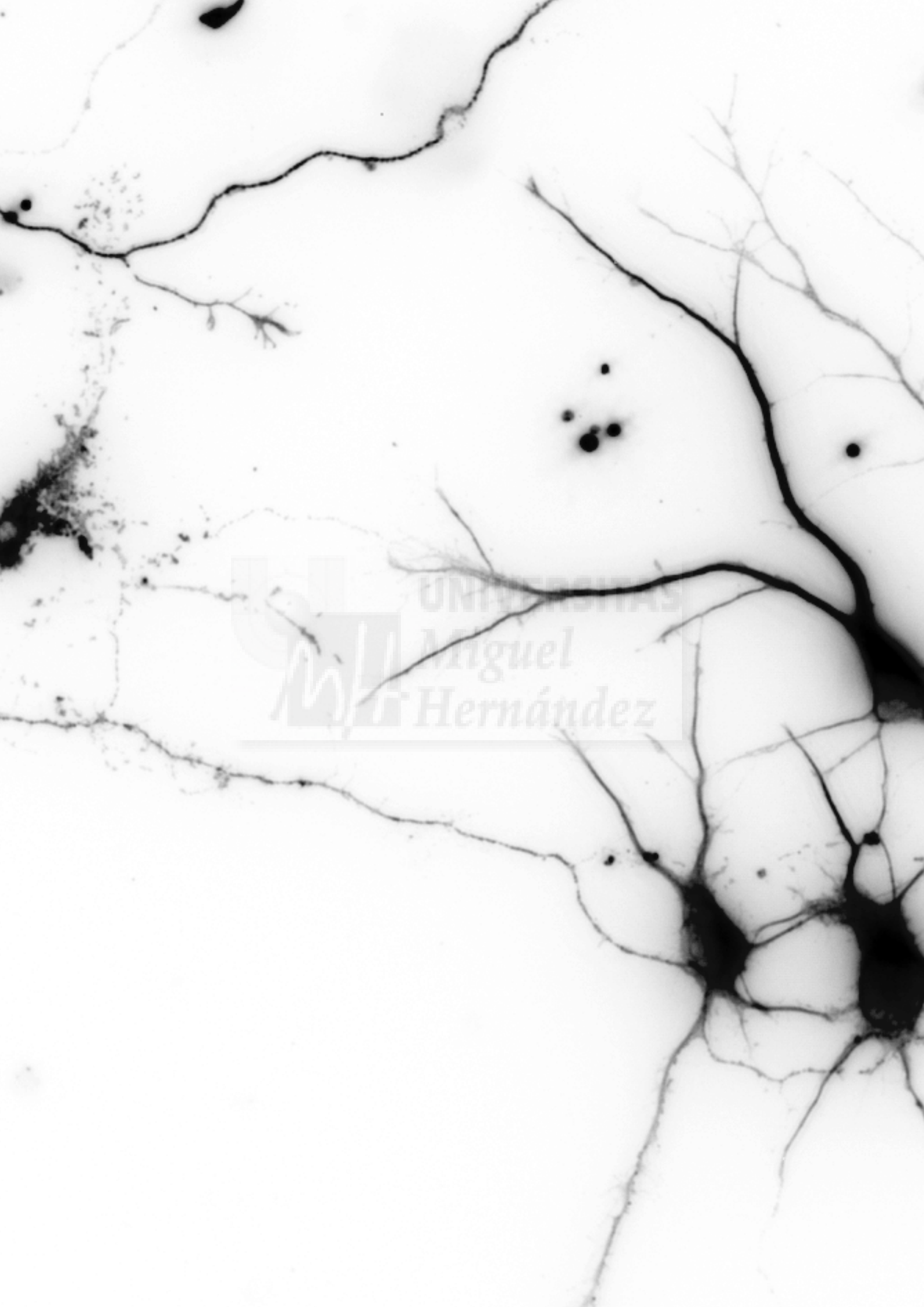
To collect tissue from the dLGN nucleus at neonatal stages, animals were sacrificed and their brain was dissected out in RNase-free conditions to prevent RNA degradation. Vibratome sections (200 μ m) were obtained and collected in ice-cold oxygenated aCSF (117mM NaCl, 4.7mM KCl, 1.2mM MgCl₂, 2.5mM CaCl₂, 1.2mM NaH₂PO₄, 25mM NaHCO₃ and 0.45% D-glucose), and the thalamic nucleus was rapidly microdissected under a microscope. The tissue was maintained overnight at 4 °C in RNA-Later (Sigma) and stored at -80 °C for subsequent RNA extraction.

RNA isolation and Affymetrix Microarray

For microarray hybridization, RNA was extracted from the tissue collected using the RNeasy Mini Kit (Qiagen), including a DNaseI step. Complimentary RNAs (two rounds of amplification) were hybridized to Affymetrix GeneChip Mouse Genome arrays 430 v2, and the signal intensities were analyzed using Partek Genomics suites (Partek, St. Louis, MI, USA) and Matlab (The MathWorks Inc, Natick, MA, USA). The data were normalized using RMA and changes in gene expression > 1.5-fold with a p-value < 0.05 were considered to reflect a significant difference in expression.

Statistics

Statistical analysis was carried out in GraphPad Prism6™ and Matlab™. Data are presented as mean and SEM. Statistical comparison between groups was performed using unpaired two-tailed Student's *t* test or Mann-Whitney U-Test non-parametric two-tailed test when data failed a Kolmogorov-Smirnov or a Shapiro Wilk normality tests. No statistical methods were used to predetermine the sample size, but our sample sizes are considered adequate for the experiments and consistent with the literature. The mice were not randomized. The investigators were blinded to sample identity except in the calcium activity experiments.



UNIVERSITAS
Miguel
Hernández

A black and white micrograph of a plant stem cross-section. The image shows a central vascular bundle with a dark pith, surrounded by a ring of large, thin-walled parenchyma cells. The outer layers consist of a cortex and an epidermis. The overall structure is radial, with vascular bundles arranged in a ring.

Discussion

UNIVERSITAS
Miguel
Hernández

Discussion

Understanding how do cortical areas acquire their functional identity is a central question that has been studied for many years. A classical paradigm used to unravel the role of afferent input in the development of the cortical territories is the deprivation of one sensory modality. To determine how the brain adapts to the sensory lost might help to better decipher the role of extrinsic and intrinsic mechanisms in cortical development. In this Thesis work, it has been demonstrated an unpredicted role of the prenatal thalamus in shaping cortical territories after input deprivation, which depends on the propagation of spontaneous calcium waves across the different thalamic sensory nuclei. Moreover, we have discovered that *Rorb* plays a crucial role in the organization of TCAs terminals in layer 4 of S1. Additionally, we have preliminary evidences that show that these experience-independent thalamic mechanisms are shared among sensory systems, as showed between somatosensory and auditory. We have elucidated common plastic adaptations in the somatosensory system when visual or auditory input is lost during embryogenesis, and the implication of *Rorb* in triggering these cross-modal changes. Finally, we have evidences that suggest that spontaneous thalamic activity is also crucial for the correct development of the corticothalamic projections in the visual system. Altogether these results contribute to elucidate the role of the thalamus and TCAs in cortical development and regionalization, and to characterize the cross-modal adaptations that take place in the brain when early sensory input is lost.

Experience-independent cross-modal reorganization of cortical areas

The classical studies of cross-modal plasticity have suggested that cortical adaptations after sensory input deprivation occur via experience-dependent increase of the intact sensory systems during the postnatal life (Bronchti et al., 1992; Rauschecker et al., 1992; Toldi et al., 1994; Zheng and Purves, 1995). Nevertheless, a definitive involvement of the sensory experience has remained controversial. Moreover, recent publications have shown that somatosensory cortical adaptations after visual deprivation are present well before the onset of sensory active experience (Fetter-Pruneda et al., 2013) (Abbott et al., 2015). Thus, these studies raised the possibility that the barrel cortex expansion in the

Discussion

blind might be triggered by experience-independent mechanisms. In the classical studies of cross-modal plasticity, deprivation of visual input was performed as early as P0 in rodents and the plasticity was analysed in adult animals. To determine whether experience-independent mechanisms might influence the size of cortical areas, we developed a method to deprive the visual input during embryogenesis in mice. In this model, we enucleated bilaterally mice at E14.5, thus the visual thalamus will never receive retinal input. Our first result was that an embryonic bilateral enucleation provokes profound cortical adaptations in the somatosensory cortex well before the sensory experience starts. Already at P4, the somatosensory cortex is enlarged and this stage is before the active whisking in mice that starts at P12 (Landers et al., 2006). This increased in size of the barrelfield is not accompanied by either changes in the somatosensory trigeminal or in the somatosensory thalamic nuclei indicating that the adaptation in the somatosensory cortex depends on changes in the thalamocortical projection.

In addition to the expansion of the spared cortical areas of the intact senses, mice enucleated on their first postnatal day show an activation of the visual cortex by auditory or somatosensory stimuli (Chabot et al., 2007). By placing DiI in the principal cortical areas (S1, V1 and A1) in our embBE model, we did not detect any evidence for a cross-modal rewiring of the thalamocortical projections. Indeed, the dLGN projects to its proper visual area (V1), showing that in the absence of the retinal axons the visual thalamocortical circuit is correctly develop, although functionally it can carry out other sensory information. Despite we have not found any apparent rewiring of the thalamocortical axons in both embBE or embBC models, we can not exclude the possibility that a cortico-cortical mechanism that may also contribute to the cross-modal cortical adaptations we observed in S1. Future studies should be aimed to analyse the cortico-cortical contribution to the expansion of the somatosensory cortex after visual or auditory deprivation.

Mechanism involved in the emergence of the thalamic waves

One of our core results is that the plasticity observed in the early-deprived animals requires cross talk among sensory modalities. The thalamus emerges as a putative core region involved in regulating this process, as it is the first relay station where sensory input converges from the distinct sensory systems. A major result derived from this

This work is that we showed a previously unknown component of thalamic spontaneous activity, the thalamic calcium waves, that modify the development of the sensory systems. These thalamic waves are propagated among the different thalamic nuclei from embryonic stages when the thalamocortical and corticothalamic projections are developing. We have found that the embryonic thalamic calcium waves are crucial for the cortical plasticity after sensory manipulations as the impairment of one sensory modality triggers profound changes in the pattern of thalamic calcium waves. Moreover, this spontaneous activity in the thalamus is crucial for the correct development of the cortical territories as the modulation of the frequency of the thalamic calcium waves, provides a mechanism to induce adaptations in the size of the cortical maps.

Thalamic calcium waves emerge embryonically, before the peripheral connectivity reaches the thalamus, which suggest that these calcium waves emerge intrinsically in this structure. Regarding the possible mechanism of its generation and propagation, it has been previously demonstrated that cortical calcium waves are modulated by the presence of gap junctions (Yuste et al., 1995; Lacar et al., 2011; Barnett et al., 2014). Here, we have shown that thalamic calcium waves are also propagated by the function of gap junctions as carbenoxolone, a general gap-junction blocker, avoids the generation of thalamic calcium waves. These waves also need membrane potential depolarization as the application of KCl leads to an increase in their frequency. In the same direction, unpublished data from our laboratory shows that the application of bicuculin, an antagonist of GABA-A receptors, leads to an increase in the frequency of waves. In sum, these results suggest that the generation and propagation of thalamic calcium waves are dependent on the electrical activity properties of the developing thalamic neurons. A hypothesis to explain how thalamic spontaneous calcium waves are generated and propagated is the following. The synchronous spontaneous activation of a group of neurons leads to a propagation of the calcium activity via gap junctions to neighbour cells involving the opening of IP₃ and ryanodine receptors (IP₃R and RYR, respectively) that allows the calcium-induced calcium release (CICR) and probably accompanied by the local paracrine release of other messengers as glutamate (Leybaert and Sanderson, 2012). Future experiments in the lab are being design to test this hypothesis by combining whole-cell patch clamp recordings, calcium imaging and pharmacological treatments.

Role of thalamic $Ror\beta$ in cortical plasticity

Spontaneous activity seems to regulate many aspects of brain development through the regulation of gene expression (Flavell and Greenberg, 2008; Mire et al., 2012; Benito and Barco, 2015; Castillo-Paterna et al., 2015; Moreno-Juan et al., 2017). We found that in the embBE mice, many genes changed in the thalamus in both dLGN and VPM. One of the genes that we found to be involved in the rearrangements of TCAs in the embBE mice microarray is *Ror β* , which is 2-fold upregulated in the VPM. It has been demonstrated an important role of cortical *Ror β* in barrel-field formation (Jabaudon et al., 2012). In this study it has been demonstrated a direct relationship between cortical *Ror β* expression, TCA innervation and barrel formation, since the interference of a correct TCA development disrupts the expression of *Ror β* in the cortex and the overexpression of this gene in the cortex is sufficient to generate barrel-like structures (Jabaudon et al., 2012). In our study we have discovered a novel function of thalamic *Ror β* where its upregulation by overexpressing *Ror β* in the thalamus in wild type mice was sufficient to increase the size of the barrelfield inducing a more complex arborisation of TCAs terminals in S1. As such, embryonic eye enucleation or cochleation trigger an overexpression of thalamic *Ror β* that predates the increase size in barrel-field by most likely modifying TCA branching in the cortex. Our results suggest that prenatal thalamic *Ror β* is a central regulator in the development of the somatosensory cortex.

It has been widely studied that the axonal branching of the thalamocortical cells is regulated by activity-dependent mechanisms (Hubel et al., 1977; Shatz and Stryker, 1978; Haruta and Hata, 2007; Uesaka et al., 2007; Alchini et al., 2017). Suppressing the spontaneous activity of thalamic cells by transfecting them with Kir2.1 leads to a reduction of their thalamic branches in culture (Yamada et al., 2010; Matsumoto et al., 2015). For the contrary, the increase of thalamic neuronal spontaneous activity by voltage-gated sodium channels activation promoted the increase of branch formation (Matsumoto et al., 2015). These results suggest that thalamic spontaneous activity is crucial for the axonal branching phenotype of the thalamocortical cells. Moreover, in this Thesis we have demonstrated that thalamic *Ror β* is regulated by spontaneous calcium activity. Additionally, *in vitro* experiments where the levels of spontaneous activity were artificially increased by adding KCl, the levels of *Ror β* were also increased in the VPM

neurons. In model where we silenced the MGv, the levels of *Rorβ* in this nucleus were reduced. Taking altogether these results show that the expression pattern of *Rorβ* can be modulated by thalamic spontaneous activity. Thus, we have discovered a new mechanism by which an activity-dependent regulation of *Rorβ* might control the expansion and plasticity of cortical areas by modulating TCA branching. Interestingly, we have analysed the *Rorβ* promoter and found that contains several motifs that are putative targets for Ca²⁺ sensitive transcription factors like CREB, AP-1 and NF-κB-binding sites (Mire et al., 2012; Benito and Barco, 2015; Castillo-Paterna et al., 2015).

Embryonic auditory deprivation: common mechanisms for cross-modal plasticity

Our results demonstrate an unprecedented role for the thalamus in the control of cross-modal plasticity in the visual-somatosensory systems (Moreno-Juan et al., 2017). By performing cochleations before the collicular axons reach the thalamus, we also collected unpublished data that shows that a similar mechanism might work between auditory and somatosensory systems. Embryonic bilateral cochleation (embBC) triggers an expansion of the somatosensory cortex before the auditory sensory onset. Interestingly, we found that despite the expansion of the S1, the VPM nucleus does not change in size similarly to what we found in the embBE mice. Furthermore, the size of the rest of the thalamic nuclei (auditory and visual) and other cortical areas (as V1 and A1) do not reveal major changes. Yet, we found a difference between both models. In the embBE mouse, the visual thalamic nucleus is reduced by 35% triggering a similar reduction of V1. In the embBC animals, axons from the IC correctly arrive to the MGv nucleus and thus afferent connections might be keeping an integral MGv and A1 sizes. A more precise analysis of the subthalamic connectivity in the embBC animals needs to be done in order to determine whether this hypothesis is correct.

As in the embBE, embryonic auditory input deprivation triggers an early postnatally (experience-independent) increase of S1. Our preliminary results also show that an increase in thalamic *Rorβ* might be involved in a common underlying mechanism. *In situ* hybridization experiments for *Rorβ* in the embBC mouse showed the upregulation of this gene in the VPM at P0. Future plans analysing the thalamic calcium waves in the VPM of the embBC animals have to be performed in order to test whether the same cross-modal changes that appear in the embBE also occur in the embBC.

Thalamic calcium waves control CTA innervation

Axons from the corticothalamic cells start to invade the dLGN at P3 (Brooks et al., 2013; Seabrook et al., 2013; Grant et al., 2016). However, although retinal axons are present in the thalamus from E15.5 (Deck et al., 2013; Moreno-Juan et al., 2017), they do not start to correctly innervate the dLGN and to establish functional synapses until P12 (Brooks et al., 2013; Seabrook et al., 2013; Grant et al., 2016). Interestingly, retinal axons are less than 10% of the total amount of synapses in the dLGN (Sherman and Guillery, 2002; Bickford et al., 2010) while the majority of the synapses present in these neurons are from TRN inputs, brainstem nuclei and V1 corticothalamic axons (CTA) (Erisir et al., 1997; Briggs and Usrey, 2008; Sherman and Guillery, 2002). Recent publications have shown the importance of retinal axons in shaping the topography of the CTAs in the dLGN (Seabrook et al., 2013; Grant et al., 2016). When mice are monocularly enucleated at birth, CTAs prematurely enter the dLGN (Grant et al., 2016). This is consistent with our unpublished data showing that in the embBE mice, CTAs (vGlut1-positive) also prematurely invade the dLGN at P4 and thus corroborate that retinal axons have a pivotal role in the control of the CTA segregation and synapses maturation in the dLGN. Indeed, the thalamic calcium waves persist in absence of retinal input although their properties are altered. Thus, the peripheral activity might modulate the thalamic intrinsic activity, as it was already suggested by other studies where different visual relay stations were recorded simultaneously (Mooney et al., 1996; Ackman et al., 2012). However, it is still possible that the role of the retinal axons in controlling the innervation of the CTAs is indirect. In this sense, we have shown that the frequency of dLGN thalamic calcium waves is increased in the embBE mice. So it is possible that CTAs invasion is controlled by thalamic spontaneous activity rather than purely by the presence or absence of retinal axons. Moreover, in a recent study where the retinal activity was silenced by injection of epibatidine in the eye, it was shown that similarly CTAs early invade the dLGN concluding that is the lack of the retinal activity the responsible factor for the aberration behaviour of the CTAs (Grant et al., 2016). To test directly this question, we check CTAs innervation by taking advantage of the $Gbx2^{Cre};Kir^{fl}$ animal model in which the thalamic spontaneous waves are eliminated (Moreno-Juan et al., 2017; N. Anton-Bolaños and G. López-Bendito, unpublished data) preserving the retinogeniculate axons. Interestingly, we found that in the absence of thalamic calcium waves, CTAs do not invade the dLGN

nucleus, at least at P6 and P8 (data not shown), as we could not find the presence of vGlut1 stained axons in the dLGN. Whether CTAs later invade this structure needs to be determined. But, how is thalamic spontaneous activity controlling the entrance of CTA into the dLGN? It is possible that thalamic activity controls the expression pattern of genes in the dLGN that might be important for CTA targeting. We have recently performed a microarray assay in which the dLGN genetic profile of the embBE mice was analysed. Thus, we have a powerful suitable dataset in which to look for specific activity-dependent genes involved in controlling the entrance of the CTAs. In the future, we aim to perform functional experiments for some of these candidate genes and study their functional role in CTAs development. Anyway, a more detailed analysis of the connectivity of CTAs in the dLGN must be done as vGlut1 is labelling corticothalamic terminals in the thalamus but is not showing directly the axons. Thus, using genetic strategies, as for example injecting virus in the V1 with specific layer 6a promoters (as Ntsr1) and thus restricting the spatial expression of fluorescent proteins, we will be able to follow the CTAs in the visual system (Olsen et al., 2012; Gerfen et al., 2013). With this sort of strategies, we will be able to analyse not only the visual system, but also the remaining sensory systems injecting the tracers in different cortical areas.

Finally, we discovered that in Th^{Kir} animals, the size of the dLGN nucleus was 33.24% smaller compared to the control animals at P7. However, measurements done at P0 in Th^{Kir} animals did not show changes in the size of the dLGN nucleus. These results prompted us to speculate that the lack of CTAs might be underlying the changes in dLGN size after the timing where CTAs must to be placed within dLGN nucleus. More studies analysing the cell death and dLGN size at different time points must to be performed in order to better achieve this hypothesis.

Thalamic spontaneous calcium waves are not indispensable for retinothalamic innervation

The role of the thalamic calcium waves in specifying the behaviour of ingrowing thalamic afferents seems to be very specific. We found that in the Th^{Kir} model, and thus silencing the thalamic waves, CTAs do not innervate the dLGN. However, surprisingly, retinothalamic innervation of the dLGN and their segregation into ipsilateral and contralateral representations of the eyes occurs perfectly within dLGN of the thalamic

Discussion

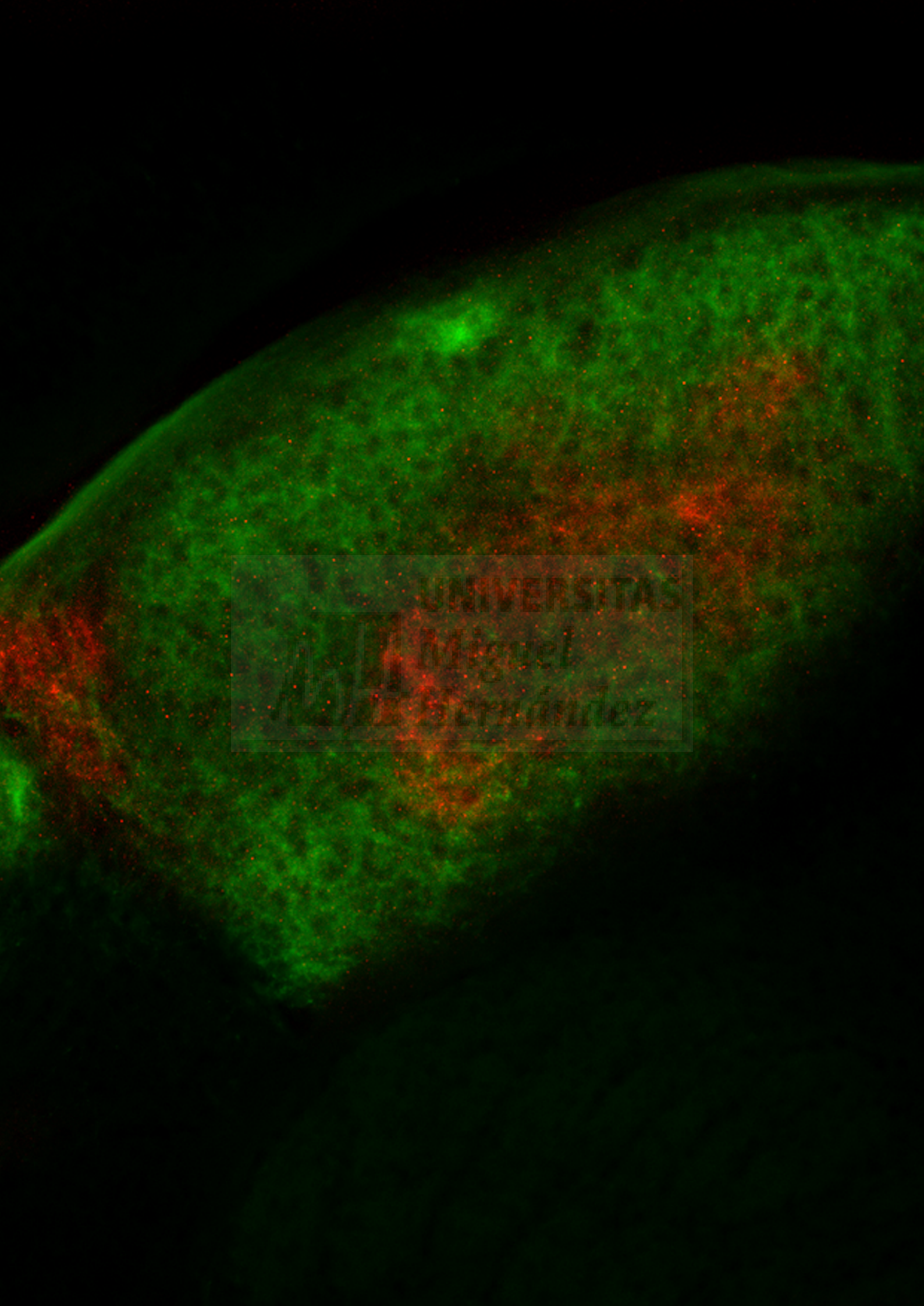
silenced mice. This is in contradiction to previous data show that cortical inputs are required for the RGCs axons to correctly innervate dLGN. Disrupting the corticogeniculate innervation by manipulations in the cortex with *Tbr1* KO or *Tra2 β* cKO mice leads to abnormal or absent innervation of the CTAs in dLGN (Shanks et al., 2016; Diao et al., 2017). The hypothesis of these studies is that the lack of corticothalamic axons triggers cell death and/or differentiation problems in dLGN neurons, making them unsuitable targets for retinal axons. A major caveat on these published data is that the models used cause a huge damage into the cortex and thus not only affect CTAs innervation of the dLGN. In our preliminary results, the lack of the CTAs in the Th^{Kir} mouse does not produce a major change in the dLGN invasion of the retinogeniculate axons. One possible explanation of these contrary phenotypes is that as vGlut1 is labelling the accumulation of this vesicular transporter in the corticothalamic terminals of the dLGN, but not the innervation of these terminals, perhaps the corticothalamic axons are invading dLGN despite they do not form correct synapses. Furthermore, as was mentioned before, more experiments with specific axonal tracers for corticogeniculate axons are needed in order to better understand these results.

Concluding remarks

Despite the great effort to understand the brain changes triggered upon sensory loss, the identity of the brain regions that are changed, the exact mechanisms that underlie cross-modal plasticity and the neural basis of behavioural compensation remain largely unknown. A better understood of how the brain is rewired after sensory deprivation is needed in order to unravel the plastic mechanisms that take place in the sensory damaged brain and to investigate possible clinic therapeutic targets promoting behavioural gains and eliminating those connections that may be maladaptive. In conclusion, the work presented in this Thesis highlight how spontaneous activity mechanism have a prominent role in early stages of development. We showed that the presence of thalamic calcium waves provides a means of communication among different sensory systems that regulates gene expression programs and drives cross-modal adaptations of cortical territories. Furthermore, this spontaneous thalamic activity is crucial for the coordination of the development of the different sensory systems. Additionally, we have shown that common mechanisms exist behind the regulation of cross-modal adaptations and that

thalamic spontaneous activity has a crucial role in the correct corticothalamic development. All these information provides novel clues to understand the compensatory cortical expansion and increased capabilities observed in blind and deaf humans (Cohen et al., 1997).





UNIVERSITAS
Miguel
Serrán

Conclusions



Conclusions

1. Embryonic visual input deprivation causes adaptations in the size of the somatosensory barrel field size at early postnatal stages, suggesting that this cross-modal plasticity occurs via experience-independent mechanisms.
2. Thalamic calcium waves communicate the different sensory thalamic nuclei regulating inter-areal cortical size before sensory experience.
3. Thalamic calcium waves are propagated via gap junctions.
4. Blockage of thalamic calcium waves triggers cortical adaptations. The silence of the thalamic auditory nucleus produces an increase in the size of the somatosensory barrel field that is predated by an increase in the frequency of waves in the somatosensory thalamic nucleus. This increase is a common mechanism also present in embBE animals.
5. Embryonic visual enucleation triggers changes in gene expression of VPM thalamic neurons at P0 and at P4.
6. *Rorb* gene is significantly upregulated in VPM neurons after embryonic visual enucleation. The increase of *Rorb* expression in the somatosensory thalamic neurons predates the enlargement of the PMBSF in embBE mice.
7. Spontaneous thalamic activity regulates the expression levels of *Rorb*.
8. Expression of *Rorb* in VPM neurons influences the total PMBSF area by modifying TCA branching *in vivo*.

Conclusions

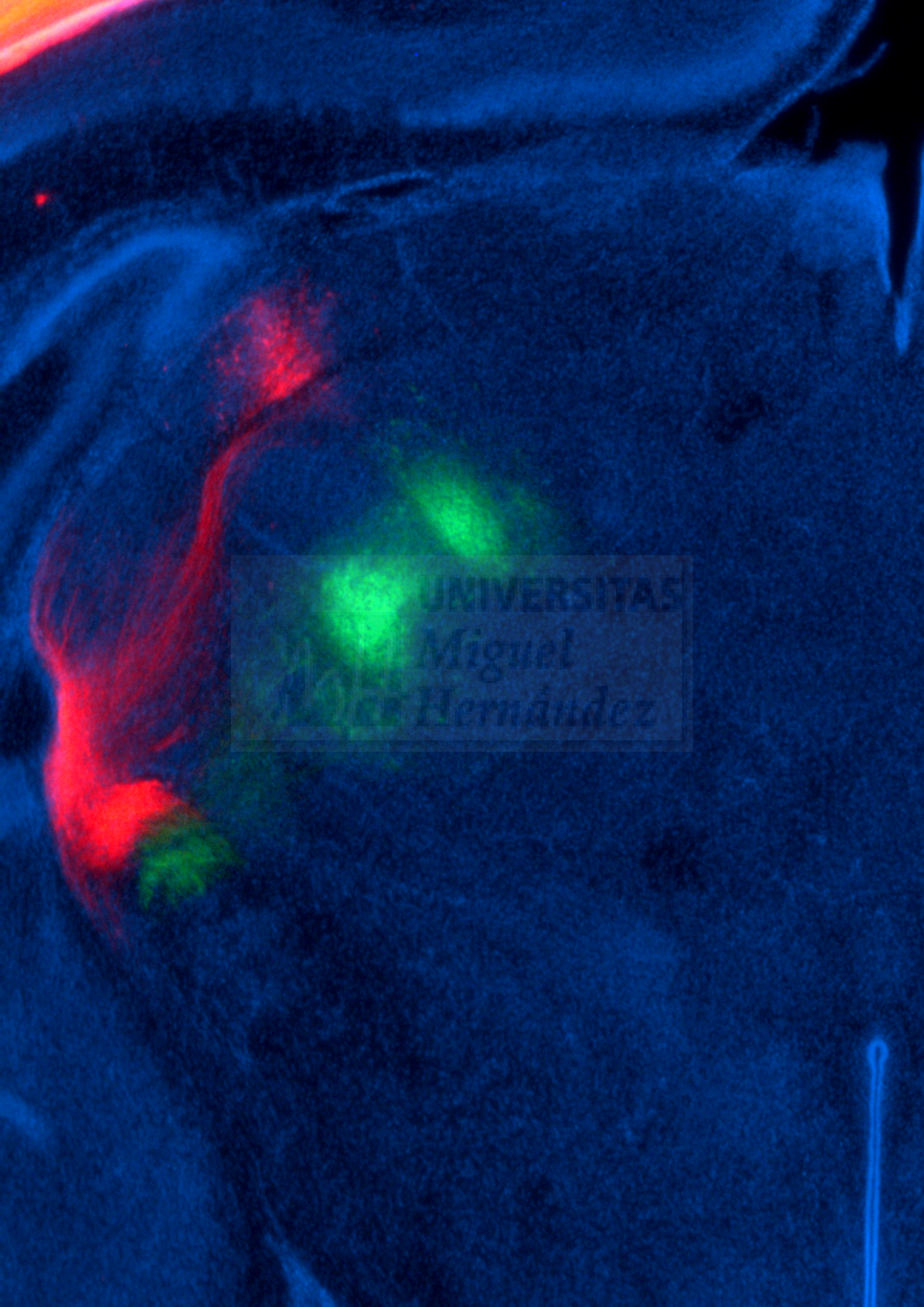
9. We have developed a new strategy to study common mechanisms behind cross-modal plasticity between different sensory systems, the embryonic auditory cochleation.
10. Embryonic auditory cochleation triggers an increase in the size of the somatosensory barrel field area similarly to what occurs in the embBE animals.
11. Embryonic auditory deprivation causes an increase in the expression levels of *Rorβ* in VPM neurons suggesting a common mechanism that regulate the somatosensory adaptations after visual or auditory deprivation.
12. Embryonic visual enucleation triggers an early invasion of the dLGN by the corticothalamic axons.
13. Embryonic visual enucleation triggers an increase in the frequency of dLGN waves at E18.5 and leads to transcriptional gene changes in this structure both at P0 and P4.
14. Thalamic spontaneous calcium waves control the invasion profile of the corticothalamic axons in dLGN.
15. The segregation of the retinal axons in dLGN is independent of the thalamic spontaneous calcium waves, and the invasion of the dLGN by corticothalamic axons.

Conclusiones

1. La enucleación visual embrionaria causa adaptaciones en el tamaño de la corteza somatosensorial de barriles en estadios embrionarios tempranos, lo que sugiere que la plasticidad cross-modal ocurre a través mecanismos independientes de la experiencia.
2. Las ondas talámicas de calcio comunican los diferentes núcleos talámicos regulando el tamaño de las áreas corticales antes de la existencia de experiencia sensorial.
3. Las ondas talámicas se propagan vía uniones gap.
4. El bloqueo de las ondas talámicas de calcio provoca adaptaciones corticales. El silenciado del núcleo talámico auditivo produce un aumento del tamaño de la corteza somatosensorial de barriles, provocado por un incremento en la frecuencia de las ondas de calcio del núcleo talámico somatosensorial. Este aumento de actividad es un mecanismo común que también está presente en los embriones enucleados.
5. La enucleación embrionaria visual provoca cambios en la expresión de genes de las neuronas talámicas del VPM a P0 y a P4.
6. La expresión del gen *Rorb* está incrementada en las neuronas del VPM tras la enucleación visual embrionaria. Este incremento en la expresión de *Rorb* en las neuronas talámicas provoca el aumento del tamaño del PMBSF en los ratones enucleados.
7. La actividad espontánea talámica regula los niveles de *Rorb*.

Conclusions

8. La expresión de *Rorb* en neuronas del VPM controla el área total del PMBSF modificando la ramificación de los axones talamocorticales *in vivo*.
9. Hemos desarrollado una nueva estrategia para estudiar la presencia de mecanismos comunes de plasticidad cross-modal entre sistemas sensoriales diferentes, la cocleotomía auditiva embrionaria.
10. La cocleotomía auditiva embrionaria provoca un aumento en el tamaño de la corteza de barriles somatosensorial de manera similar a como ocurre en los animales enucleados en estadios embrionarios.
11. La privación auditiva embrionaria causa un aumento en la expresión de *Rorb* en las neuronas del VPM, lo que sugiere la existencia de mecanismos comunes que regulan adaptaciones somatosensoriales tras la pérdida visual o auditiva.
12. La enucleación visual embrionaria provoca cambios en la inervación temprana de los axones corticotálamicos en el núcleo dLGN.
13. La enucleación visual embrionaria provoca un aumento en la frecuencia de ondas de calcio en el dLGN a E18.5 y conlleva cambios en la expresión genética de esta estructura a P0 y a P4.
14. Las ondas talámicas de calcio controlan el perfil de invasión de los axones corticotálamicos en el dLGN.
15. La segregación de los axones de la retina en el dLGN es independiente de las ondas de actividad talámica espontánea y también de la invasión del dLGN por los axones corticotálamicos.



UNIVERSITAS
Miguel
Hernández

References

UNIVERSITAS
Miguel
Alonso Hernández

References

Abbott CW, Kozanian OO, Huffman KJ (2015) The effects of lifelong blindness on murine neuroanatomy and gene expression. *Front Aging Neurosci* 7:381–13.

Abdel-Majid RM, Leong WL, Schalkwyk LC, Smallman DS, Wong ST, Storm DR, Fine A, Dobson MJ, Guernsey DL, Neumann PE (1998) Loss of adenylyl cyclase I activity disrupts patterning of mouse somatosensory cortex. *Nat Genet* 19:289–291.

Ackman JB, Burbridge TJ, Crair MC (2012) Retinal waves coordinate patterned activity throughout the developing visual system. *Nature* 490:219–225.

Agmon A, Yang LT, Jones EG, O'Dowd DK (1995) Topological precision in the thalamic projection to neonatal mouse barrel cortex. *Journal of Neuroscience* 15:549–561.

Alchini R, Sato H, Matsumoto N, Shimogori T, Sugo N, Yamamoto N (2017) Nucleocytoplasmic Shuttling of Histone Deacetylase 9 Controls Activity-Dependent Thalamocortical Axon Branching. *Sci Rep* 7:6024.

Allendoerfer KL, Shatz CJ (1994) The subplate, a transient neocortical structure: its role in the development of connections between thalamus and cortex. *Annu Rev Neurosci* 17:185–218.

Angelucci A, Clasca F, Bricolo E, Cramer KS, Sur M (1997) Experimentally induced retinal projections to the ferret auditory thalamus: development of clustered eye-specific patterns in a novel target. *Journal of Neuroscience* 17:2040–2055.

Angelucci A, Clasca F, Sur M (1998) Brainstem inputs to the ferret medial geniculate nucleus and the effect of early deafferentation on novel retinal projections to the auditory thalamus. *J Comp Neurol* 400:417–439.

Antonini A, Fagiolini M, Stryker MP (1999) Anatomical correlates of functional plasticity in mouse visual cortex. *Journal of Neuroscience* 19:4388–4406.

Antonini A, Stryker MP (1996) Plasticity of geniculocortical afferents following brief or prolonged monocular occlusion in the cat. *J Comp Neurol* 369:64–82.

Arai Y, Pierani A (2014) Development and evolution of cortical fields. *Neuroscience Research* 86:66–76.

References

Araneda R, Renier L, Ebner-Karestinou D, Dricot L, De Volder AG (2017) Hearing, feeling or seeing a beat recruits a supramodal network in the auditory dorsal stream. *Eur J Neurosci* 45:1439–1450.

Armentano M, Chou S-J, Srubek Tomassy G, Leingärtner A, O'Leary DDM, Studer M (2007) COUP-TFI regulates the balance of cortical patterning between frontal/motor and sensory areas. *Nat Neurosci* 10:1277–1286.

Ashmore J, Avan P, Brownell WE, Dallos P, Dierkes K, Fettiplace R, Grosh K, Hackney CM, Hudspeth AJ, Jülicher F, Lindner B, Martin P, Meaud J, Petit C, Santos Sacchi JR, Canlon B (2010) The remarkable cochlear amplifier. *Hearing Research* 266:1–17.

Auladell C, Perez-Sust P, Super H, Soriano E (2000) The early development of thalamocortical and corticothalamic projections in the mouse. *Anat Embryol (Berl)* 201:169–179.

Bagnall MW, Hull C, Bushong EA, Ellisman MH, Scanziani M (2011) Multiple Clusters of Release Sites Formed by Individual Thalamic Afferents onto Cortical Interneurons Ensure Reliable Transmission. *Neuron* 71:180–194.

Ballester-Rosado CJ, Sun H, Huang JY, Lu HC (2016) mGluR5 Exerts Cell-Autonomous Influences on the Functional and Anatomical Development of Layer IV Cortical Neurons in the Mouse Primary Somatosensory Cortex. *Journal of Neuroscience* 36:8802–8814.

Barnett HM, Gjorgjieva J, Weir K, Comfort C, Fairhall AL, Moody WJ (2014) Relationship between individual neuron and network spontaneous activity in developing mouse cortex. *Journal of Neurophysiology* 112:3033–3045.

Bavelier D, Neville HJ (2002) Cross-modal plasticity: where and how? *Nature Reviews Neuroscience* 3:443–452.

Benito E, Barco A (2015) The neuronal activity-driven transcriptome. *Mol Neurobiol* 51:1071–1088.

Berglund AM, Ryugo DK (1987) Hair cell innervation by spiral ganglion neurons in the mouse. *J Comp Neurol* 255:560–570.

Bickford ME, Slusarczyk A, Dilger EK, Krahe TE, Kucuk C, Guido W (2010) Synaptic development of the mouse dorsal lateral geniculate nucleus. *J Comp Neurol* 518:622–635.
Bicknese AR, Sheppard AM, O'Leary DD, Pearlman AL (1994) Thalamocortical axons extend along a chondroitin sulfate proteoglycan-enriched pathway coincident with the

neocortical subplate and distinct from the efferent path. *Journal of Neuroscience* 14:3500–3510.

Bielle F, Marcos-Mondéjar P, Leyva-Díaz E, Lokmane L, Mire E, Mailhes C, Keita M, García N, Tessier-Lavigne M, Garel S, López-Bendito G (2011) Emergent Growth Cone Responses to Combinations of Slit1 and Netrin 1 in Thalamocortical Axon Topography. *Current Biology* 21:1748–1755.

Bishop KM, Garel S, Nakagawa Y, Rubenstein JLR, O'Leary DDM (2003) Emx1 and Emx2 cooperate to regulate cortical size, lamination, neuronal differentiation, development of cortical efferents, and thalamocortical pathfinding. *J Comp Neurol* 457:345–360.

Braisted JE, Ringstedt T, O'Leary DDM (2009) Slits Are Chemorepellents Endogenous to Hypothalamus and Steer Thalamocortical Axons into Ventral Telencephalon. *Cerebral Cortex* 19:i144–i151.

Braisted JEEA (1999) Thalamocortical Axons Are Influenced by Chemorepellent and Chemoattractant Activities Localized to Decision Points along Their Path. :1–11.

Briggs F, Usrey WM (2008) Emerging views of corticothalamic function. *Current Opinion in Neurobiology* 18:403–407.

Bronchti G, Schonenberger N, Welker E, Van der Loos H (1992) Barreldfield expansion after neonatal eye removal in mice. *Neuroreport* 3:489–492.

Brooks JM, Su J, Levy C, Wang JS, Seabrook TA, Guido W, Fox MA (2013) A molecular mechanism regulating the timing of corticogeniculate innervation. *CellReports* 5:573–581.

Buchel C, Price C, Friston K (1998) A multimodal language region in the ventral visual pathway. *Nature* 394:274–277.

Bulfone A, Puelles L, Porteus MH, Frohman MA, Martin GR, Rubenstein JL (1993) Spatially restricted expression of *Dlx-1*, *Dlx-2* (*Tes-1*), *Gbx-2*, and *Wnt-3* in the embryonic day 12.5 mouse forebrain defines potential transverse and longitudinal segmental boundaries. *Journal of Neuroscience* 13:3155–3172.

Calvert GA (2001) Crossmodal processing in the human brain: insights from functional neuroimaging studies. *Cerebral Cortex* 11:1110–1123.

References

Cases O, Vitalis T, Seif I, De Maeyer E, Sotelo C, Gaspar P (1996) Lack of barrels in the somatosensory cortex of monoamine oxidase A-deficient mice: role of a serotonin excess during the critical period. *Neuron* 16:297–307.

Castillo-Paterna M, Moreno-Juan V, Filipchuk A, Rodriguez-Malmierca L, Susin R, Lopez Bendito G (2015) DCC functions as an accelerator of thalamocortical axonal growth downstream of spontaneous thalamic activity. *EMBO reports* 16:851–862.

Catalano SM, Shatz CJ (1998) Activity-dependent cortical target selection by thalamic axons. *Science* 281:559–562.

Chabot N, Robert S, Tremblay R, Miceli D, Boire D, Bronchti G (2007) Audition differently activates the visual system in neonatally enucleated mice compared with anophthalmic mutants. *European Journal of Neuroscience* 26:2334–2348.

Chen L, Guo Q, Li JYH (2009) Transcription factor Gbx2 acts cell-nonautonomously to regulate the formation of lineage-restriction boundaries of the thalamus. *Development* 136:1317–1326.

Chou SJ, Babot Z, Leingartner A, Studer M, Nakagawa Y, O'Leary DDM (2013) Geniculocortical Input Drives Genetic Distinctions Between Primary and Higher-Order Visual Areas. *Science* 340:1239–1242.

Cichon J, Gan W-B (2015) Branch-specific dendritic Ca²⁺ spikes cause persistent synaptic plasticity. *Nature* 520:180–185.

Clark WE (1932) A MORPHOLOGICAL STUDY OF THE LATERAL GENICULATE BODY. *Br J Ophthalmol* 16:264–284.

Clause A, Kim G, Sonntag M, Weisz CJC, Vetter DE, Rübtsamen R, Kandler K (2014) The Precise Temporal Pattern of Prehearing Spontaneous Activity Is Necessary for Tonotopic Map Refinement. *Neuron* 82:822–835.

Cohen LG, Celnik P, Pascual-Leone A, Corwell B, Falz L, Dambrosia J, Honda M, Sadato N, Gerloff C, Catala MD, Hallett M (1997) Functional relevance of cross-modal plasticity in blind humans. *Nature* 389:180–183.

Constantinople CM, Bruno RM (2013) Deep Cortical Layers Are Activated Directly by Thalamus. *Science* 340:1591–1594.

Couchman K, Garrett A, Deardorff AS, Rattay F, Resatz S, Fyffe R, Walmsley B, Leão RN (2011) Lateral superior olive function in congenital deafness. *Hearing Research* 277:163–175.

Crandall SR, Cruikshank SJ, Connors BW (2015) A Corticothalamic Switch: Controlling the Thalamus with Dynamic Synapses. *Neuron* 86:768–782.

Cruz-Martín A, El-Danaf RN, Osakada F, Sriram B, Dhande OS, Nguyen PL, Callaway EM, Ghosh A, Huberman AD (2014) A dedicated circuit links direction-selective retinal ganglion cells to the primary visual cortex. *Nature* 507:358–361.

Çavdar S, Bay HH, Yıldız SD, Akakın D, Şirvancı S, Onat F (2014) Comparison of numbers of interneurons in three thalamic nuclei of normal and epileptic rats. *Neurosci Bull* 30:451–460.

Davis ZW, Chapman B, Cheng HJ (2015) Increasing Spontaneous Retinal Activity before Eye Opening Accelerates the Development of Geniculate Receptive Fields. *Journal of Neuroscience* 35:14612–14623.

De Carlos JA, O'Leary DD (1992) Growth and targeting of subplate axons and establishment of major cortical pathways. *Journal of Neuroscience* 12:1194–1211.

Deck M, Lokmane L, Chauvet S, Mailhes C, Keita M, Niquille M, Yoshida M, Yoshida Y, Lebrand C, Mann F, Grove EA, Garel S (2013) Pathfinding of Corticothalamic Axons Relies on a Rendezvous with Thalamic Projections. *Neuron* 77:472–484.

del Rio JA, de Lecea L, Ferrer I, Soriano E (1994) The development of parvalbumin-immunoreactivity in the neocortex of the mouse. *Brain Res Dev Brain Res* 81:247–259.

Dhande OS, Stafford BK, Lim J-HA, Huberman AD (2015) Contributions of Retinal Ganglion Cells to Subcortical Visual Processing and Behaviors. *Annu Rev Vis Sci* 1:291–328.

Diamond IT, Jones EG, Powell TP (1969) The projection of the auditory cortex upon the diencephalon and brain stem in the cat. *Brain Res* 15:305–340.

Diao Y, Cui L, Chen Y, Burbridge TJ, Han W, Wirth B, Sestan N, Crair MC, Zhang J (2017) Reciprocal Connections Between Cortex and Thalamus Contribute to Retinal Axon Targeting to Dorsal Lateral Geniculate Nucleus. *Cerebral Cortex*:1–15.

Dupont E, Hanganu IL, Kilb W, Hirsch S, Luhmann HJ (2005) Rapid developmental switch in the mechanisms driving early cortical columnar networks. *Nature* 439:79–83.

References

Dye CA, Abbott CW, Huffman KJ (2012) Bilateral enucleation alters gene expression and intraneocortical connections in the mouse. *Neural Dev* 7:5.

Erisir A, Van Horn SC, Bickford ME, Sherman SM (1997) Immunocytochemistry and distribution of parabrachial terminals in the lateral geniculate nucleus of the cat: a comparison with corticogeniculate terminals. *J Comp Neurol* 377:535–549.

Erzurumlu RS, Jhaveri S (1992) Emergence of connectivity in the embryonic rat parietal cortex. *Cerebral Cortex* 2:336–352.

Espinosa JS, Stryker MP (2012) Development and plasticity of the primary visual cortex. *Neuron* 75:230–249.

Espinosa JS, Wheeler DG, Tsien RW, Luo L (2009) Uncoupling Dendrite Growth and Patterning: Single-Cell Knockout Analysis of NMDA Receptor 2B. *Neuron* 62:205–217.

Fagiolini M, Hensch TK (2000) Inhibitory threshold for critical-period activation in primary visual cortex. *Nature* 404:183–186.

Fetter-Pruneda I, Geovannini-Acuña H, Santiago C, Ibararán-Viniegra AS, Martínez-Martínez E, Sandoval-Velasco M, Uribe-Figueroa L, Padilla-Cortés P, Mercado-Célis G, Gutiérrez-Ospina G (2013) Shifts in Developmental Timing, and Not Increased Levels of Experience-Dependent Neuronal Activity, Promote Barrel Expansion in the Primary Somatosensory Cortex of Rats Enucleated at Birth Allodi S, ed. *PLoS ONE* 8:e54940–14.

Firth SI, Wang C-T, Feller MB (2005) Retinal waves: mechanisms and function in visual system development. *Cell Calcium* 37:425–432.

Flavell SW, Greenberg ME (2008) Signaling mechanisms linking neuronal activity to gene expression and plasticity of the nervous system. *Annu Rev Neurosci* 31:563–590.

Fox K, Schlaggar BL, Glazewski S, O'Leary DD (1996) Glutamate receptor blockade at cortical synapses disrupts development of thalamocortical and columnar organization in somatosensory cortex. *Proceedings of the National Academy of Sciences* 93:5584–5589.

Frangeul L, Pouchelon G, Telley L, Lefort S, Lüscher C, Jabaudon D (2016) A cross-modal genetic framework for the development and plasticity of sensory pathways. *Nature* 538:96–98.

- Franklin SR, Brunso-Bechtold JK, Henkel CK (2006) Unilateral cochlear ablation before hearing onset disrupts the maintenance of dorsal nucleus of the lateral lemniscus projection patterns in the rat inferior colliculus. *Neuroscience* 143:105–115.
- Franklin SR, Brunso-Bechtold JK, Henkel CK (2008) Bilateral cochlear ablation in postnatal rat disrupts development of banded pattern of projections from the dorsal nucleus of the lateral lemniscus to the inferior colliculus. *Neuroscience* 154:346–354.
- Friauf E, Lohmann C (1999) Development of auditory brainstem circuitry. Activity-dependent and activity-independent processes. *Cell Tissue Res* 297:187–195.
- Friauf E, Shatz CJ (1991) Changing patterns of synaptic input to subplate and cortical plate during development of visual cortex. *Journal of Neurophysiology* 66:2059–2071.
- Frost DO, Caviness VSJ (1980) Radial organization of thalamic projections to the neocortex in the mouse. *J Comp Neurol* 194:369–393.
- Frost DO, Schneider GE (1979) Plasticity of retinofugal projections after partial lesions of the retina in newborn Syrian hamsters. *J Comp Neurol* 185:517–567.
- Froud KE, Wong ACY, Cederholm JME, Klugmann M, Sandow SL, Julien J-P, Ryan AF, Housley GD (2015) Type II spiral ganglion afferent neurons drive medial olivocochlear reflex suppression of the cochlear amplifier. *Nat Commun* 6:7115.
- Fu Y, Kaneko M, Tang Y, Alvarez-Buylla A, Stryker MP (2015) A cortical disinhibitory circuit for enhancing adult plasticity. *Elife* 4:e05558.
- Fukuchi-Shimogori T (2001) Neocortex Patterning by the Secreted Signaling Molecule FGF8. *Science* 294:1071–1074.
- Gabriele ML, Brunso-Bechtold JK, Henkel CK (2000a) Development of afferent patterns in the inferior colliculus of the rat: projection from the dorsal nucleus of the lateral lemniscus. *J Comp Neurol* 416:368–382.
- Gabriele ML, Brunso-Bechtold JK, Henkel CK (2000b) Plasticity in the development of afferent patterns in the inferior colliculus of the rat after unilateral cochlear ablation. *Journal of Neuroscience* 20:6939–6949.
- Garel S (2002) The early topography of thalamocortical projections is shifted in *Ebf1* and *Dlx1/2* mutant mice. *Development* 129:5621–5634.

References

Garel S, López-Bendito G (2014) ScienceDirectInputs from the thalamocortical system on axon pathfinding mechanisms. *Current Opinion in Neurobiology* 27:143–150.

Garel S, Rubenstein JLR (2004) Intermediate targets in formation of topographic projections: inputs from the thalamocortical system. *Trends in Neurosciences* 27:533–539.

Garrett ME, Nauhaus I, Marshel JH, Callaway EM (2014) Topography and areal organization of mouse visual cortex. *Journal of Neuroscience* 34:12587–12600.

Gerfen CR, Paletzki R, Heintz N (2013) GENSAT BAC Cre-Recombinase Driver Lines to Study the Functional Organization of Cerebral Cortical and Basal Ganglia Circuits. *Neuron* 80:1368–1383.

Gezelius H, López-Bendito G (2016) Thalamic neuronal specification and early circuit formation. *Devel Neurobio*:1–14.

Gezelius H, Moreno-Juan V, Mezzera C, Thakurela S, Rodriguez-Malmierca LM, Pistolic J, Benes V, Tiwari VK, López-Bendito G (2017) Genetic Labeling of Nuclei-Specific Thalamocortical Neurons Reveals Putative Sensory-Modality Specific Genes. *Cerebral Cortex* 27:5054–5069.

Gheorghita F, Kraftsik R, Dubois R, Welker E (2006) Structural Basis for Map Formation in the Thalamocortical Pathway of the Barrelless Mouse. *Journal of Neuroscience* 26:10057–10067.

Godement P, Salaun J, Imbert M (1984) Prenatal and postnatal development of retinogeniculate and retinocollicular projections in the mouse. *J Comp Neurol* 230:552–575.

Golding B, Pouchelon G, Bellone C, Murthy S, Di Nardo AA, Govindan S, Ogawa M, Shimogori T, Lüscher C, Dayer A, Jabaudon D (2014) Retinal Input Directs the Recruitment of Inhibitory Interneurons into Thalamic Visual Circuits. *Neuron* 81:1057–1069.

Golshani P, Goncalves JT, Khoshkhoo S, Mostany R, Smirnakis S, Portera-Cailliau C (2009) Internally Mediated Developmental Desynchronization of Neocortical Network Activity. *Journal of Neuroscience* 29:10890–10899.

Grant E, Hoerder-Suabedissen A, Molnár Z (2012) Development of the corticothalamic projections. *Front Neurosci* 6:53.

- Grant E, Hoerder-Suabedissen A, Molnár Z (2016) The Regulation of Corticofugal Fiber Targeting by Retinal Inputs. *Cerebral Cortex* 26:1336–1348.
- Greig LC, Woodworth MB, Greppi C, Macklis JD (2016) Ctip1 Controls Acquisition of Sensory Area Identity and Establishment of Sensory Input Fields in the Developing Neocortex. *Neuron* 90:261–277.
- Grove EA, Fukuchi-Shimogori T (2003) GENERATING THE CEREBRAL CORTICAL AREAS. *Annu Rev Neurosci* 26:355–380.
- Grubb MS, Rossi FM, Changeux JP, Thompson ID (2003) Abnormal functional organization in the dorsal lateral geniculate nucleus of mice lacking the beta 2 subunit of the nicotinic acetylcholine receptor. *Neuron* 40:1161–1172.
- Guillery RW (1967) Patterns of fiber degeneration in the dorsal lateral geniculate nucleus of the cat following lesions in the visual cortex. *J Comp Neurol* 130:197–221.
- Guillery RW (1995) Retinal representations. *Science* 267:1038.
- Guillery RW, Sherman SM (2002) The thalamus as a monitor of motor outputs. *Philosophical Transactions of the Royal Society B: Biological Sciences* 357:1809–1821.
- Hamasaki T, Leingärtner A, Ringstedt T, O'Leary DDM (2004) EMX2 Regulates Sizes and Positioning of the Primary Sensory and Motor Areas in Neocortex by Direct Specification of Cortical Progenitors. *Neuron* 43:359–372.
- Hammer S, Monavarfeshani A, Lemon T, Su J, Fox MA (2015) Multiple Retinal Axons Converge onto Relay Cells in the Adult Mouse Thalamus. *CellReports* 12:1575–1583.
- Hanganu IL, Okabe A, Lessmann V, Luhmann HJ (2009) Cellular mechanisms of subplate-driven and cholinergic input-dependent network activity in the neonatal rat somatosensory cortex. *Cerebral Cortex* 19:89–105.
- Hanganu-Opatz IL (2010) Between molecules and experience: role of early patterns of coordinated activity for the development of cortical maps and sensory abilities. *Brain Res Rev* 64:160–176.
- Hannan AJ, Blakemore C, Katsnelson A, Vitalis T, Huber KM, Bear M, Roder J, Kim D, Shin HS, Kind PC (2001) PLC-beta1, activated via mGluRs, mediates activity-dependent differentiation in cerebral cortex. *Nat Neurosci* 4:282–288.

References

Haruta M, Hata Y (2007) Experience-driven axon retraction without binocular imbalance in developing visual cortex. *Current Biology* 17:37–42.

Hashisaki GT, Rubel EW (1989) Effects of unilateral cochlea removal on anteroventral cochlear nucleus neurons in developing gerbils. *J Comp Neurol* 283:5–73.

Hayes SG, Murray KD, Jones EG (2003) Two epochs in the development of gamma-aminobutyric acidergic neurons in the ferret thalamus. *J Comp Neurol* 463:45–65.

Hensch TK (2005) Critical period plasticity in local cortical circuits. *Nature Reviews Neuroscience* 6:877–888.

Higashi S, Molnar Z, Kurotani T, Toyama K (2002) Prenatal development of neural excitation in rat thalamocortical projections studied by optical recording. *Neuroscience* 115:1231–1246.

Hirtz JJ, Boesen M, Braun N, Deitmer JW, Kramer F, Lohr C, Muller B, Nothwang HG, Striessnig J, Lohrke S, Friauf E (2011) Cav1.3 Calcium Channels Are Required for Normal Development of the Auditory Brainstem. *Journal of Neuroscience* 31:8280–8294.

Hoerder-Suabedissen A, Molnár Z (2015) Development, evolution and pathology of neocortical subplate neurons. *Nature Publishing Group* 16:133–146.

Hoogland PV, Welker E, Van der Loos H (1987) Organization of the projections from barrel cortex to thalamus in mice studied with *Phaseolus vulgaris*-leucoagglutinin and HRP. *Experimental Brain Research* 68:73–87.

Hubel DH, Wiesel TN, Stryker MP (1977) Orientation columns in macaque monkey visual cortex demonstrated by the 2-deoxyglucose autoradiographic technique. *Nature* 269:328–330.

Huberman AD, Manu M, Koch SM, Susman MW, Lutz AB, Ullian EM, Baccus SA, Barres BA (2008) Architecture and activity-mediated refinement of axonal projections from a mosaic of genetically identified retinal ganglion cells. *Neuron* 59:425–438.

Huberman AD, Speer CM, Chapman B (2006) Spontaneous retinal activity mediates development of ocular dominance columns and binocular receptive fields in v1. *Neuron* 52:247–254.

Huberman AD, Stellwagen D, Chapman B (2002) Decoupling eye-specific segregation from lamination in the lateral geniculate nucleus. *Journal of Neuroscience* 22:9419–9429.

Hull C, Isaacson JS, Scanziani M (2009) Postsynaptic Mechanisms Govern the Differential Excitation of Cortical Neurons by Thalamic Inputs. *Journal of Neuroscience* 29:9127–9136.

Inan M (2006) Barrel Map Development Relies on Protein Kinase A Regulatory Subunit IIbeta-Mediated cAMP Signaling. *Journal of Neuroscience* 26:4338–4349.

Iwasato T, Erzurumlu RS, Huerta PT, Chen DF, Sasaoka T, Ulupinar E, Tonegawa S (1997) NMDA receptor-dependent refinement of somatotopic maps. *Neuron* 19:1201–1210.

Iwasato T, Inan M, Kanki H, Erzurumlu RS, Itohara S, Crair MC (2008) Cortical Adenylyl Cyclase 1 Is Required for Thalamocortical Synapse Maturation and Aspects of Layer IV Barrel Development. *Journal of Neuroscience* 28:5931–5943.

Jabaudon D, J Shnider S, J Tischfield D, J Galazo M, Macklis JD (2012) ROR Induces Barrel-like Neuronal Clusters in the Developing Neocortex. *Cerebral Cortex* 22:996–1006.

Jacobs EC, Campagnoni C, Kampf K, Reyes SD, Kalra V, Handley V, Xie Y-Y, Hong-Hu Y, Spreur V, Fisher RS, Campagnoni AT (2007) Visualization of corticofugal projections during early cortical development in a τ -GFP-transgenic mouse. *European Journal of Neuroscience* 25:17–30.

Jager P, Ye Z, Yu X, Zagoraoui L, Prekop H-T, Partanen J, Jessell TM, Wisden W, Brickley SG, Delogu A (2016) Tectal-derived interneurons contribute to phasic and tonic inhibition in the visual thalamus. *Nat Commun* 7:1–14.

Jagger DJ (2003) Membrane Properties of Type II Spiral Ganglion Neurons Identified in a Neonatal Rat Cochlear Slice. *J Physiol*:1–9.

Jaubert-Miazza L, Green E, Lo F-S, Bui K, Mills J, Guido W (2005) Structural and functional composition of the developing retinogeniculate pathway in the mouse. *Vis Neurosci* 22:661–676.

Jensen KF, Killackey HP (1987) Terminal arbors of axons projecting to the somatosensory cortex of the adult rat. I. The normal morphology of specific thalamocortical afferents. *Journal of Neuroscience* 7:3529–3543.

References

- Jhaveri S, Erzurumlu RS, Crossin K (1991) Barrel construction in rodent neocortex: role of thalamic afferents versus extracellular matrix molecules. *Proceedings of the National Academy of Sciences* 88:4489–4493.
- Jones EG (2002) Thalamic circuitry and thalamocortical synchrony. *Philosophical Transactions of the Royal Society B: Biological Sciences* 357:1659–1673.
- Jones EG, Powell TP (1968) The projection of the somatic sensory cortex upon the thalamus in the cat. *Brain Res* 10:369–391.
- Jones EG, Rubenstein JLR (2004) Expression of regulatory genes during differentiation of thalamic nuclei in mouse and monkey. *J Comp Neurol* 477:55–80.
- Jones, E.G. (2007) *The Thalamus*, 2nd ed. Cambridge University Press. Cambridge, UK
- Kandler K, Clause A, Noh J (2009) Tonotopic reorganization of developing auditory brainstem circuits. *Nat Neurosci* 12:711–717.
- Kanold PO, Luhmann HJ (2010) The Subplate and Early Cortical Circuits. *Annu Rev Neurosci* 33:23–48.
- Kelley MW, Talreja DR, Corwin JT (1995) Replacement of hair cells after laser microbeam irradiation in cultured organs of corti from embryonic and neonatal mice. *Journal of Neuroscience* 15:3013–3026.
- Kiang NY, Rho JM, Northrop CC, Liberman MC, Ryugo DK (1982) Hair-cell innervation by spiral ganglion cells in adult cats. *Science* 217:175–177.
- Kilb W, Kirischuk S, Luhmann HJ (2011) Electrical activity patterns and the functional maturation of the neocortex. *Eur J Neurosci* 34:1677–1686.
- Killackey HP, Belford G, Ryugo R, Ryugo DK (1976) Anomalous organization of thalamocortical projections consequent to vibrissae removal in the newborn rat and mouse. *Brain Res* 104:309–315.
- Killackey HP, Rhoades RW, Bennett-Clarke CA (1995) The formation of a cortical somatotopic map. *Trends in Neurosciences* 18:402–407.
- Kim G, Kandler K (2003) Elimination and strengthening of glycinergic/GABAergic connections during tonotopic map formation. *Nat Neurosci* 6:282–290.

Kivrak BG, Erzurumlu RS (2012) Development of the principal nucleus trigeminal lemniscal projections in the mouse. *J Comp Neurol* 521:299–311.

Kopecky BJ, Duncan JS, Elliot KL, Fritsch B (2012) Three-dimensional reconstructions from optical sections of thick mouse inner ears using confocal microscopy. *Journal of Microscopy* 248:292–298.

Kotak VC, Sanes DH (1996) Developmental influence of glycinergic transmission: regulation of NMDA receptor-mediated EPSPs. *Journal of Neuroscience* 16:1836–1843.

Lacar B, Young SZ, Platel J-C, Bordey A (2011) Gap junction-mediated calcium waves define communication networks among murine postnatal neural progenitor cells. *Eur J Neurosci* 34:1895–1905.

Landers M, Haidarliu S, Philip Zeigler H (2006) Development of rodent macrovibrissae: effects of neonatal whisker denervation and bilateral neonatal enucleation. *Somatosens Mot Res* 23:11–17.

Leake PA, Snyder RL, Hradek GT (2002) Postnatal refinement of auditory nerve projections to the cochlear nucleus in cats. *J Comp Neurol* 448:6–27.

Leclerc C, Saint-Amour D, Lavoie ME, Lassonde M, Lepore F (2000) Brain functional reorganization in early blind humans revealed by auditory event-related potentials. *Neuroreport* 11:545–550.

Lessard N, Pare M, Lepore F, Lassonde M (1998) Early-blind human subjects localize sound sources better than sighted subjects. *Nature* 395:278–280.

Levanen S, Hamdorf D (2001) Feeling vibrations: enhanced tactile sensitivity in congenitally deaf humans. *Neuroscience Letters* 301:75–77.

Leybaert L, Sanderson MJ (2012) Intercellular Ca²⁺ waves: mechanisms and function. *Physiol Rev* 92:1359–1392.

Leyva-Díaz E, del Toro D, Menal MJ, Cambray S, Susín R, Tessier-Lavigne M, Klein R, Egea J, López-Bendito G (2014) FLRT3 Is a Robo1-Interacting Protein that Determines Netrin-1 Attraction in Developing Axons. *Current Biology* 24:494–508.

Li H, Fertuzinhos S, Mohns E, Hnasko TS, Verhage M, Edwards R, Sestan N, Crair MC (2013) Laminar and Columnar Development of Barrel Cortex Relies on Thalamocortical Neurotransmission. *Neuron* 79:970–986.

References

- Li Y, Erzurumlu RS, Chen C, Jhaveri S, Tonegawa S (1994) Whisker-related neuronal patterns fail to develop in the trigeminal brainstem nuclei of NMDAR1 knockout mice. *Cell* 76:427–437.
- Liberman MC, Brown MC (1986) Physiology and anatomy of single olivocochlear neurons in the cat. *Hearing Research* 24:17–36.
- Lickiss T, Cheung AFP, Hutchinson CE, Taylor JSH, Molnár Z (2012) Examining the relationship between early axon growth and transcription factor expression in the developing cerebral cortex. *Journal of Anatomy* 220:201–211.
- Lim DJ, Anniko M (1985) Developmental morphology of the mouse inner ear. A scanning electron microscopic observation. *Acta Otolaryngol Suppl* 422:1–69.
- Lim DJ, Kalinec F (1998) Cell and molecular basis of hearing. *Kidney Int Suppl* 65:S104–S113.
- Litvina EY, Chen C (2017) Functional Convergence at the Retinogeniculate Synapse. *Neuron* 96:330–338.e335.
- Liu H, Kim S-Y, Fu Y, Wu X, Ng L, Swaroop A, Forrest D (2013) An isoform of retinoid-related orphan receptor β directs differentiation of retinal amacrine and horizontal interneurons. *Nat Commun* 4:1813.
- López-Bendito G, Cautinat A, Sánchez JA, Bielle F, Flames N, Garratt AN, Talmage DA, Role LW, Charnay P, Marín O, Garel S (2006) Tangential Neuronal Migration Controls Axon Guidance: A Role for Neuregulin-1 in Thalamocortical Axon Navigation. *Cell* 125:127–142.
- López-Bendito G, Molnár Z (2003) Thalamocortical development: how are we going to get there? *Nature Reviews Neuroscience* 4:276–289.
- Lu H-C, She W-C, Plas DT, Neumann PE, Janz R, Crair MC (2003) Adenylyl cyclase I regulates AMPA receptor trafficking during mouse cortical “barrel” map development. *Nat Neurosci* 6:939–947.
- Lu HC (2006) Role of Efficient Neurotransmitter Release in Barrel Map Development. *Journal of Neuroscience* 26:2692–2703.
- Luhmann HJ (2017) Review of imaging network activities in developing rodent cerebral cortex in vivo. *Neurophoton* 4:031202–031209.

Luhmann HJ, Sinning A, Yang J-W, Reyes-Puerta V, Stüttgen MC, Kirischuk S, Kilb W (2016) Spontaneous Neuronal Activity in Developing Neocortical Networks: From Single Cells to Large-Scale Interactions. *Front Neural Circuits* 10:40.

Ma PM, Woolsey TA (1984) Cytoarchitectonic correlates of the vibrissae in the medullary trigeminal complex of the mouse. *Brain Res* 306:374–379.

Macaluso E, Frith CD, Driver J (2001) Multimodal mechanisms of attention related to rates of spatial shifting in vision and touch. *Experimental Brain Research* 137:445–454.

Mallamaci A, Muzio L, Chan CH, Parnavelas J, Boncinelli E (2000) Area identity shifts in the early cerebral cortex of *Emx2*^{-/-} mutant mice. *Nat Neurosci* 3:679–686.

Mallamaci A, Stoykova A (2006) Gene networks controlling early cerebral cortex arealization. *European Journal of Neuroscience* 23:847–856.

Mandai K, Reimert DV, Ginty DD (2014) *Linx* Mediates Interaxonal Interactions and Formation of the Internal Capsule. *Neuron* 83:93–103.

Mann ZF, Kelley MW (2011) Development of tonotopy in the auditory periphery. *Hearing Research* 276:2–15.

Martini FJ, Moreno-Juan V, Filipchuk A, Valdeolmillos M, López-Bendito G (2017) Impact of thalamocortical input on barrel cortex development. *Neuroscience*:1–10.

Matsumoto N, Hoshiko M, Sugo N, Fukazawa Y, Yamamoto N (2015) Synapse-dependent and independent mechanisms of thalamocortical axon branching are regulated by neuronal activity. *Devel Neurobio* 76:323–336.

McKay SM, Oleskevich S (2007) The role of spontaneous activity in development of the endbulb of Held synapse. *Hearing Research* 230:53–63.

McQuillen PS, DeFreitas MF, Zada G, Shatz CJ (2002) A novel role for p75^{NTR} in subplate growth cone complexity and visual thalamocortical innervation. *Journal of Neuroscience* 22:3580–3593.

Meyer AC, Frank T, Khimich D, Hoch G, Riedel D, Chapochnikov NM, Yarin YM, Harke B, Hell SW, Egner A, Moser T (2009) Tuning of synapse number, structure and function in the cochlea. *Nat Neurosci* 12:444–453.

Miller B, Chou L, Finlay BL (1993) The early development of thalamocortical and corticothalamic projections. *J Comp Neurol* 335:16–41.

References

Mire E, Mezzera C, az EL-DI, Paternain AV, Squarzoni P, Bluy L, Castillo-Paterna M, López MJ, Peregrín S, Tessier-Lavigne M, Garel S, Galcerán J, Lerma J, López-Bendito (2012) Spontaneous activity regulates Robo1 transcription to mediate a switch in thalamocortical axon growth. *Nat Neurosci*:1–12.

Mitrovic N, Mohajeri H, Schachner M (1996) Effects of NMDA receptor blockade in the developing rat somatosensory cortex on the expression of the glia-derived extracellular matrix glycoprotein tenascin-C. *Eur J Neurosci* 8:1793–1802.

Miyashita-Lin EM, Hevner R, Wassarman KM, Martinez S, Rubenstein JL (1999) Early neocortical regionalization in the absence of thalamic innervation. *Science* 285:906–909.

Mizuno H, Luo W, Tarusawa E, Saito YM, Sato T, Yoshimura Y, Itohara S, Iwasato T (2014) NMDAR-Regulated Dynamics of Layer 4 Neuronal Dendrites during Thalamocortical Reorganization in Neonates. *Neuron* 82:365–379.

Molnar Z, Cordery P (1999) Connections between cells of the internal capsule, thalamus, and cerebral cortex in embryonic rat. *J Comp Neurol* 413:1–25.

Molnar Z, Hannan AJ (2000) Development of thalamocortical projections in normal and mutant mice. *Results Probl Cell Differ* 30:293–332.

Molnár Z (1998) Mechanisms Underlying the Early Establishment of Thalamocortical Connections in the Rat. :1–23.

Molnár Z (2012) Development of the corticothalamic projections. :1–14.

Molnár Z, Garel S, López-Bendito G, Maness P, Price DJ (2012) Mechanisms controlling the guidance of thalamocortical axons through the embryonic forebrain. *European Journal of Neuroscience* 35:1573–1585.

Molyneaux BJ, Arlotta P, Menezes JRL, Macklis JD (2007) Neuronal subtype specification in the cerebral cortex. *Nature Reviews Neuroscience* 8:427–437.

Moreno-Juan V, Filipchuk A, Antón-Bolaños N, Mezzera C, Gezelius H, Rodríguez-Malmierca LM, Susín R, Schaad O, Iwasato T, Schüle R, Rutlin M, Nelson S, Ducret S, Valdeolmillos M, Rijli FM, López-Bendito G (2017) Prenatal thalamic waves regulate cortical area size prior to sensory processing. *Nat Commun* 8:1–14.

Morgan JL, Berger DR, Wetzel AW, Lichtman JW (2016) The Fuzzy Logic of Network Connectivity in Mouse Visual Thalamus. *Cell* 165:192–206.

Mostafapour SP, Cochran SL, Del Puerto NM, Rubel EW (2000) Patterns of cell death in mouse anteroventral cochlear nucleus neurons after unilateral cochlea removal. *J Comp Neurol* 426:561–571.

Muir-Robinson G, Hwang BJ, Feller MB (2002) Retinogeniculate axons undergo eye-specific segregation in the absence of eye-specific layers. *Journal of Neuroscience* 22:5259–5264.

Murray KD, Choudary PV, Jones EG (2007) Nucleus- and cell-specific gene expression in monkey thalamus. *Proceedings of the National Academy of Sciences* 104:1989–1994.

Myers (2003) *Choreography of Early Thalamocortical Development*. :1–9.

Nakagawa Y, Johnson JE, O'Leary DD (1999) Graded and areal expression patterns of regulatory genes and cadherins in embryonic neocortex independent of thalamocortical input. *Journal of Neuroscience* 19:10877–10885.

Nakagawa Y, O'Leary DD (2001) Combinatorial expression patterns of LIM-homeodomain and other regulatory genes parcellate developing thalamus. *Journal of Neuroscience* 21:2711–2725.

Nakagawa Y, Shimogori T (2012) Diversity of thalamic progenitor cells and postmitotic neurons. *Eur J Neurosci* 35:1554–1562.

Ni B, Wu X, Yan GM, Wang J, Paul SM (1995) Regional expression and cellular localization of the Na(+)-dependent inorganic phosphate cotransporter of rat brain. *Journal of Neuroscience* 15:5789–5799.

Noctor SC, Martínez-Cerdeño V, Ivic L, Kriegstein AR (2004) Cortical neurons arise in symmetric and asymmetric division zones and migrate through specific phases. *Nat Neurosci* 7:136–144.

Noh J, Seal RP, Garver JA, Edwards RH, Kandler K (2010) Glutamate co-release at GABA/glycinergic synapses is crucial for the refinement of an inhibitory map. *Nat Neurosci* 13:232–238.

O'Leary DD (1989) Do cortical areas emerge from a protocortex? *Trends in Neurosciences* 12:400–406.

References

- O'Leary DDM, Chou S-J, Hamasaki T, Sahara S, Takeuchi A, Thuret S, Leingärtner A (2007) Regulation of laminar and area patterning of mammalian neocortex and behavioural implications. *Novartis Found Symp* 288:141–59–discussion159–64–276–81.
- Oberlaender M, de Kock CPJ, Bruno RM, Ramirez A, Meyer HS, Dercksen VJ, Helmstaedter M, Sakmann B (2011) Cell Type-Specific Three-Dimensional Structure of Thalamocortical Circuits in a Column of Rat Vibrissal Cortex. *Cerebral Cortex* 22:2375–2391.
- Oleskevich S, Walmsley B (2002) Synaptic transmission in the auditory brainstem of normal and congenitally deaf mice. *J Physiol* 540:447–455.
- Oleskevich S, Youssoufian M, Walmsley B (2004) Presynaptic plasticity at two giant auditory synapses in normal and deaf mice. *J Physiol* 560:709–719.
- Olsen SR, Bortone DS, Adesnik H, Scanziani M (2012) Gain control by layer six in cortical circuits of vision. *Nature* 483:47–52.
- O'Leary DD, Sahara S (2008) Genetic regulation of arealization of the neocortex. *Current Opinion in Neurobiology* 18:90–100.
- Pasternak JR, Woolsey TA (1975) The number, size and spatial distribution of neurons in lamina IV of the mouse SmI neocortex. *J Comp Neurol* 160:291–306.
- Penn AA, Riquelme PA, Feller MB, Shatz CJ (1998) Competition in retinogeniculate patterning driven by spontaneous activity. *Science* 279:2108–2112.
- Persico AM, Mengual E, Moessner R, Hall FS, Revay RS, Sora I, Arellano J, DeFelipe J, Gimenez-Amaya JM, Conciatori M, Marino R, Baldi A, Cabib S, Pascucci T, Uhl GR, Murphy DL, Lesch KP, Keller F (2001) Barrel pattern formation requires serotonin uptake by thalamocortical afferents, and not vesicular monoamine release. *Journal of Neuroscience* 21:6862–6873.
- Petersen CCH (2007) The Functional Organization of the Barrel Cortex. *Neuron* 56:339–355.
- Petros TJ, Rebsam A, Mason CA (2008) Retinal Axon Growth at the Optic Chiasm: To Cross or Not to Cross. *Annu Rev Neurosci* 31:295–315.
- Pouchelon G, Gambino F, Bellone C, Telley L, Vitali I, Lüscher C, Holtmaat A, Jabaudon D (2014) Modality-specific thalamocortical inputs instruct the identity of postsynaptic L4 neurons. *Nature* 511:471–474.

Price DJ (2012) The importance of combinatorial gene expression in early mammalian thalamic patterning and thalamocortical axonal guidance. :1–15.

Price DJ, Kennedy H, Dehay C, Zhou L, Mercier M, Jossin Y, Goffinet AM, Tissir F, Blakey D, Molnár Z (2006) The development of cortical connections. *European Journal of Neuroscience* 23:910–920.

Rakic P (1988) Specification of cerebral cortical areas. *Science* 241:170–176.

Ralston HJ3 (1969) The synaptic organization of lemniscal projections to the ventrobasal thalamus of the cat. *Brain Res* 14:99–115.

Rash BG, Grove EA (2006) Area and layer patterning in the developing cerebral cortex. *Current Opinion in Neurobiology* 16:25–34.

Rauschecker JP, Tian B, Korte M, Egert U (1992) Crossmodal changes in the somatosensory vibrissa/barrel system of visually deprived animals. *Proceedings of the National Academy of Sciences* 89:5063–5067.

Rebillard G, Carlier E, Rebillard M, Pujol R (1977) Enhancement of visual responses on the primary auditory cortex of the cat after an early destruction of cochlear receptors. *Brain Res* 129:162–164.

Rebsam A, Petros TJ, Mason CA (2009) Switching retinogeniculate axon laterality leads to normal targeting but abnormal eye-specific segregation that is activity dependent. *J Neurosci* 29:14855–14863.

Reichova I (2004) Somatosensory Corticothalamic Projections: Distinguishing Drivers From Modulators. *Journal of Neurophysiology* 92:2185–2197.

Rice FL, Gomez C, Barstow C, Burnet A, Sands P (1985) A comparative analysis of the development of the primary somatosensory cortex: interspecies similarities during barrel and laminar development. *J Comp Neurol* 236:477–495.

Richards LJ, Koester SE, Tuttle R, O'Leary DD (1997) Directed growth of early cortical axons is influenced by a chemoattractant released from an intermediate target. *Journal of Neuroscience* 17:2445–2458.

Roder B, Teder-Salejarvi W, Sterr A, Rosler F, Hillyard SA, Neville HJ (1999) Improved auditory spatial tuning in blind humans. *Nature* 400:162–166.

References

Roe AW, Pallas SL, Hahm JO, Sur M (1990) A map of visual space induced in primary auditory cortex. *Science* 250:818–820.

Rompani SB, Müllner FE, Wanner A, Zhang C, Roth CN, Yonehara K, Roska B (2017) Different Modes of Visual Integration in the Lateral Geniculate Nucleus Revealed by Single-Cell- Initiated Transsynaptic Tracing. *Neuron* 93:767–776.e6.

Roska, B, & Meister, M (2014) The Retina Dissects the Visual Scene into Distinct Features. In: *The New Visual Neurosciences* (Werner, JS, Chalupa, LM, eds), pp 163–182.

Rossi FM, Pizzorusso T, Porciatti V, Marubio LM, Maffei L, Changeux JP (2001) Requirement of the nicotinic acetylcholine receptor beta 2 subunit for the anatomical and functional development of the visual system. *Proceedings of the National Academy of Sciences* 98:6453–6458.

Rouiller EM, Welker E (2000) A comparative analysis of the morphology of corticothalamic projections in mammals. *Brain Res Bull* 53:727–741.

Rubel EW, Fritsch B (2002) Auditory system development: primary auditory neurons and their targets. *Annu Rev Neurosci* 25:51–101.

Rubenstein JL, Martinez S, Shimamura K, Puelles L (1994) The embryonic vertebrate forebrain: the prosomeric model. *Science* 266:578–580.

Rudhard Y, Kneussel M, Nassar MA, Rast GF, Annala AJ, Chen PE, Tigaret CM, Dean I, Roes J, Gibb AJ, Hunt SP, Schoepfer R (2003) Absence of Whisker-related pattern formation in mice with NMDA receptors lacking coincidence detection properties and calcium signaling. *Journal of Neuroscience* 23:2323–2332.

Russell FA, Moore DR (1995) Afferent reorganisation within the superior olivary complex of the gerbil: development and induction by neonatal, unilateral cochlear removal. *J Comp Neurol* 352:607–625.

Salichon N, Gaspar P, Upton AL, Picaud S, Hanoun N, Hamon M, De Maeyer E, Murphy DL, Mossner R, Lesch KP, Hen R, Seif I (2001) Excessive activation of serotonin (5-HT) 1B receptors disrupts the formation of sensory maps in monoamine oxidase a and 5-ht transporter knock-out mice. *Journal of Neuroscience* 21:884–896.

Sanes DH, Song J, Tyson J (1992) Refinement of dendritic arbors along the tonotopic axis of the gerbil lateral superior olive. *Brain Res Dev Brain Res* 67:47–55.

Sanes DH, Takacs C (1993) Activity-dependent refinement of inhibitory connections. *Eur J Neurosci* 5:570–574.

Scalia F, Grant AC, Reyes M, Lettvin JY (1995) Functional properties of regenerated optic axons terminating in the primary olfactory cortex. *Brain Res* 685:187–197.

Schlaggar BL, O'Leary DD (1994) Early development of the somatotopic map and barrel patterning in rat somatosensory cortex. *J Comp Neurol* 346:80–96.

Schneider GE (1973) Early lesions of superior colliculus: factors affecting the formation of abnormal retinal projections. *Brain Behav Evol* 8:73–109.

Schug N, Braig C, Zimmermann U, Engel J, Winter H, Ruth P, Blin N, Pfister M, Kalbacher H, Knipper M (2006) Differential expression of otoferlin in brain, vestibular system, immature and mature cochlea of the rat. *European Journal of Neuroscience* 24:3372–3380.

Seabrook TA, El-Danaf RN, Krahe TE, Fox MA, Guido W (2013) Retinal Input Regulates the Timing of Corticogeniculate Innervation. *Journal of Neuroscience* 33:10085–10097.

Sehara K, Kawasaki H (2011) Neuronal Circuits with Whisker-Related Patterns. *Mol Neurobiol* 43:155–162.

Shams L, Kamitani Y, Thompson S, Shimojo S (2001) Sound alters visual evoked potentials in humans. *Neuroreport* 12:3849–3852.

Shanks JA, Ito S, Schaevitz L, Yamada J, Chen B, Litke A, Feldheim DA (2016) Corticothalamic Axons Are Essential for Retinal Ganglion Cell Axon Targeting to the Mouse Dorsal Lateral Geniculate Nucleus. *Journal of Neuroscience* 36:5252–5263.

Shatz CJ, Stryker MP (1978) Ocular dominance in layer IV of the cat's visual cortex and the effects of monocular deprivation. *J Physiol* 281:267–283.

Shatz CJ, Stryker MP (1988) Prenatal tetrodotoxin infusion blocks segregation of retinogeniculate afferents. *Science* 242:87–89.

She W-C, Quairiaux C, Albright MJ, Wang Y-C, Sanchez DE, Chang P-S, Welker E, Lu H-C (2009) Roles of mGluR5 in synaptic function and plasticity of the mouse thalamocortical pathway. *Eur J Neurosci* 29:1379–1396.

References

Sherman SM, Guillery RW (1998) On the actions that one nerve cell can have on another: distinguishing "drivers" from "modulators". *Proceedings of the National Academy of Sciences* 95:7121–7126.

Sherman SM, Guillery RW (2002) The role of the thalamus in the flow of information to the cortex. *Philosophical Transactions of the Royal Society B: Biological Sciences* 357:1695–1708.

Shi W, Xianyu A, Han Z, Tang X, Li Z, Zhong H, Mao T, Huang K, Shi S-H (2017) Ontogenetic establishment of order-specific nuclear organization in the mammalian thalamus. *Nat Neurosci* 20:516–528.

Shibata S, Kakazu Y, Okabe A, Fukuda A, Nabekura J (2004) Experience-dependent changes in intracellular Cl⁻ regulation in developing auditory neurons. *Neuroscience Research* 48:211–220.

Shimogori T (2005) Fibroblast Growth Factor 8 Regulates Neocortical Guidance of Area-Specific Thalamic Innervation. *Journal of Neuroscience* 25:6550–6560.

Siegel F, Heimel JA, Peters J, Lohmann C (2012) Peripheral and Central Inputs Shape Network Dynamics in the Developing Visual Cortex *In Vivo*. *Current Biology* 22:253–258.

Simons DJ, Durham D, Woolsey TA (1984) Functional organization of mouse and rat SmI barrel cortex following vibrissal damage on different postnatal days. *Somatosens Res* 1:207–245.

Song H, Lee B, Pyun D, Guimera J, Son Y, Yoon J, Baek K, Wurst W, Jeong Y (2015) *Ascl1* and *Helt* act combinatorially to specify thalamic neuronal identity by repressing *Dlx5* activation. *Developmental Biology* 398:280–291.

Spitzer NC (2006) Electrical activity in early neuronal development. *Nature* 444:707–712.

Stocker AM, O'Leary DDM (2016) *Emx1* Is Required for Neocortical Area Patterning Mallo M, ed. *PLoS ONE* 11:e0149900–e0149911.

Strutz J (1981) Efferent innervation of the cochlea. *Ann Otol Rhinol Laryngol* 90:158–160.

Sur M, Pallas SL, Roe AW (1990) Cross-modal plasticity in cortical development: differentiation and specification of sensory neocortex. *Trends in Neurosciences* 13:227–233.

Thiers FA, Nadol JBJ, Liberman MC (2008) Reciprocal synapses between outer hair cells and their afferent terminals: evidence for a local neural network in the mammalian cochlea. *J Assoc Res Otolaryngol* 9:477–489.

Tierney TS, Russell FA, Moore DR (1997) Susceptibility of developing cochlear nucleus neurons to deafferentation-induced death abruptly ends just before the onset of hearing. *J Comp Neurol* 378:295–306.

Toldi J, Laskawi R, Landgrebe M, Wolff JR (1996) Biphasic reorganization of somatotopy in the primary motor cortex follows facial nerve lesions in adult rats. *Neuroscience Letters* 203:179–182.

Toldi J, Rojik I, Feher O (1994) Neonatal monocular enucleation-induced cross-modal effects observed in the cortex of adult rat. *Neuroscience* 62:105–114.

Tolner EA, Sheikh A, Yukin AY, Kaila K, Kanold PO (2012) Subplate neurons promote spindle bursts and thalamocortical patterning in the neonatal rat somatosensory cortex. *Journal of Neuroscience* 32:692–702.

Tronche F, Kellendonk C, Kretz O, Gass P, Anlag K, Orban PC, Bock R, Klein R, Schutz G (1999) Disruption of the glucocorticoid receptor gene in the nervous system results in reduced anxiety. *Nat Genet* 23:99–103.

Tsukano H, Horie M, Ohga S, Takahashi K, Kubota Y, Hishida R, Takebayashi H, Shibuki K (2017) Reconsidering Tonotopic Maps in the Auditory Cortex and Lemniscal Auditory Thalamus in Mice. *Front Neural Circuits* 11:14.

Uemura M, Nakao S, Suzuki ST, Takeichi M, Hirano S (2007) OL-protocadherin is essential for growth of striatal axons and thalamocortical projections. *Nat Neurosci* 10:1151–1159.

Uesaka N, Hayano Y, Yamada A, Yamamoto N (2007) Interplay between laminar specificity and activity-dependent mechanisms of thalamocortical axon branching. *Journal of Neuroscience* 27:5215–5223.

Vale C, Sanes DH (2000) Afferent regulation of inhibitory synaptic transmission in the developing auditory midbrain. *Journal of Neuroscience* 20:1912–1921.

Vale C, Sanes DH (2002) The effect of bilateral deafness on excitatory and inhibitory synaptic strength in the inferior colliculus. *European Journal of Neuroscience* 16:2394–2404.

References

- Vale C, Schoorlemmer J, Sanes DH (2003) Deafness disrupts chloride transporter function and inhibitory synaptic transmission. *Journal of Neuroscience* 23:7516–7524.
- Valverde F (1968) Structural changes in the area striata of the mouse after enucleation. *Experimental Brain Research* 5:274–292.
- Van der Loos H, Woolsey TA (1973) Somatosensory cortex: structural alterations following early injury to sense organs. *Science* 179:395–398.
- Varoqui H, Schafer MKH, Zhu H, Weihe E, Erickson JD (2002) Identification of the differentiation-associated Na⁺/PI transporter as a novel vesicular glutamate transporter expressed in a distinct set of glutamatergic synapses. *Journal of Neuroscience* 22:142–155.
- Voss P, Lassonde M, Gougoux F, Fortin M, Guillemot J-P, Lepore F (2004) Early- and late-onset blind individuals show supra-normal auditory abilities in far-space. *Current Biology* 14:1734–1738.
- Vue TY, Aaker J, Taniguchi A, Kazemzadeh C, Skidmore JM, Martin DM, Martin JF, Treier M, Nakagawa Y (2007) Characterization of progenitor domains in the developing mouse thalamus. *J Comp Neurol* 505:73–91.
- Vue TY, Lee M, Tan YE, Werkhoven Z, Wang L, Nakagawa Y (2013) Thalamic control of neocortical area formation in mice. *Journal of Neuroscience* 33:8442–8453.
- Wang Q, Burkhalter A (2007) Area map of mouse visual cortex. *J Comp Neurol* 502:339–357.
- Watson RF (2006) Involvement of Protein Kinase A in Patterning of the Mouse Somatosensory Cortex. *Journal of Neuroscience* 26:5393–5401.
- Weller WL, Johnson JI (1975) Barrels in cerebral cortex altered by receptor disruption in newborn, but not in five-day-old mice (Cricetidae and Muridae). *Brain Res* 83:504–508.
- Wijetunge LS, Till SM, Gillingwater TH, Ingham CA, Kind PC (2008) mGluR5 Regulates Glutamate-Dependent Development of the Mouse Somatosensory Cortex. *Journal of Neuroscience* 28:13028–13037.
- Wimmer VC, Broser PJ, Kuner T, Bruno RM (2010) Experience-induced plasticity of thalamocortical axons in both juveniles and adults. *J Comp Neurol* 518:4629–4648.

- Yamada A, Uesaka N, Hayano Y, Tabata T, Kano M, Yamamoto N (2010) Role of pre- and postsynaptic activity in thalamocortical axon branching. *Proceedings of the National Academy of Sciences* 107:7562–7567.
- Yang J-W, An S, Sun J-J, Reyes-Puerta V, Kindler J, Berger T, Kilb W, Luhmann HJ (2013) Thalamic network oscillations synchronize ontogenetic columns in the newborn rat barrel cortex. *Cerebral Cortex* 23:1299–1316.
- Youssoufian M, Couchman K, Shivdasani MN, Paolini AG, Walmsley B (2008) Maturation of auditory brainstem projections and calyces in the congenitally deaf (dn/dn) mouse. *J Comp Neurol* 506:442–451.
- Yu X, Chung S, Chen D-Y, Wang S, Dodd SJ, Walters JR, Isaac JTR, Koretsky AP (2012) Thalamocortical Inputs Show Post-Critical-Period Plasticity. *Neuron* 74:731–742.
- Yuste R, Nelson DA, Rubin WW, Katz LC (1995) Neuronal domains in developing neocortex: mechanisms of coactivation. *Neuron* 14:7–17.
- Zeltser LM (2005) Shh-dependent formation of the ZLI is opposed by signals from the dorsal diencephalon. *Development* 132:2023–2033.
- Zembrzycki A, Chou S-J, Ashery-Padan R, Stoykova A, O'Leary DDM (2013) Sensory cortex limits cortical maps and drives top-down plasticity in thalamocortical circuits. *Nat Neurosci* 16:1060–1067.
- Zembrzycki A, Griesel G, Stoykova A, Mansouri A (2007) Genetic interplay between the transcription factors Sp8 and Emx2 in the patterning of the forebrain. *Neural Dev* 2:8–18.
- Zheng D, Purves D (1995) Effects of increased neural activity on brain growth. *Proceedings of the National Academy of Sciences* 92:1802–1806.
- Zhou C, Qiu Y, Pereira FA, Crair MC, Tsai SY, Tsai MJ (1999) The nuclear orphan receptor COUP-TFI is required for differentiation of subplate neurons and guidance of thalamocortical axons. *Neuron* 24:847–859.

